DOE/BC/14600-53
Distribution Category UC-122

SUPRI HEAVY OIL RESEARCH PROGRAM

SUPRI 92

Annual Report for the Period
October 1, 1991--September 30, 1992

By
William E. Brigham
Henry J. Ramey Jr.
Louis M. Castanier

August 1993

Work Performed Under Contract No. DE-FG22-90BC14600

Prepared for
U.S. Department of Energy
Assistant Secretary for Fossil Energy

Thomas Reid, Project Manager
Bartlesville Project Office
P.O. Box 1398
Bartlesville, OK 74005

Prepared by
Stanford University
Petroleum Research Institute
Stanford, CA 94305

CONTENTS

LIST OF TABLES

LIST OF FIGURES

SUMMARY

The goal of the Stanford University Petroleum Research Institute is to conduct research directed toward increasing the recovery of heavy oils. Presently, SUPRI is working in five main directions:

1. FLOW PROPERTIES STUDIES - To assess the influence of different reservoir conditions (temperature and pressure) on the absolute and relative permeability to oil and water and on capillary pressure.

2. IN-SITU COMBUSTION - To evaluate the effect of different reservoir parameters on the *in-situ* combustion process. This project includes the study of the kinetics of the reactions.

3. STEAM WITH ADDITIVES - To develop and understand the mechanisms of the process using commercially available surfactants for reduction of gravity override and channeling of steam.

4. FORMATION EVALUATION - To develop and improve techniques of formation evaluation such as tracer tests and pressure transient tests.

5. FIELD SUPPORT SERVICES - To provide technical support for design and monitoring of DOE sponsored or industry initiated field projects.

1.1. A STUDY OF END EFFECTS IN DISPLACEMENT EXPERIMENTS

(Suhail Qadeer)

1.1.1 INTRODUCTION

The study of end effects in displacement experiments continued. Both experiments and numerical simulations are being used in this study. The results from this work indicate that the flow near the inlet and outlet of the core is non–linear. There is a strong saturation gradient along the length of the core in drainage displacements, even at high flow rates. This saturation gradient causes a non–monotonic saturation profile in subsequent imbibition displacement. Relative permeability calculations using models which assume monotonic saturation profiles, or linear flow models, should be used with caution.

1.1.2 EXPERIMENTAL APPARATUS AND PROCEDURES

The details of experimental apparatus used in this study have been presented in a previous SUPRI report (Brigham *et al.* 1990) . The analysis of the results from previous experiments, presented in last years report (Brgiham *et al.* 1992) , indicated a strong possibility of bypassing of the fluids around the core. The bypassing resulted in high wetting phase saturations near the outlet end of the core and low pressure drops. It was observed that the heat shrinkable Teflon sleeve looses its elasticity in the process of heat treatment and the applied overburden pressure is not enough to assure a seal between the sleeve and the core. The overburden pressure can not be increased because of the design limitations of the core holder.

It was therefore decided to apply a very thin layer of epoxy over the surface of the core before applying the Teflon sleeve. The epoxy is thick enough during this process that its penetration into the core is negligible. This was confirmed by cutting a test sample of the core after the application of the epoxy and teflon sleeve. The pressure drop and saturation measurements now confirm that the problem of bypassing has been solved. The teflon sleeve provides a reliable means of avoiding any reaction between the fluids and the outer rubber sleeve, which provides the necessary mechanical strength for the application of the overburden pressure. The end plugs for these experiments had distribution grooves in them. The geometry of these grooves is shown in Figure 1.1.1.

It was observed in previous runs that,because of the time involved in scanning, it is not possible to scan the core at different locations along its length to create saturation profiles at different times and observe the progress of the flood. It was therefore decided to keep the core stationary during the early phase of each displacement. At the beginning of a displacement run the CT scans were performed near the center of the core (at location # 13) until the flood front had passed that section of the core. The scan location was then moved near the outlet end of the core (location # 20) and the procedure was repeated. After breakthrough of the injected phase, the core was scanned at twenty locations along the length of the core. This procedure permitted us to dynamically observe the progress of the flood and also to generate the 3–D saturation profiles at the end of each flood.

1.1.3 RESULTS FROM DISPLACEMENT EXPERIMENTS

The core was initially saturated with 8% sodium bromide brine. A total of five drainage and four imbibition displacement experiments were conducted using Core-2. After saturating the

core with brine and measuring the absolute permeability, primary drainage displacement was done at a rate of 8.0 cc/min, followed by a sequence of imbibition and displacement experiments at 8.0, 4.0, and 2.0 cc/min. At the end of the 2.0 cc/min. drainage, the flow rate of oil was increased to 8.0 cc/min. for Drainage-4. This was followed by imbibition and drainage runs at 8.0 cc/min. The complete sequence of experiments is given in Table 1.1.1.

The saturations were calculated using two methods. In the first method the average saturation for each cross-section scanned was calculated based upon the average CT numbers for the cross-section. The second method of calculations uses the CT numbers for each volume element (a voxel) which is 0.5 mm by 0.5 mm by 17 mm. This method allows the construction of 3-D saturation maps. These maps provide a valuable insight into the flow mechanics at small scale. The details of the calculation procedure are given in a previous SUPRI report

The saturation profiles after each displacement experiment were calculated from average CT numbers across each cross-section. The results are graphed in Figures 1.1.2 and 1.1.3. These saturations were measured after the production of the displaced fluids had become negligible. It is obvious from these graphs that the measurements of saturation by CT are quite consistent. The maximum deviation being less than $\pm 5\%$. The saturation profiles after the drainage displacements are graphed in Figure 1.1.2. The graphs show saturation gradients at the outlet end.

The first scan location, which is very near the inlet end, also showed higher water saturation. This result is most probably caused by the inclusion of the end plug, into the X-ray field. This end plug is fabricated from stainless steal, causing the CT numbers to be higher. This effect is more obvious in the imbibition saturation profiles graphed in Figure 1.1.3. The irreducible brine saturation, based upon the minimum saturation measured is around 32%. If we base the irreducible saturation on the average saturation of the core it will be around 40%.

Concerning the saturation profiles after imbibition displacements, shown in Figure 1.1.3, the saturation is much more uniform throughout the core. As explained earlier, the first saturation point near the inlet end is probably in error. The value of brine saturation at irreducible oil saturation is around 68%. Again if we base our measurements on the average core saturation the value will be slightly higher, about 70%.

The 3-D saturation maps from 8.0 cc/min. and 2.0 cc/min imbibition and drainage displacements are shown in Figures 1.1.4 to 1.1.7. The blue areas indicate 100% brine and red indicates brine at irreducible saturation. It can be seen that the saturations are quite heterogeneous throughout the core. Each fluid has established its own flow channel through the core. The drainage maps show large saturation gradient across the length of the core. The brine seems to occupy most of the area at the outlet face of the core (the right hand faces in the Figures 1.1.5 to 1.1.7). Some voxels at the outlet face have very high oil saturations, providing the necessary path for the oil to flow out of the core.

1.1.4 NUMERICAL SIMULATIONS

ECLIPSE, a commercial black oil simulator was used in this study. The preliminary simulation runs were made using 1-D, and 2-D rectangular grids. The purpose of these runs was to study the effect of gravity in the laboratory displacements. It was noted that the gravity effects can be neglected. To properly include the geometrical configuration of the end plugs, however it is necessary to use a 2-D radial (r-z) grid. All of the results presented in this study are from 2-D, r-z simulations. To simulate the inlet and outlet end plugs, it was assumed that the fluids enter and leave the core only through the concentric circular grooves. In the calculations four wells are used at each end of the core, one for each circular groove. The wells at the injection end are operated under group control. The total injection rate for the group is specified. The simulator automatically adjusts the individual well injection rates to match the injectivity and the pressure

field near the wells, maintaining the total specified flow rate for the group. The injectivity of each well is set such that it is proportional to the area for its corresponding groove. Similarly, at the production end, a constant bottom hole pressure for the wells is specified. The individual rates now correspond to the productivity index and the pressure gradient at the well. The schematic for this injection/production scheme is shown in Figure 1.1.8. For these runs, typical capillary pressure and relative permeability curves for Berea sandstone were used. These curves are shown in Figure 1.1.9. This method was necessary in the absence of measured capillary pressure and relative permeability curves. The measurement of the capillary pressure for our cores is in progress. The relative permeability curves calculated from the displacement experiments reported herein will be used in subsequent simulation runs.

1.1.5 RESULTS FROM NUMERICAL SIMULATIONS

The simulation runs were conducted at the same rates as the physical experiments, i.e. 8.0, 4.0, and 2.0 cc/min. The simulations were started with the core at 100% saturated with brine. The first run was primary drainage at 8.0 cc/min. The saturation maps for the primary drainage are shown is Figure 1.1.10. It was noted from the simulations that most of the fluids are taken by the innermost injector which is at the center of the core face. Thus the front moved faster through the center of the core. For unit viscosity ratio displacements, the primary drainage process is inherently stable. Although the front moved faster in the middle of the core near the inlet end, it became uniform as it moved further into the core. At latter times the saturation was uniform radially through most of the core. The effect of non-uniform injection and production from the core faces is obvious from the bending of the contours near both ends of the core. A strong saturation gradient does exist along the length of the core. Figure 1.1.11 shows the saturation profile based upon the average saturation at each cross section. The saturation gradients are quite obvious from this graph.

The next run was the simulation of an imbibition experiment at a rate of 8.0 cc/min. The saturation maps are shown in Figure 1.1.12. Considering the front mobility ratios, the imbibition displacement is a stable one. The saturation contours show that the brine moves more rapidly near the center of the core, causing a nonuniform saturation distribution at cross-sections near the inlet and outlet ends. This is again caused by the non-uniform injection and production across the faces of the core. The saturation distributions become more uniform further away from the ends of the core. The average saturation profiles are plotted in Figure 1.1.13. It should be noted that during the imbibition displacement, the average saturations do not decrease monotonically through the core, but go through a minimum. This is the result of the strong saturation gradient present at the end of the previous drainage displacement process. At the end of this imbibition there is a small saturation gradient near the outlet end. This run was followed by an 8.0 cc/min. drainage displacement.

The drainage displacement at 8.0 cc/min. is an unstable process. The mobility ratio is around 5.0. The saturation maps from this displacement are presented in Figure 1.1.14. The unstable behavior of this displacement is clear from the curved saturation contours. After breakthrough, the saturations across the cross sections became more uniform, but there are strong saturation gradients along the length of the core. These are again more obvious from the average saturation profiles shown in Figure 1.1.15.

The runs at 8.0 cc/min. were followed by 4.0 cc/min. and then 2.0 cc/min. imbibition and drainage displacements. The results from these are qualitatively similar to those discussed above at 8.0 cc/min. The saturation maps and the saturation profiles for runs at 4.0 cc/min. and 2.0 cc/min. are shown in Figure 1.1.16 to Figure 1.1.23. The effect of rate on the calculated final saturation profiles is shown in Figures 1.1.24 and 1.1.25. The final profiles from the three imbibition runs lie

directly on top of each other. There is noticeable difference in the saturation profiles at the end of the drainage displacements. These differences are caused by the large capillary outlet end effect. The saturations are higher for the low rate displacements, the difference being about 1% for each flow rate change.

A more interesting difference is shown if we graph the saturation profiles for the 4.0 cc/min and 2.0 cc/min. imbibition displacements at a total fluid injection of 0.166 PV. This graph is shown in Figure 1.1.26. It can be seen that the profile for the 2.0 cc/min. imbibition displacement has moved ahead of the run at 4.0 cc/min. This is caused by the fact that the average saturation in the core was higher at the beginning of the displacement at 2.0 cc/min. A similar trend is shown for the 8.0 cc/min. imbibition displacement, in which the front moved even slower than the 4.0 cc/min run. Although the front seems to advance faster in the lower rate runs, the time of breakthrough was the same, for the three runs. This result is because the wetting phase is held at the core face because of the capillary discontinuity.

1.1.6 CONCLUSIONS AND RECOMMENDATIONS

From the experimental results it is clear that the saturation is not uniform throughout the core at the end of a drainage process. This results in non–monotonic variation of saturations during the subsequent imbibition displacement. Conventional analysis, such as the JBN method for calculating relative permeabilities, make assumptions that (i) flow is linear and (ii) saturations are changing monotonically. The numerical simulation results indicate that even with the distribution grooves the injection of the fluids is non–uniform across the cross–section of the core. Thus the injection is almost hemispherical flow near the inlet at early stages of the displacements. Even at later stages the flow is not linear throughout the core. This behavior can result in serious errors in the calculated relative permeabilities.

In the future work the relative permeabilities from the displacement experiments will be calculated using a history matching technique using both a radial coordinate finite difference simulator and a linear model. The differences will be compared to provide guidelines for calculating relative permeabilities which are more representative of the rock and freer from experimental artifacts. The relative permeabilities will then be used in the simulator to generate more data at different conditions. More experiments will be performed using different flow rates and different fluids.

Run Name	Injected Fluids	Flow Rate cc/min.
Primary Drainage	Oil	8.0
Imbibition–1	Brine	8.0
Drainage–1	Oil	8.0
Imbibition–2	Brine	4.0
Drainage–2	Oil	4.0
Imbibition–3	Brine	2.0
Drainage–3	Oil	2.0
Drainage–4	Oil	8.0
Imbibition–4	Brine	8.0
Drainage–5	Oil	8.0

Table 1.1.1: Sequence of Experiments.

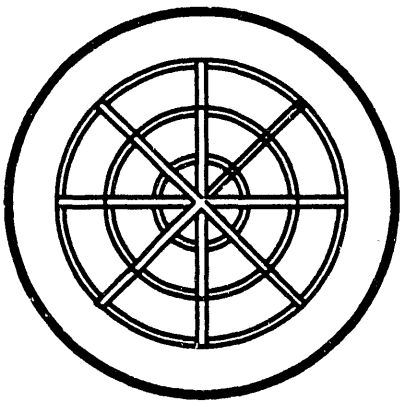

Figure 1.1.1: Schematic of the End Plug used for Distributing Fluids.

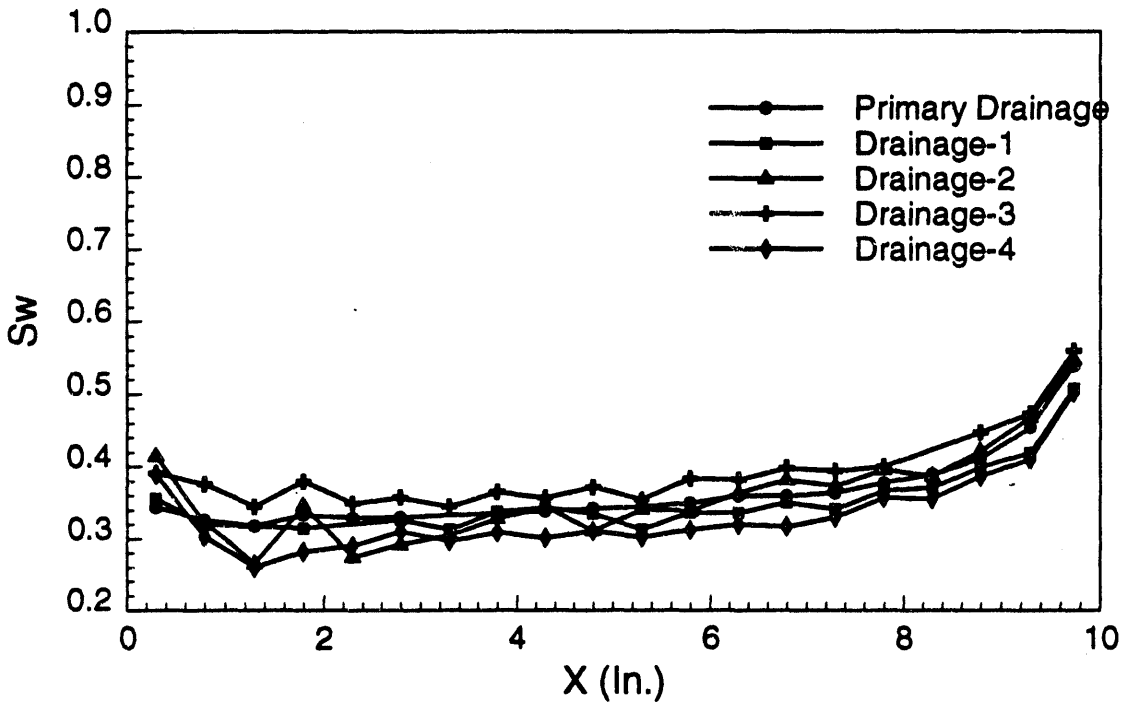

Figure 1.1.2: Saturation Profiles after Drainage Displacement Experiments.

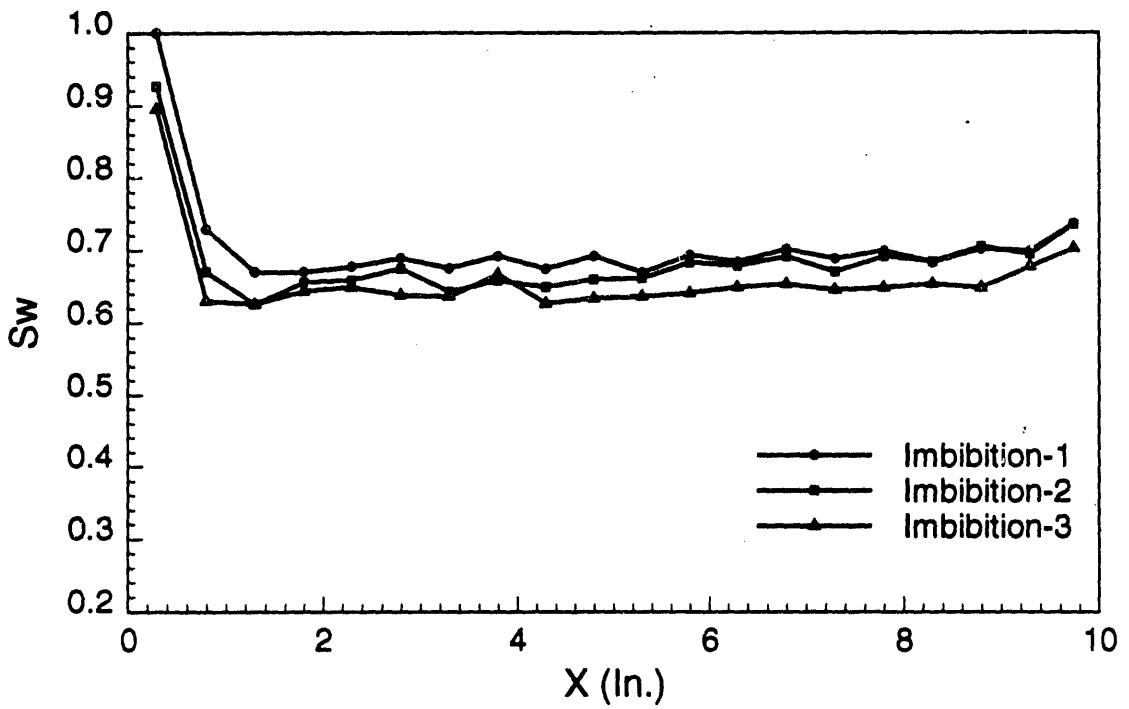

Figure 1.1.3: Saturation Profiles after Imbibition Displacement Experiments.

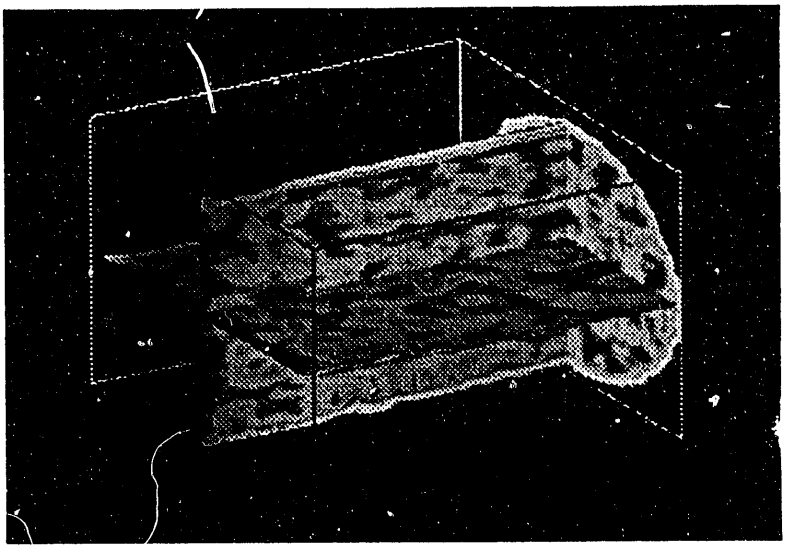

Figure 1.1.4: 3-D Saturation Map at the End of 8.0 cc/min. Imbibition.

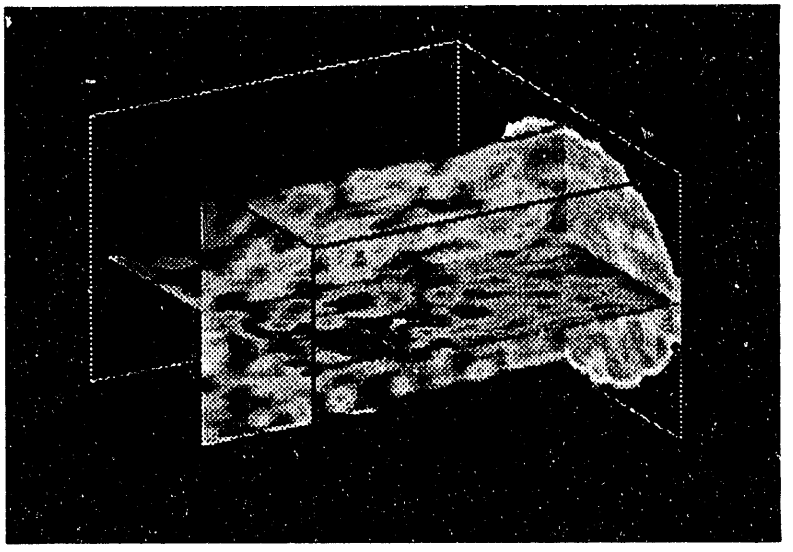

Figure 1.1.5: 3-D Saturation Map at the End of 8.0 cc/min. Drainage.

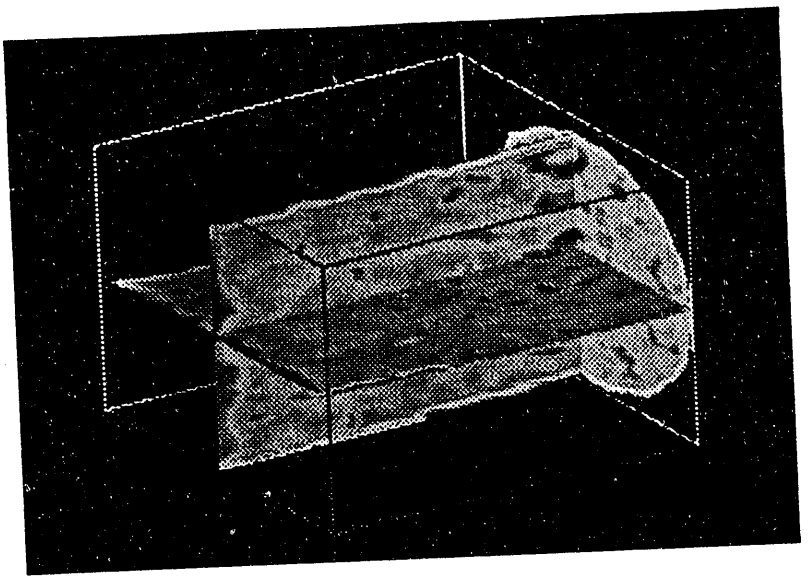

Figure 1.1.6: 3-D Saturation Map at the End of 2.0 cc/min. Imbibition.

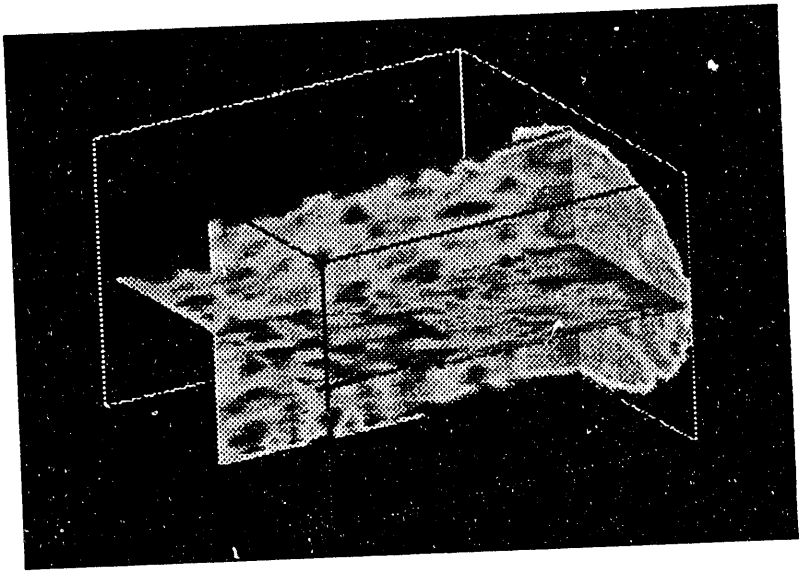

Figure 1.1.7: 3-D Saturation Map at the End of 2.0 cc/min. Drainage.

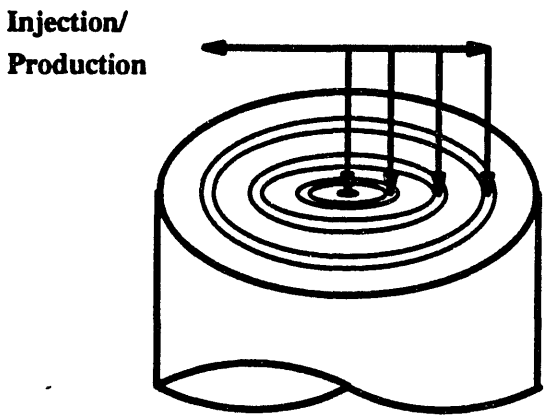

Figure 1.1.8: Schematic of the Injection and Production Wells Used in the Numerical Simulations.

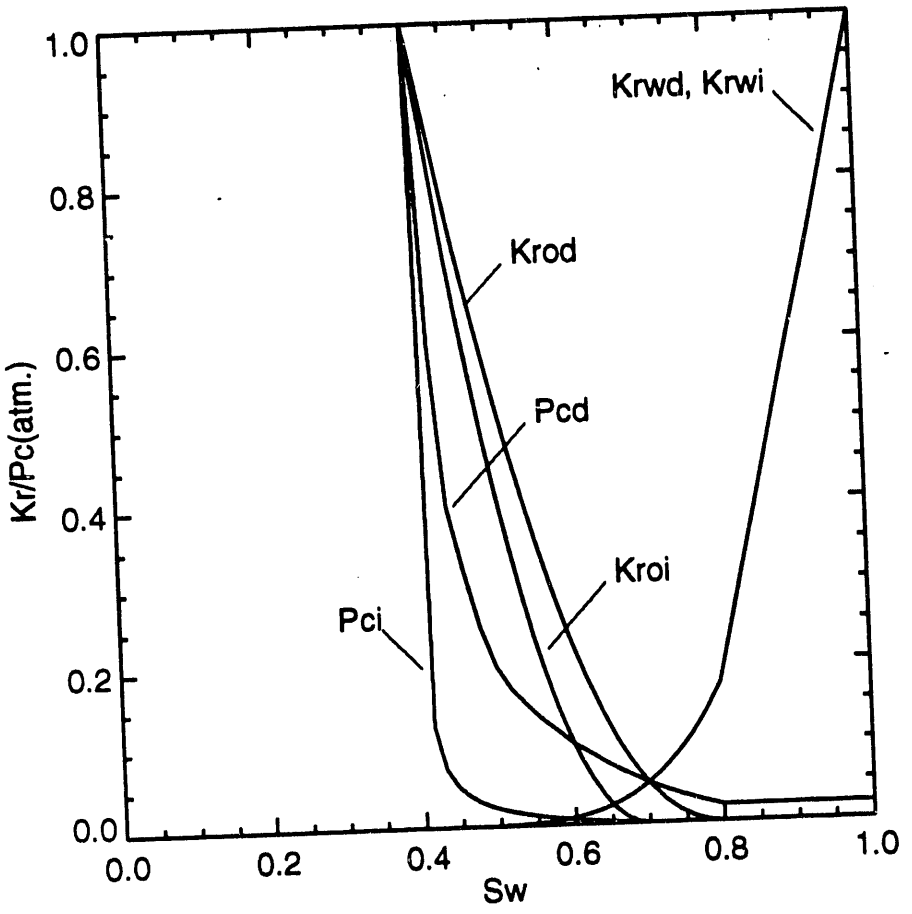

Figure 1.1.9: Capillary Pressure and Relative Permeability Curves Used in The Numerical Simulations.

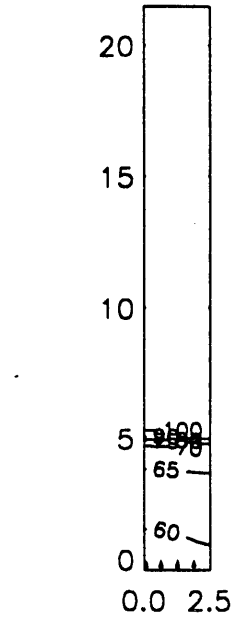

RUN 24A, Time= 0.020

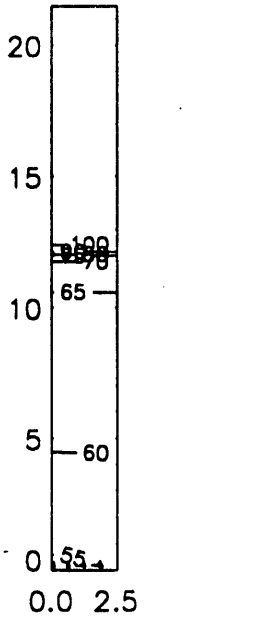

RUN 24A, Time= 0.050

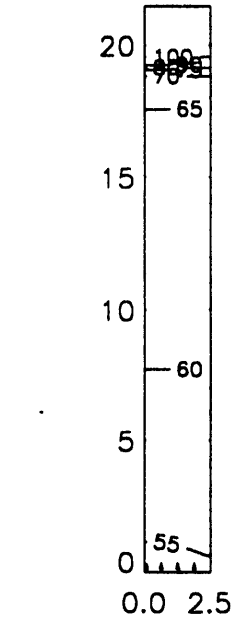

RUN 24A, Time= 0.080

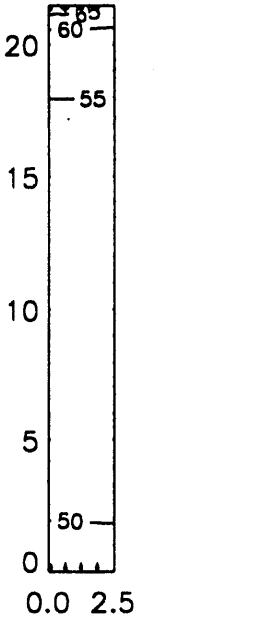

RUN 24A, Time= 1.000

Figure 1.1.10: Saturation Maps from Primary Drainage Simulation Run.

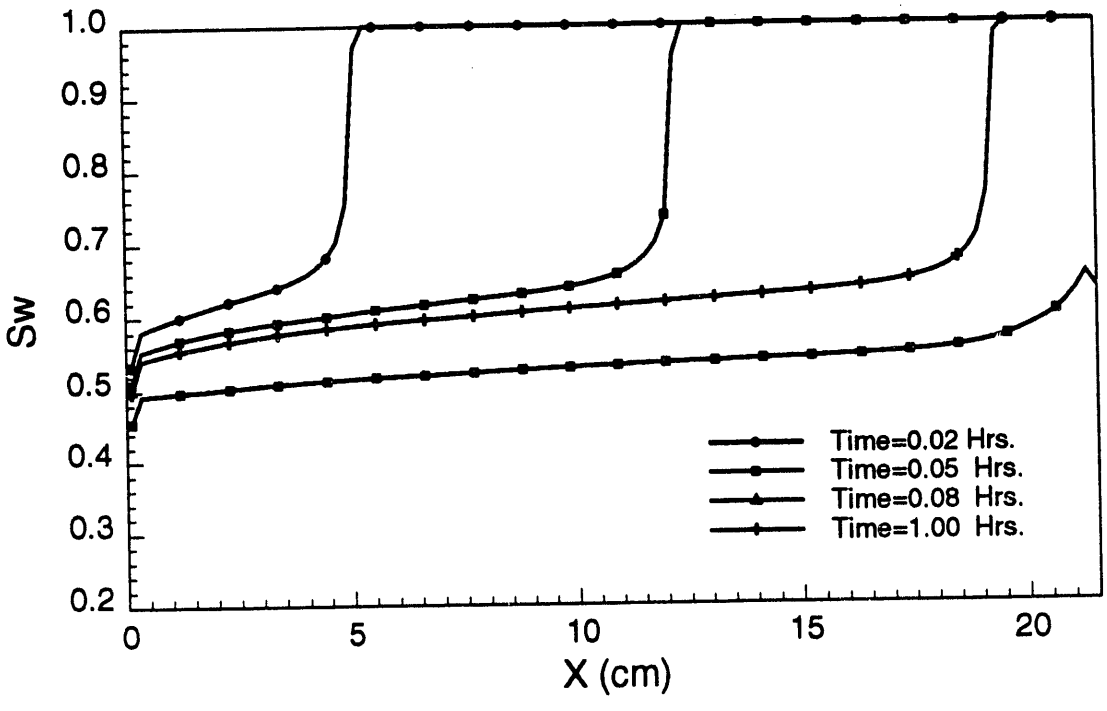

Figure 1.1.11: Saturation Profiles from Primary Drainage Simulation Run.

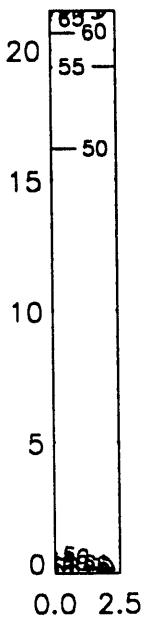

RUN 25A, Time= 0.001

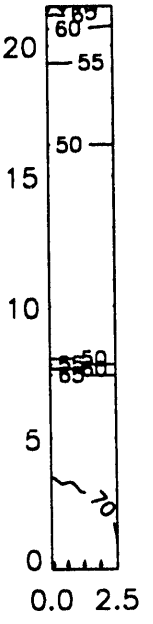

RUN 25A, Time= 0.020

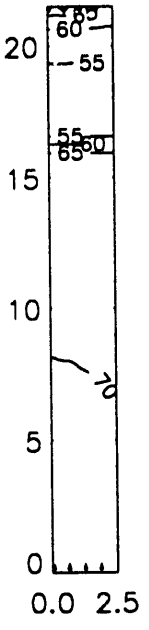

RUN 25A, Time= 0.040

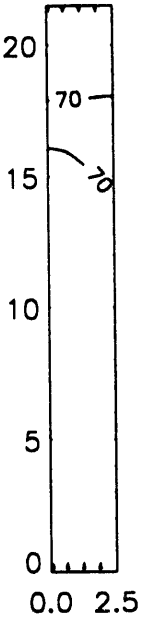

RUN 25A, Time= 0.070

Figure 1.1.12: Saturation Maps from Imbibition Run at 8.0 cc/min.

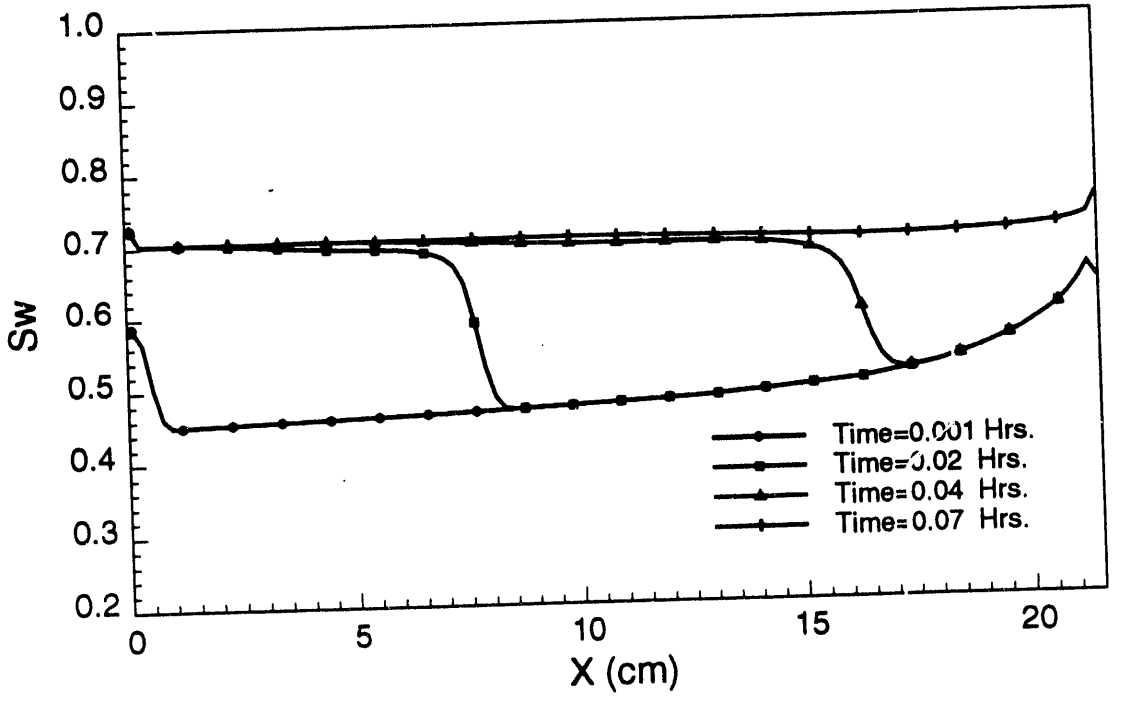

Figure 1.1.13: Saturation Profiles from Imbibition Run at 8.0 cc/min.

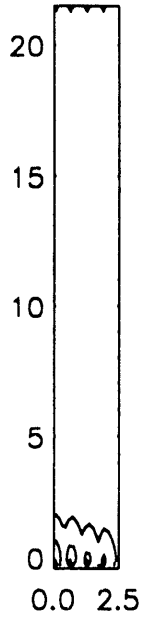

RUN 26A, Time= 0.001

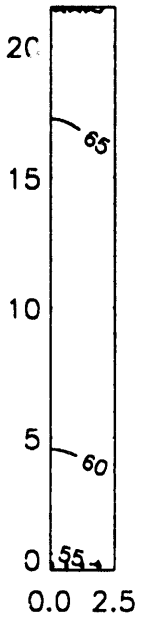

RUN 26A, Time= 0.020

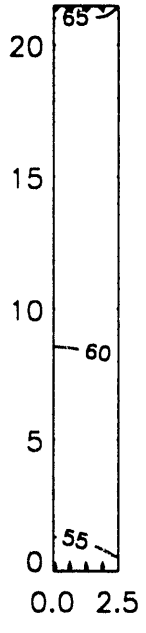

RUN 26A, Time= 0.040

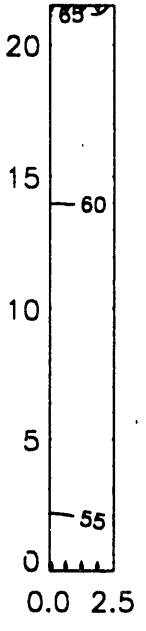

RUN 26A, Time= 0.070

Figure 1.1.14: Saturation Maps from Drainage Run at 8.0 cc/min.

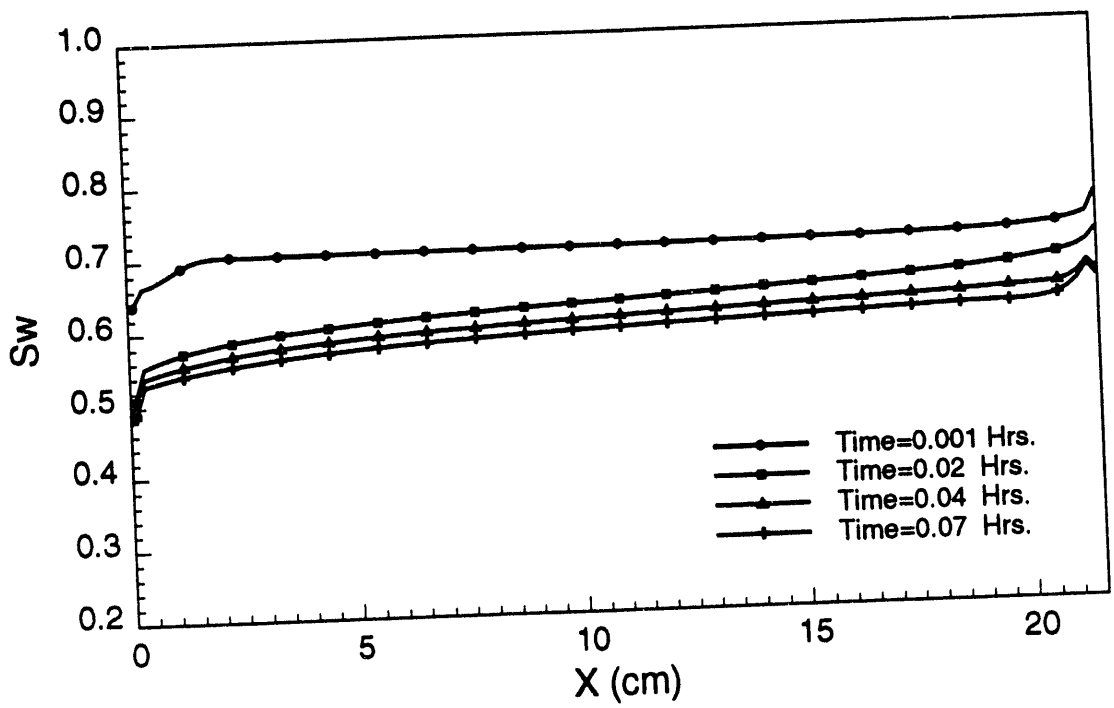

Figure 1.1.15: Saturation Profiles from Drainage Run at 8.0 cc/min.

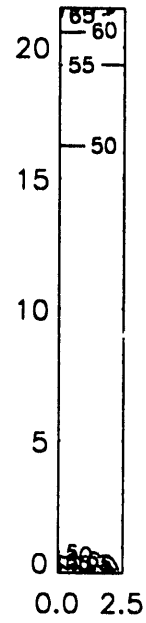

RUN 27A, Time= 0.002

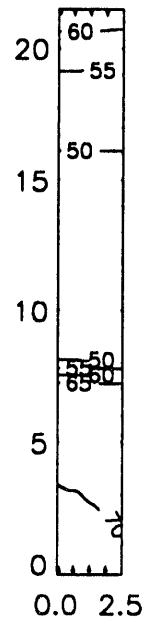

RUN 27A, Time= 0.040

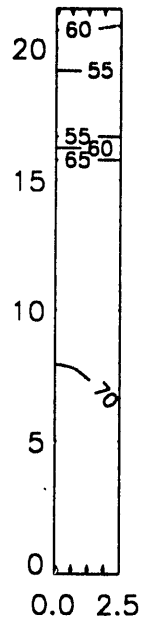

RUN 27A, Time= 0.080

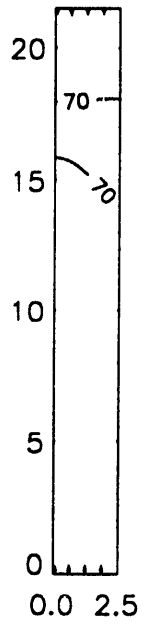

RUN 27A, Time= 0.140

Figure 1.1.16: Saturation Maps from Imbibition Run at 4.0 cc/min.

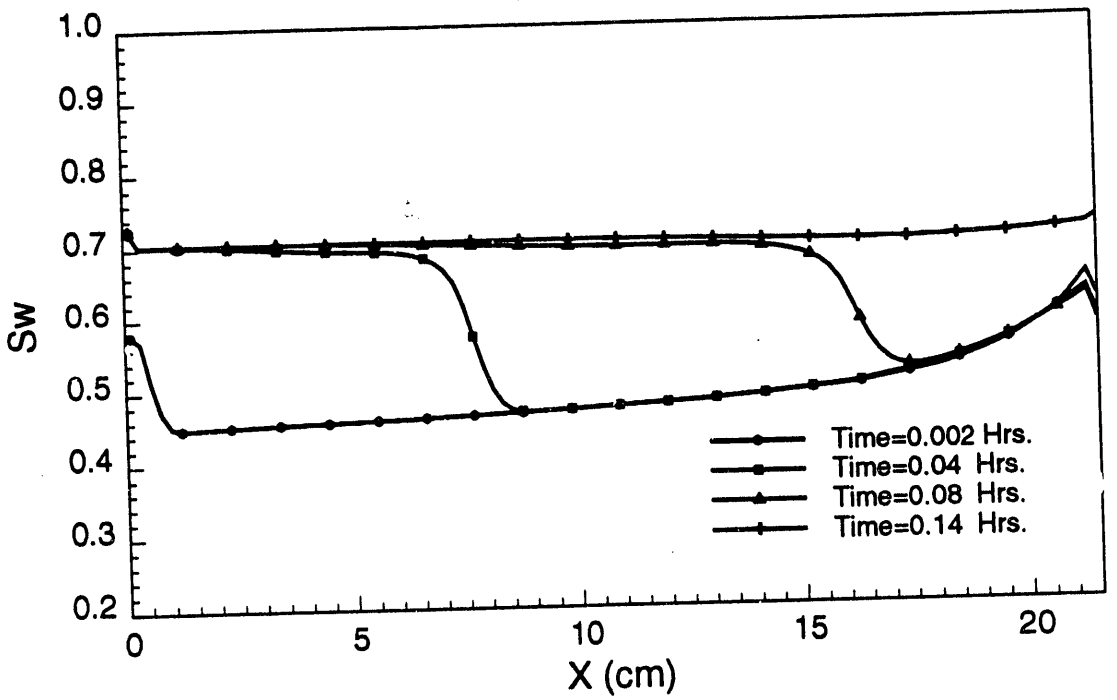

Figure 1.1.17: Saturation Profiles from Imbibition Run at 4.0 cc/min.

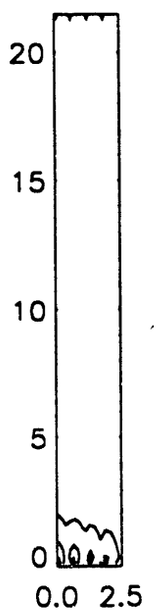

RUN 28A, Time= 0.002

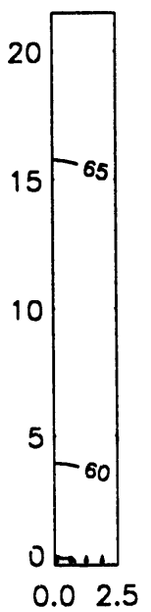

RUN 28A, Time= 0.040

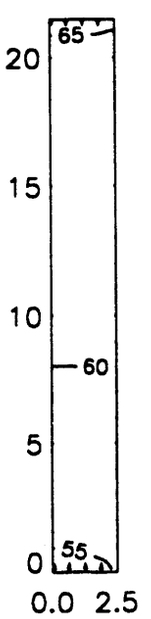

RUN 28A, Time= 0.080

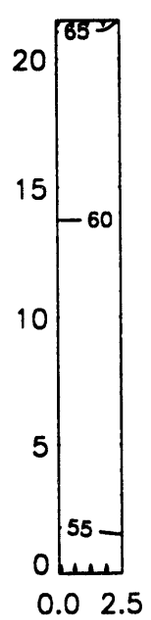

RUN 28A, Time= 0.140

Figure 1.1.18: Saturation Maps from Drainage Run at 4.0 cc/min.

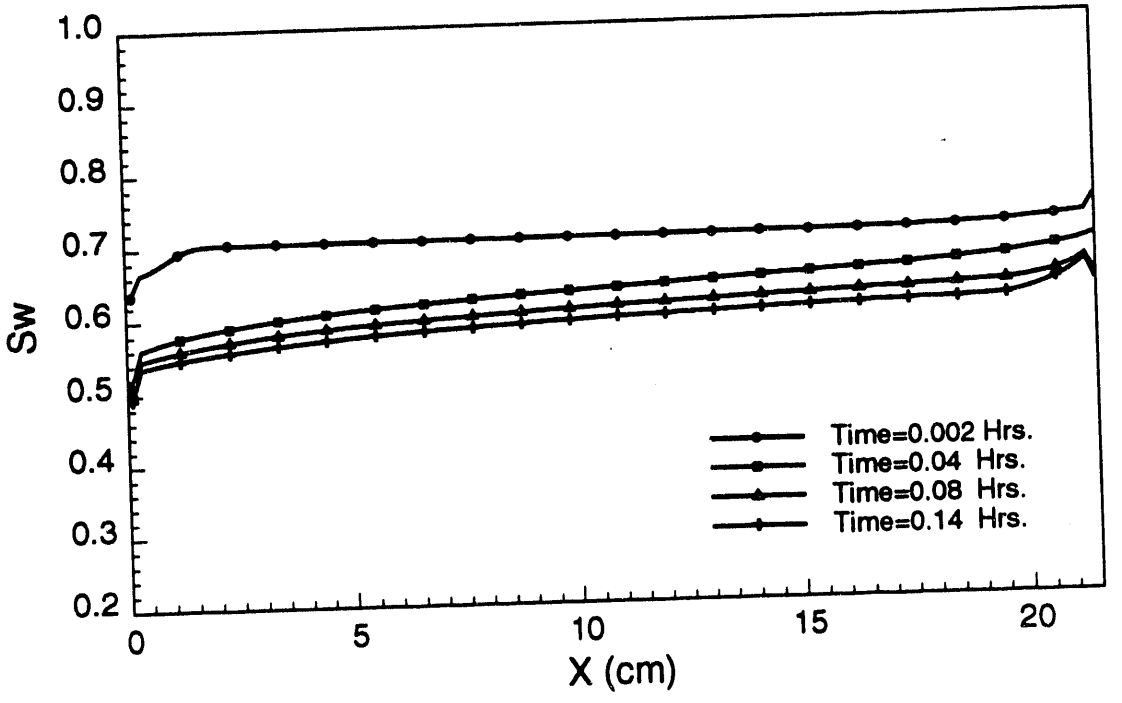

Figure 1.1.19: Saturation Profiles from Drainage Run at 4.0 cc/min.

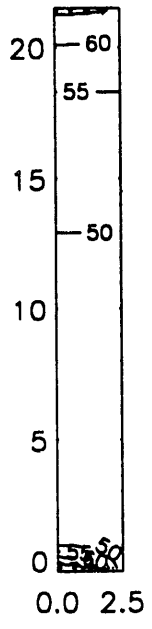

RUN 29A, Time= 0.004

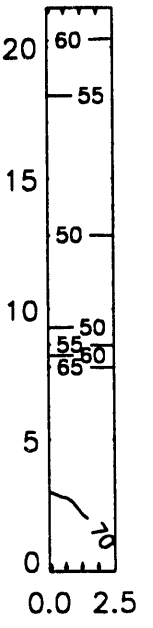

RUN 29A, Time= 0.080

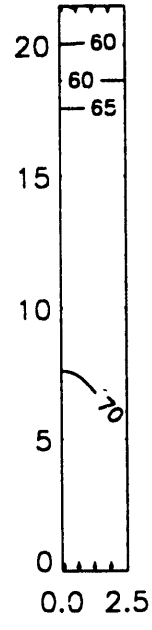

RUN 29A, Time= 0.160

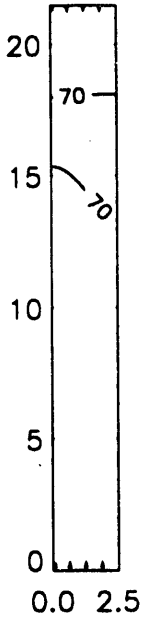

RUN 29A, Time= 0.280

Figure 1.1.20: Saturation Maps from Imbibition Run at 2.0 cc/min.

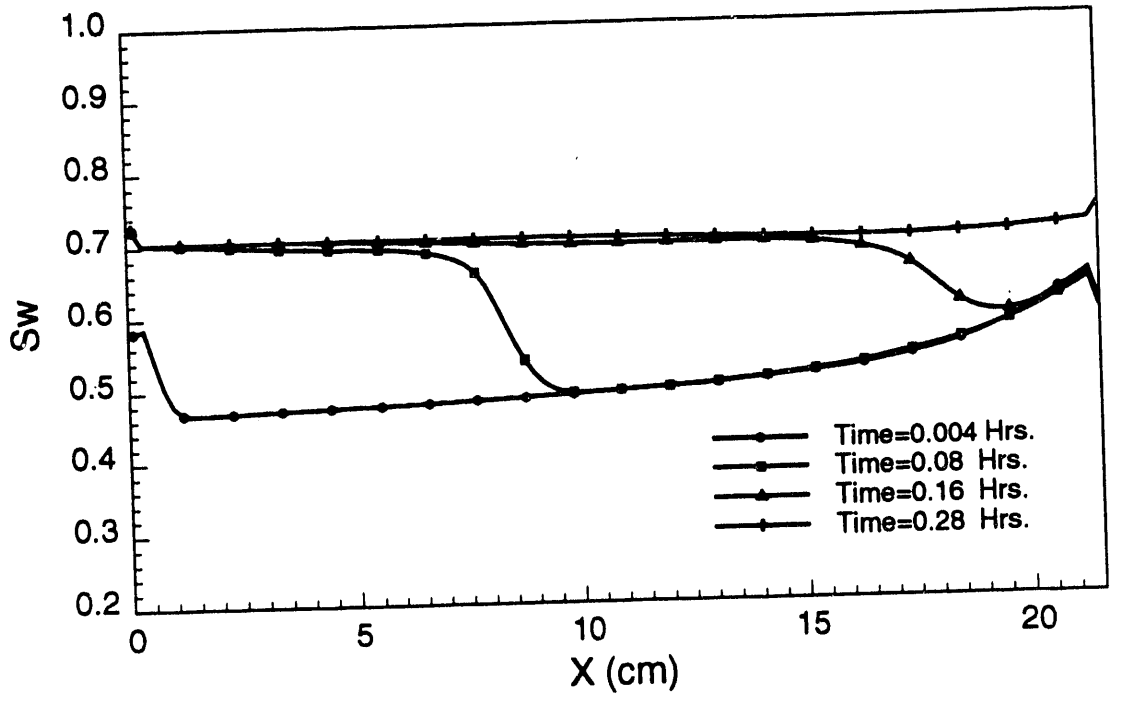

Figure 1.1.21: Saturation Profiles from Imbibition Run at 2.0 cc/min.

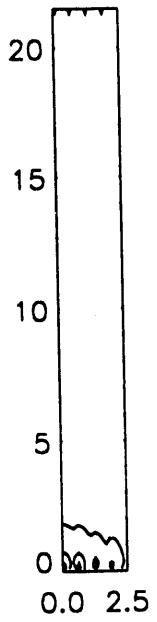

RUN 30A, Time= 0.004

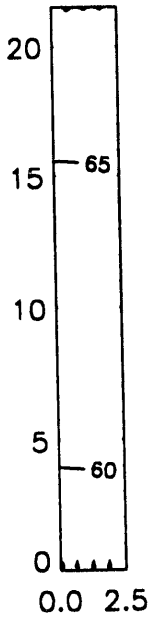

RUN 30A, Time= 0.080

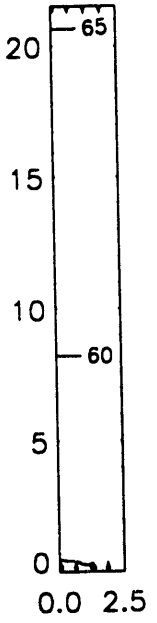

RUN 30A, Time= 0.160

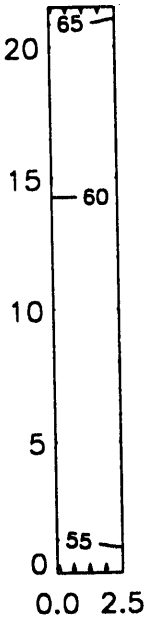

RUN 30A, Time= 0.280

Figure 1.1.22: Saturation Maps from Drainage Run at 2.0 cc/min.

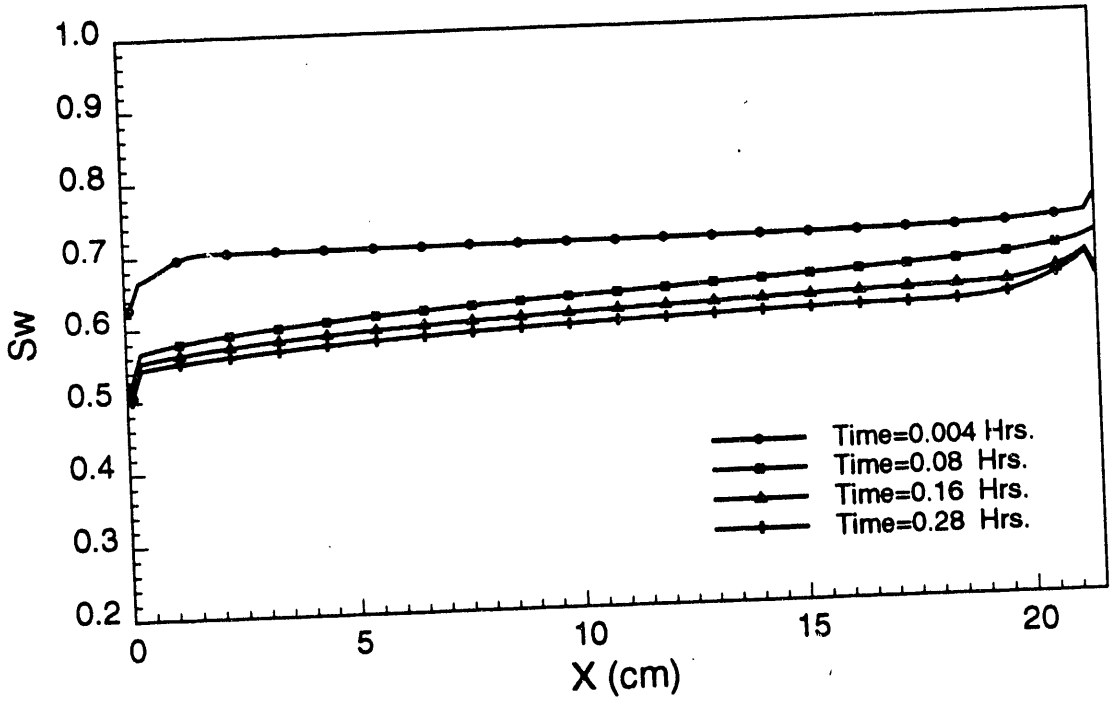

Figure 1.1.23: Saturation Profiles from Drainage Run at 2.0 cc/min.

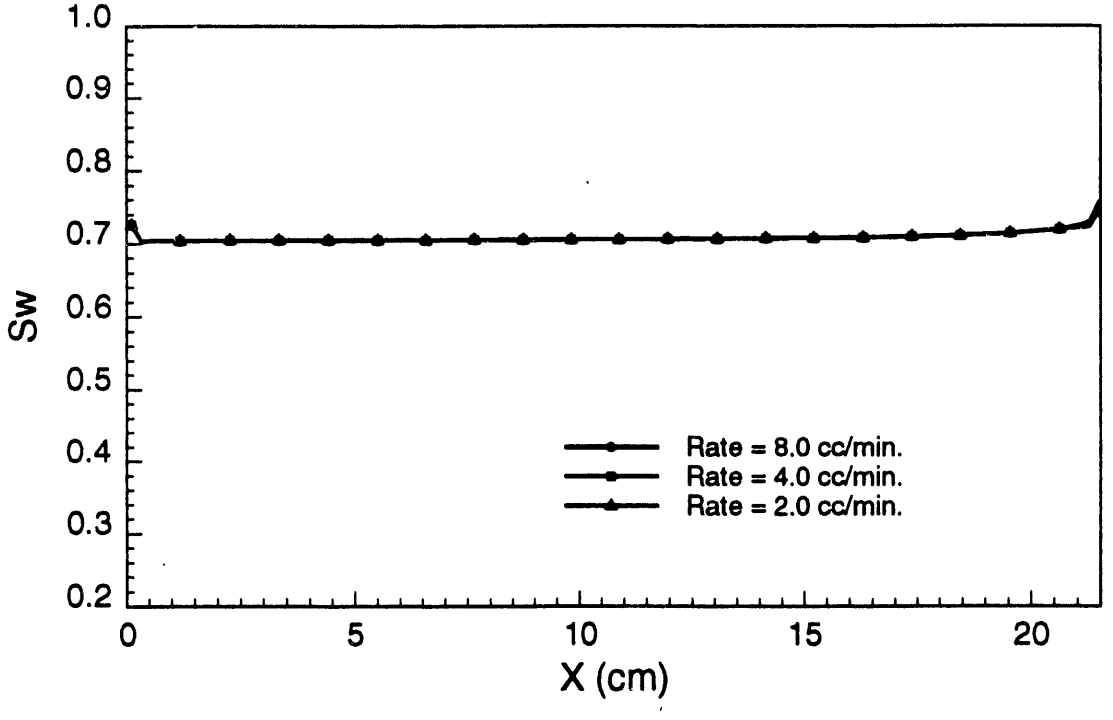

Figure 1.1.24: Saturation Profiles from Imbibition Runs at Different Flow Rates.

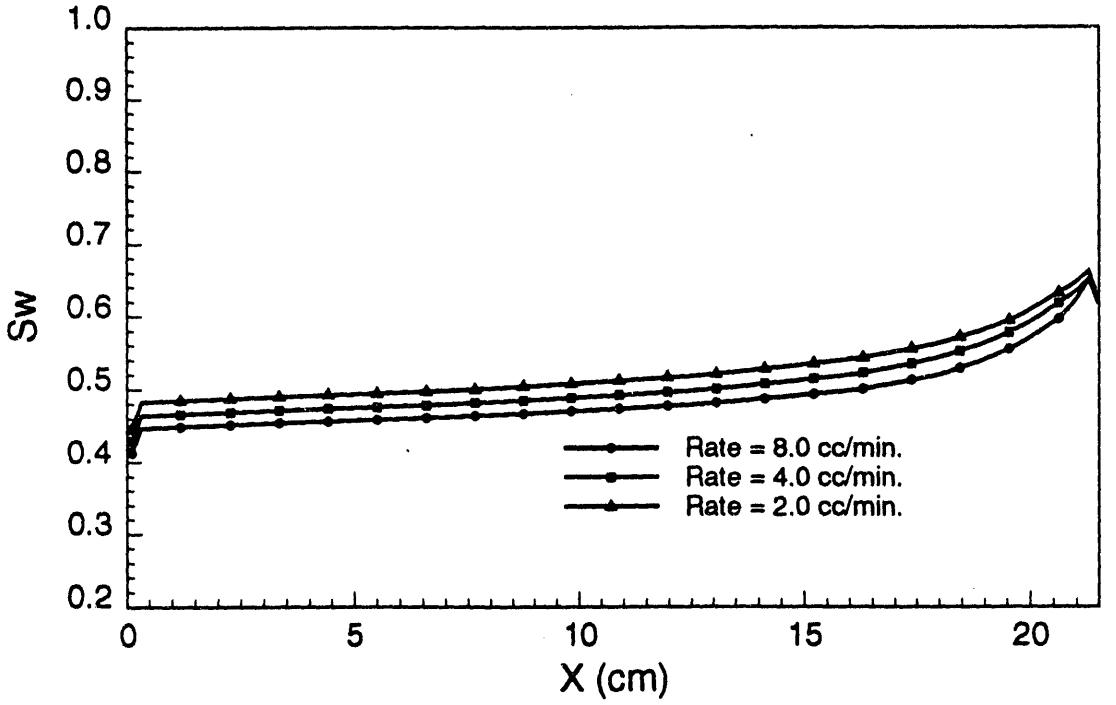

Figure 1.1.25: Saturation Profiles from Drainage Runs at Different Flow Rates.

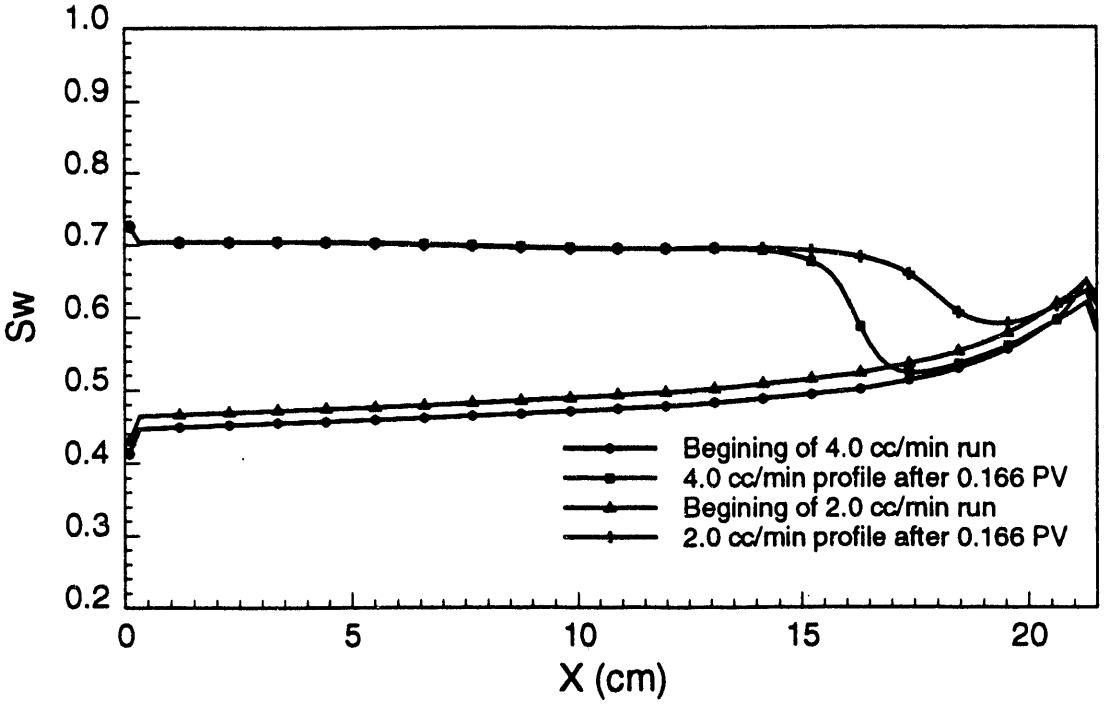

Figure 1.1.26: Comparison of Saturation Profiles at Different Flow Rates.

1.2. SOFTWARE DEVELOPMENT FOR CT DATA INTERPRETATION

(Pascal Rondeu)

1.2.1 INTRODUCTION

As the use of computer software becomes increasingly important for the research experiments, it becomes a necessity to control internally developed software. Despite the fact that SUPRI-A in-house programs are generally well written and relatively free of mistakes, they often lack documentation or on-line help. They also need to be used in a consistent way by different researchers. Usually, once the scanner users have done their experiment, they follow a set procedure of computer use that enables them to quantitatively extract and interpret the information from the CT scans. The goal of this project is to facilitate those tasks by providing both the computer environment and the software needed for post-processing of information. To do that, a software package will be developed and tested on the SUPRI-A computers dedicated to CT data analysis.

1.2.2 HARDWARE DESCRIPTION

The CT scanner works with two "D6 200 Eclipse" computers that enable the user to view and store the scans on a magnetic tape storage device. The resulting images are 320*320 pixel images with 16 gray levels. The scanner console is connected to a Mac IIcx capture board used for qualitative measurements and presentation purposes. The data files are transferred to the network via the DEC 5000/240 magnetic tape storage device and then to a Sun Sparc station fully dedicated to data and image processing of the scans. It is important to use the data files as efficiently as possible on these three hardware platforms.

1.2.3 PLANNED SOFTWARE GOALS

I will first describe the tasks to be performed by the planned software and then outline the work and schedule planned for this project.

1.2.3.1 Role of the Software

Once the scans have been made, the order of operations to extract quantitative values from the data is generally a three step process described as follows.

The first step is file and format manipulation. The CT scanner (an EMI 5005 of 1978 vintage) produces two kinds of data files that are hard to process. This problem is mainly due to the scanner's age. It is therefore necessary to convert these files to a more standard format. File manipulation includes the naming, removal, storing and compression facilities that are needed to handle the large number of files required for routine operation of the scanner. The proposed software will provide those services without using the Unix file system, which is too user unfriendly, and without the C language procedures for file handling, which is not well known by most petroleum engineers.

The second step is data computation. This process appears to be unique for each experiment, but some basic computations can be provided by the software. These include calculation of density, porosity and saturations for two and three phase experiments, and addition and subtraction of data between various scans. These calculations can be done for a whole file or for a

certain region of interest as often as needed. Some of these calculation routines already have been written by other researchers as stand alone applications, and these will be gathered within the new software to ease their use for newcomers. For calculation software that is not yet written, I will define a standard way to write interface and input- output functions in C or FORTRAN so that any new program modules can be easily incorporated into the software and can take advantage of the file management facility.

The third step is data and image processing including color 3D display, contour mapping and graphs. This step is generally done with a sophisticated high-level programmable tool kit such as IMSL/IDL (Interactive Development Language) . As such a tool kit is easy to use and powerful, it is a good idea to make sure that any new applications are built according to our specific needs but are also internally compatible. The IMSL/IDL offers a programmable language that will enable us to define a format for standard graphs and pictures. The CT interpretation software package will provided data files in a format readable by IMSL/IDL, and custom applications will be made within the tool kit.

1.2.3.2 General Features of the Software

The software will be built on a Unix platform and will use the OSF/Motif layer of the X Window Release 5 version. All dialogs will focus on the ease of use and provide comprehensive help. Interactive dialog will work according to OSF/Motif user interface recommendations so that the new applications fit well with the existing software environment. Because of the large number of files that are handled during each CT experiment, two working modes must be provided; one fully interactive, and one batch mode. Batch work can be launched from the software package and will carry a separate process identification number. The input and output file names will be taken from a specific file. The format of that file will depend on the operation to be performed. The software will provide a construction tool for each of these files.

1.2.3.3 Software Engineering Organization

The software is being developed using a Spiral life cycle, with three spirals (one for each step cited above). Each spiral will follow a V life cycle with a prototype phase. This prototype will be consolidated for the final version during the Design Phase. A single software requirement specifications document will be produced for the whole project. Then for each spiral three major documents will validate the different phases: (1) a software design description document, (2) a test design document, and (3) a user documentation. the software requirement specifications document will focus on two properties that the software must fulfill; portability and usability (as defined by IEEE).

1.2.4 PLANNED WORK FOR 1993

As the project started at the end of 1992, it is too early to determine the exact date for the testing of the first version. However, one can expect a working prototype by the end of the first quarter of 1993, and a "beta" working version at the end of the second quarter. A first working version should be available during the third or fourth quarter. The software should bring significant increase in computer use and will allow petroleum engineering researchers to be less involved in computer programming; thus they will be able to focus their work on the petroleum research, itself.

1.3. STEAM/WATER RELATIVE PERMEABILITY USING CAT SCANNER

(R. Holt)

1.3.1 INTRODUCTION

A new project is presently in its planning stages. The project will employ CT technology to study the relative permeability behavior of steam and water in geologic materials. Presently, equipment is being designed, and experimental procedures are being conceived. The relative permeability of steam and water is an important phenomenon in thermal oil recovery processes, in geothermal applications, and certain environmental clean up processes. The use of the CAT scanner makes it possible to track steam saturations in experiments where steam and water are flowing simulaneously within a core.

1.3.2 EQUIPMENT

Preliminary design considerations are as follows. A cylindrical core holder will be of length one foot and diameter 2 to 4 inches. The core holder will be placed in a vertical orientation. On the outside of the core holder will be one inch of an appropriate insulation, such as Fiberfrax. The core, then saturated with liquid phase water, will have steam injected at the top. Production will be collected at the bottom of the core. Data collected will be saturation distributions versus time (via CT number), production and injection versus time, and temperature and/or pressure profiles versus time.

1.3.3 PRELIMINARY SIMULATION

One concern is that due to heat losses the injected steam will travel down the center of the core creating a complicated 3-D steam front. Therefore, the steam displacing water situation described above was simulated numerically using TETRAD, a commercially available reservoir simulator. It was found that with either the 2 or 4 inch diameter design that heat losses are not expected to impact the experiments greatly, if at least one inch of Fiberfrax is used. In fact, with one inch of Fiberfrax, the heat loss is such a small fraction of the total heat injected that the experiments are virtually isothermal.

2.1. KINETICS OF IN-SITU COMBUSTION

(D. Mamora)

ABSTRACT

Experimental research has been carried out to investigate two parameters which are important in in-situ combustion: the nature of the fuel at the combustion zone, and the main factors that affect fuel deposition.

The previous kinetic and combustion tube experimental apparatus has been modified for greater accuracy in measurements and ease of operation. The main modifications are as follows. Equipment, fittings and lines common to both types of experiments have been integrated, minimizing redundancy and dead volumes. All instruments, gages and control valves have been mounted on panels, for ease of operation and monitoring. A gas chromatograph with an automatic gas sampler has been installed for measuring nitrogen concentration in the produced gas. A new, dual-thermowell system for the combustion tube has been fabricated, enabling one moveable and nine, stationary thermocouple measurements to be made. This enables fast temperature measurements to be made, high resolution of the temperature profile at the combustion zone and ease of operation. A new program on the personal computer has been created which controls not only data recording, but also plots on screen the critical data for ease of monitoring of the experiments.

A total of 14 kinetic and four combustion tube experiments have been carried out. Three crude oils have been used: Cold Lake bitumen (11.5°API), Huntington Beach oil (20.8°API) and Hamaca (Venezuela) crude oil (10.2°API). To investigate the nature of the fuel, kinetic runs have been made using carbon and a mixture of carbon and crude oil. In addition, elemental analysis, differential scanning calorimetry (DSC) and thermogravimetric analysis (TGA) have been conducted on selected crude samples. Based on the results of these experiments, the following conclusions can be made.

1. In combustion tube experiments, high combustion zone temperatures (about 500°C) are obtained when clay or fine sands (170–270 mesh) are present to provide a large reaction surface area. Consequently, almost all the injected oxygen is utilized at the combustion zone. Hence, hydrocarbons ahead of the combustion front do not undergo low-temperature oxidation (LTO). This results in atomic hydrogen-carbon (H/C) ratios which are only slightly lower than those of the original crudes. This also suggests that distillation is the main mechanism for fuel deposition.

2. In contrast, if there is no clay or fine sands, relatively cool burns (about 350°C) are obtained since the reaction surface area is reduced. A substantial amount of oxygen is present ahead of the combustion zone. This results in low-temperature oxidation of the crude oil to form an oxygenated hydrocarbon fuel.

3. In kinetic experiments, oxidation reactions take place in a medium containing abundant oxygen. Consequently, low-temperature oxidation of the crude occurs, which results in the formation of an oxygenated hydrocarbon fuel for high-temperature oxidation (HTO). Atomic oxygen-carbon ratios in the range of about 0.4 to 0.9 are inferred from these experiments.

Oxygen from the oxygenated hydrocarbon fuel takes part in the high-temperature oxidation reactions and has to be considered in the calculation of atomic H/C and m-ratios, where the m-ratio

is the molar ratio, $CO/(CO + CO_2)$, in the produced gas. This correction is done by carrying out the calculations on the basis of total gas volume. This new calculation method has enabled a direct comparison of atomic H/C ratios obtained from combustion tube and kinetic experiments (Table 2.1).

A new oxidation reaction model for kinetic experiments has been developed. An example of kinetic data analysis using the new model is illustrated in Figs. 2.1.1 – 2.1.6. These figures illustrate the following concepts. Fig. 2.1.1 shows the Arrhenius graph of HTO data: the crosses pertain to fuel which lies only in the toroids between the sand grains, while the circles include fuel deposited on the sand grain surface. When both fuel geometries are included, the data falls on a straight line trend over a broad range of temperature. The HTO activation energy is determined from the slope of this straight line. Based on this HTO activation energy, the fuel height as a function of time is calculated (Fig. 2.1.2). This result is used to calculate the oxygen consumption curve for HTO, shown by the solid line in Fig. 2.1.3. The LTO data (dashed line) is obtained by subtracting the calculated HTO curve from the experimental data. An Arrhenius graph of the LTO data is constructed, as shown in Fig. 2.1.4. A straight line can be drawn through the LTO data. From the slope of this straight line, the LTO activation energy is obtained. Based on this LTO activation energy, the LTO curve is calculated. The calculated LTO curve is shown as a solid line in Fig. 2.1.5. The calculated HTO and LTO curves are added to yield the total oxygen consumption curve which is indicated by the solid line in Fig. 2.1.6. The oxygen consumption curve based on the new model are in good agreement with experimental data.

The main differences between the new and previous oxidation reaction models for kinetic experiments are as follows.

New model	Previous model
a) Two reaction stages: low- and high-temperature oxidations.	a) Three reaction stages: low-, medium- and high-temperature oxidations.
b) Fuel is an oxygenated hydrocarbon.	b) Fuel is carbon.
c) Varying, reaction-surface area incorporated.	c) Reaction-surface area assumed constant.

A technical report on this research will be published in June, 1993.

Table 2.1.1: Comparison of H/C and m-Ratios

Crude	Mixture	Kinetics experiments: Old method H/C	Kinetics experiments: Old method m	Kinetics experiments: New method H/C	Kinetics experiments: New method m	Combustion tube expts. H/C	Combustion tube expts. m
Cold Lake bitumen	crude + 20-30 mesh sand	0.2	0.280	1.74	0.291	1.62	0.311
Hamaca crude oil	crude + 20-30 mesh sand	1.51	0.288	4.47	0.305	4.35	0.312
Hamaca crude oil	crude + 20-30 mesh sand + clay	0.00	0.264	1.81	0.274	1.63	0.298
Hamaca crude oil	crude + 20-30 mesh + 170-270 mesh sand	0.8	0.280	1.75	0.285	1.77	0.308

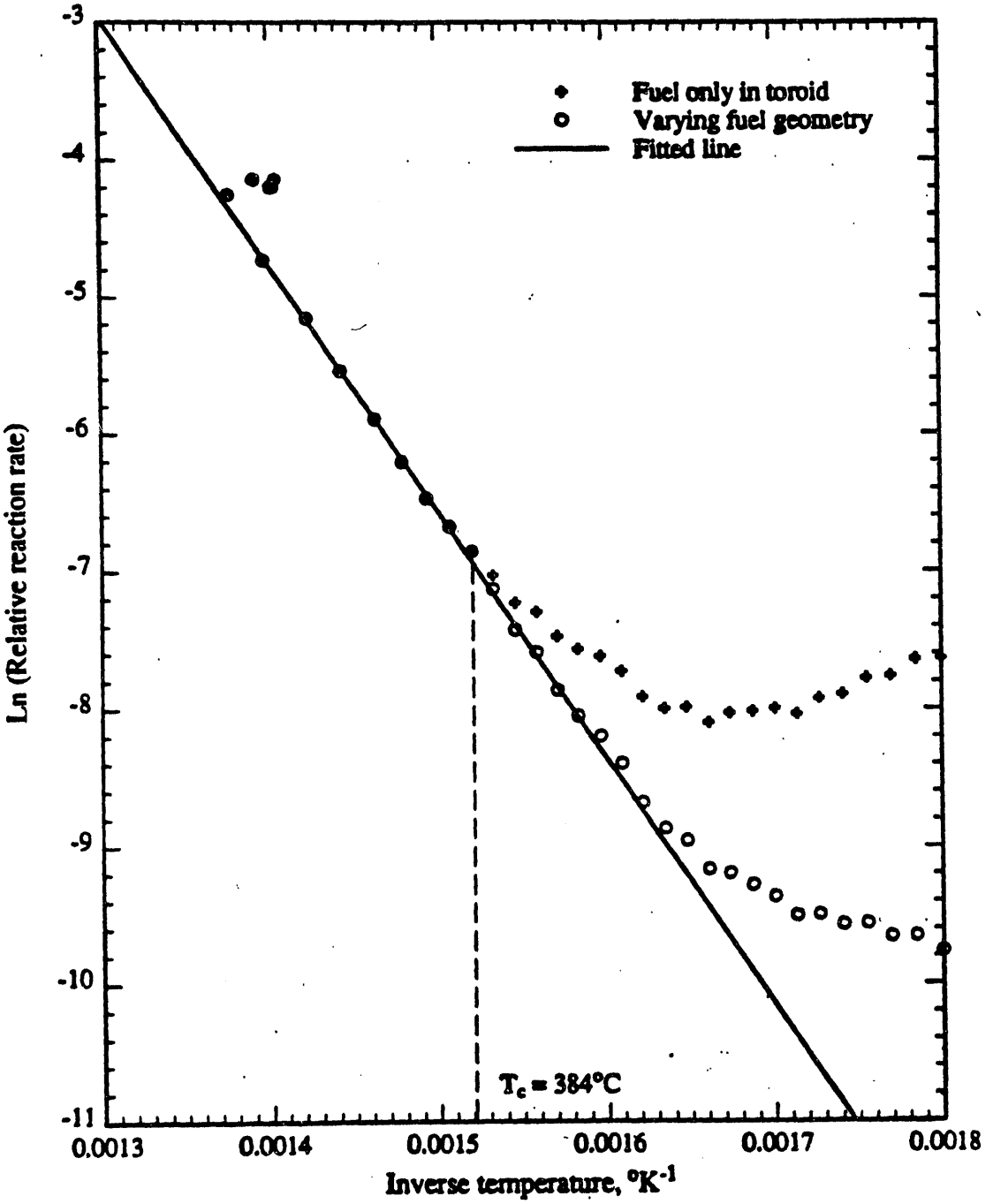

2.1.1 Arrhenius graph for HTO data (run no. CL5)

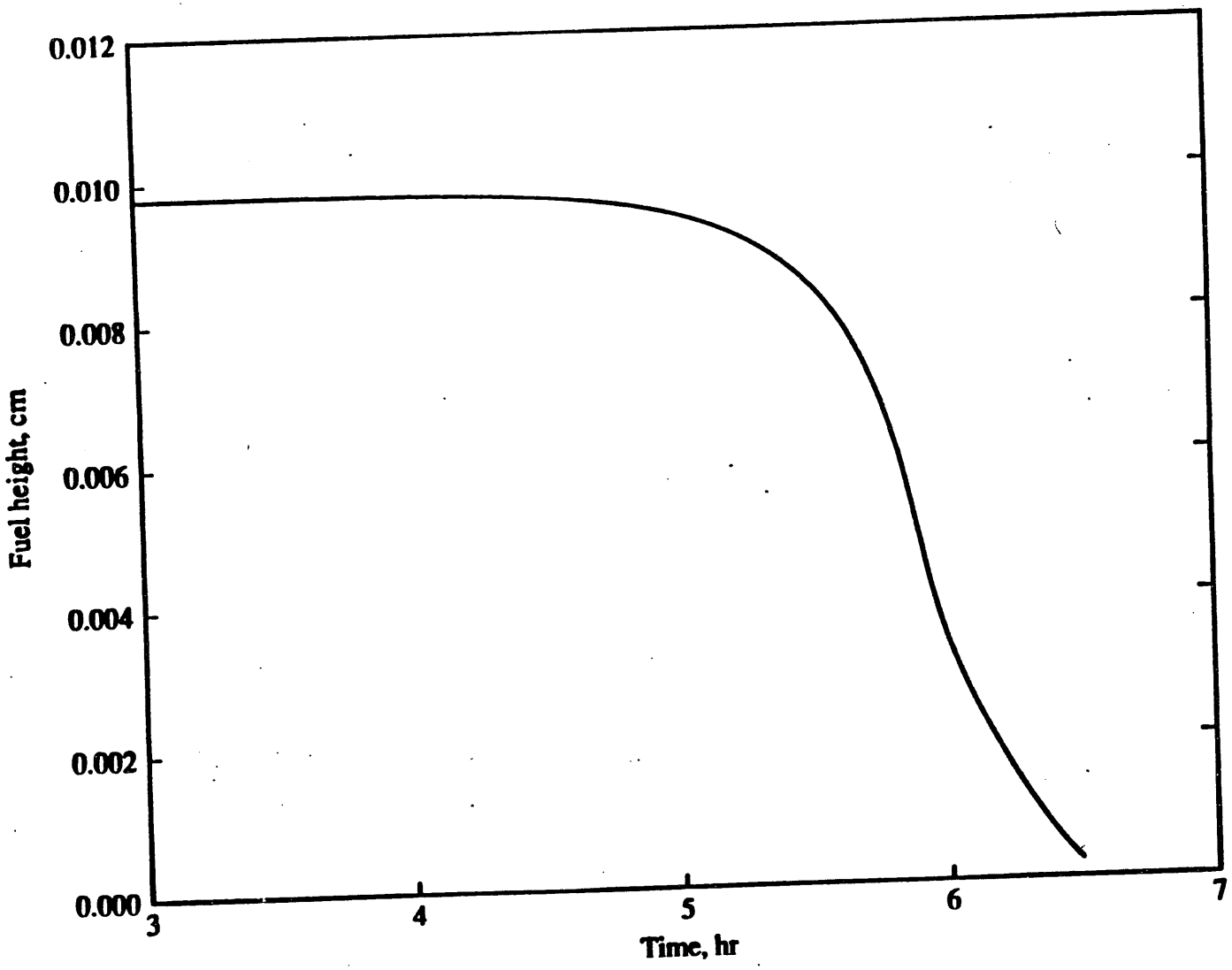

2.1.2 Fuel height versus time (run no. CL5)

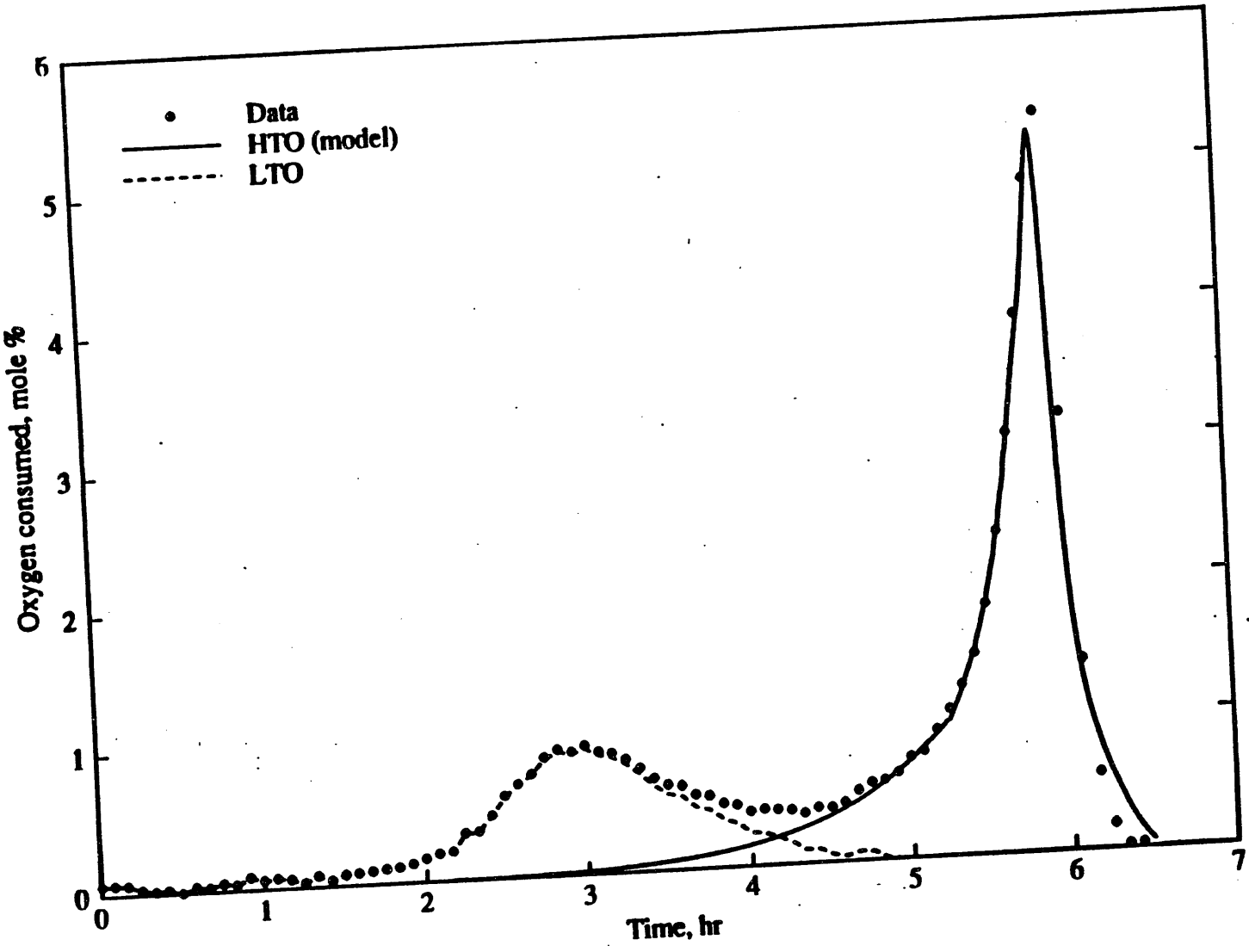

2.1.3 Oxygen consumption at HTO: model results and data (run no. CL5)

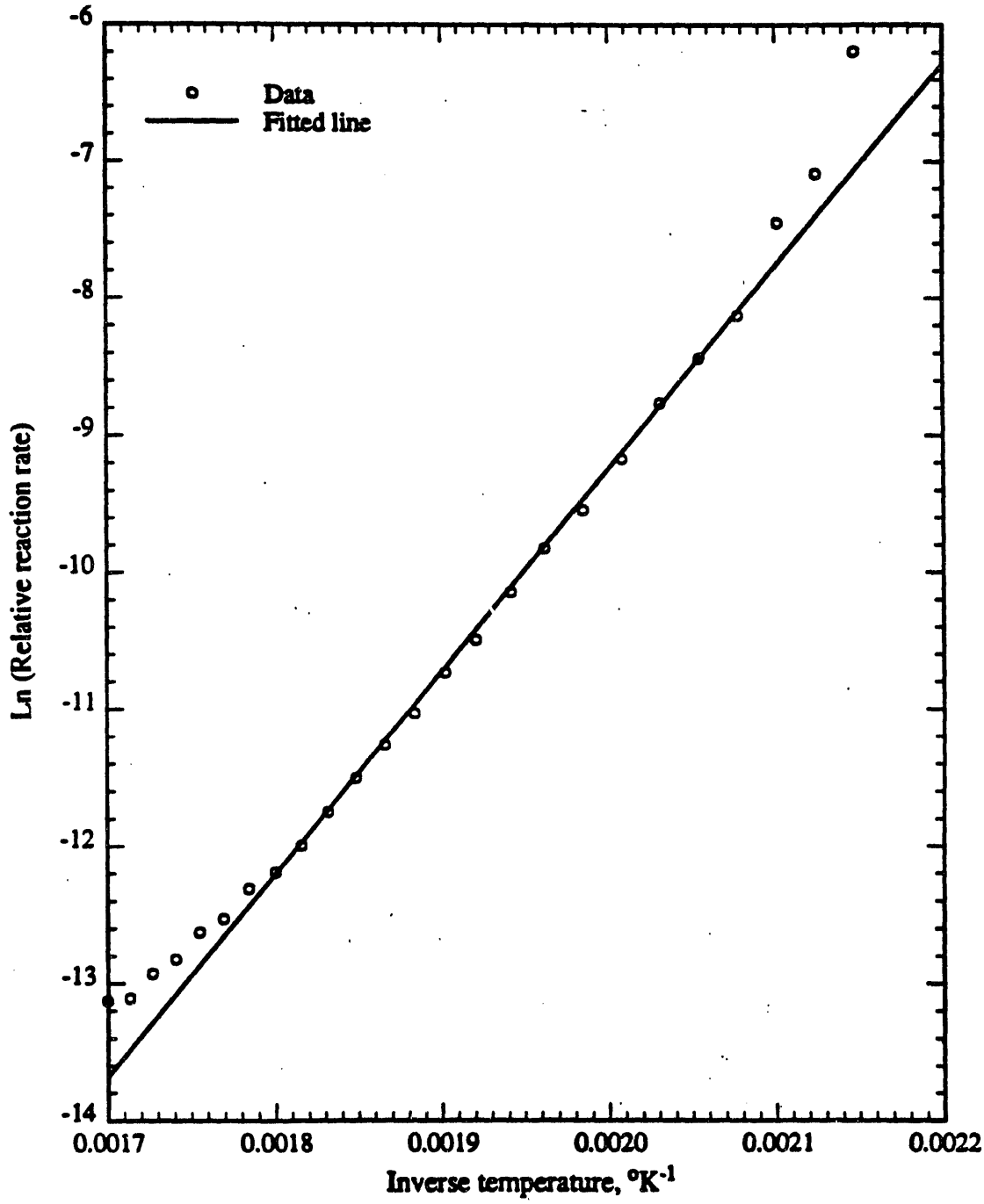

2.1.4 Arrhenius graph for LTO data (run no. CL5)

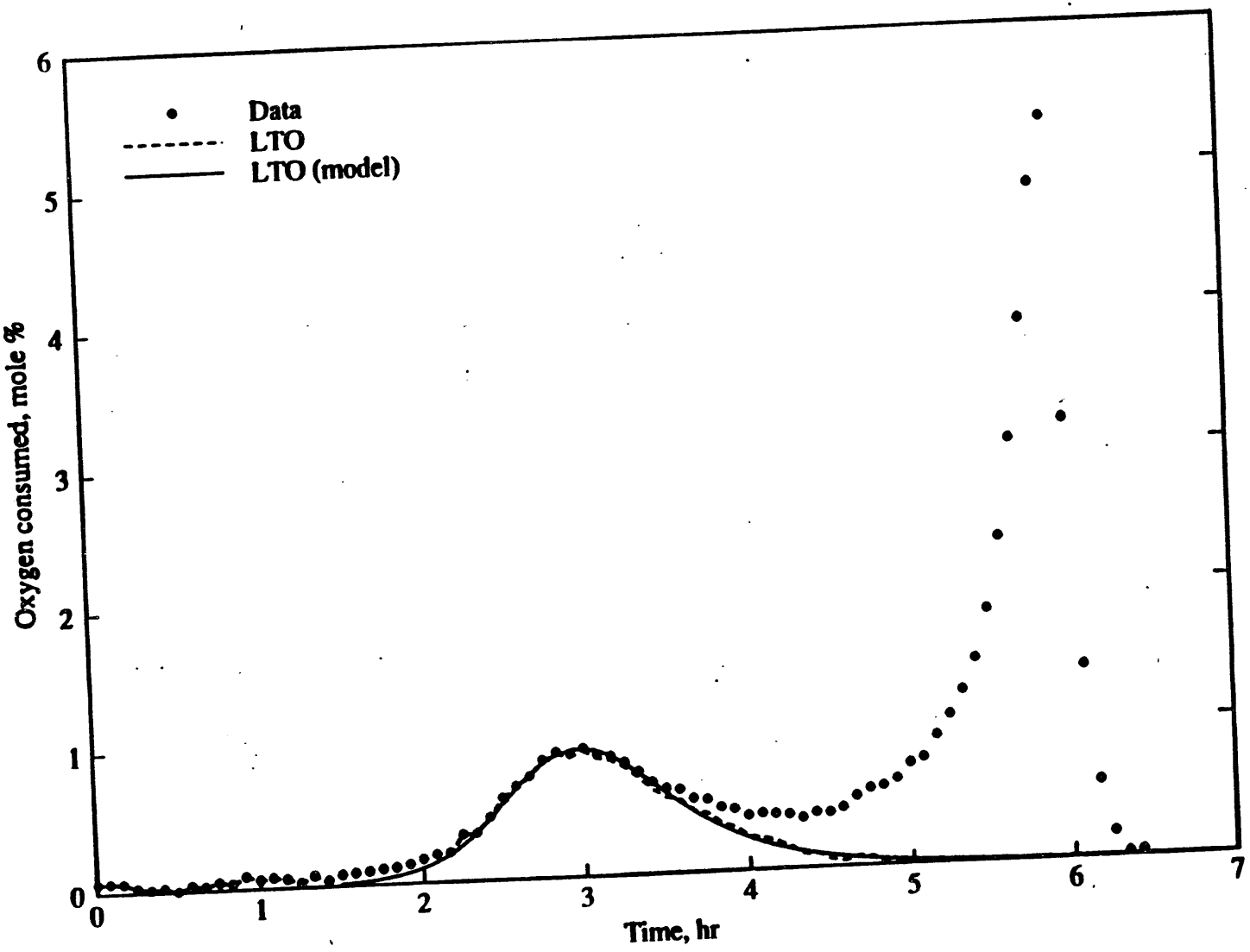

2.1.5 Oxygen consumption at LTO: model results and data (run no. CL5)

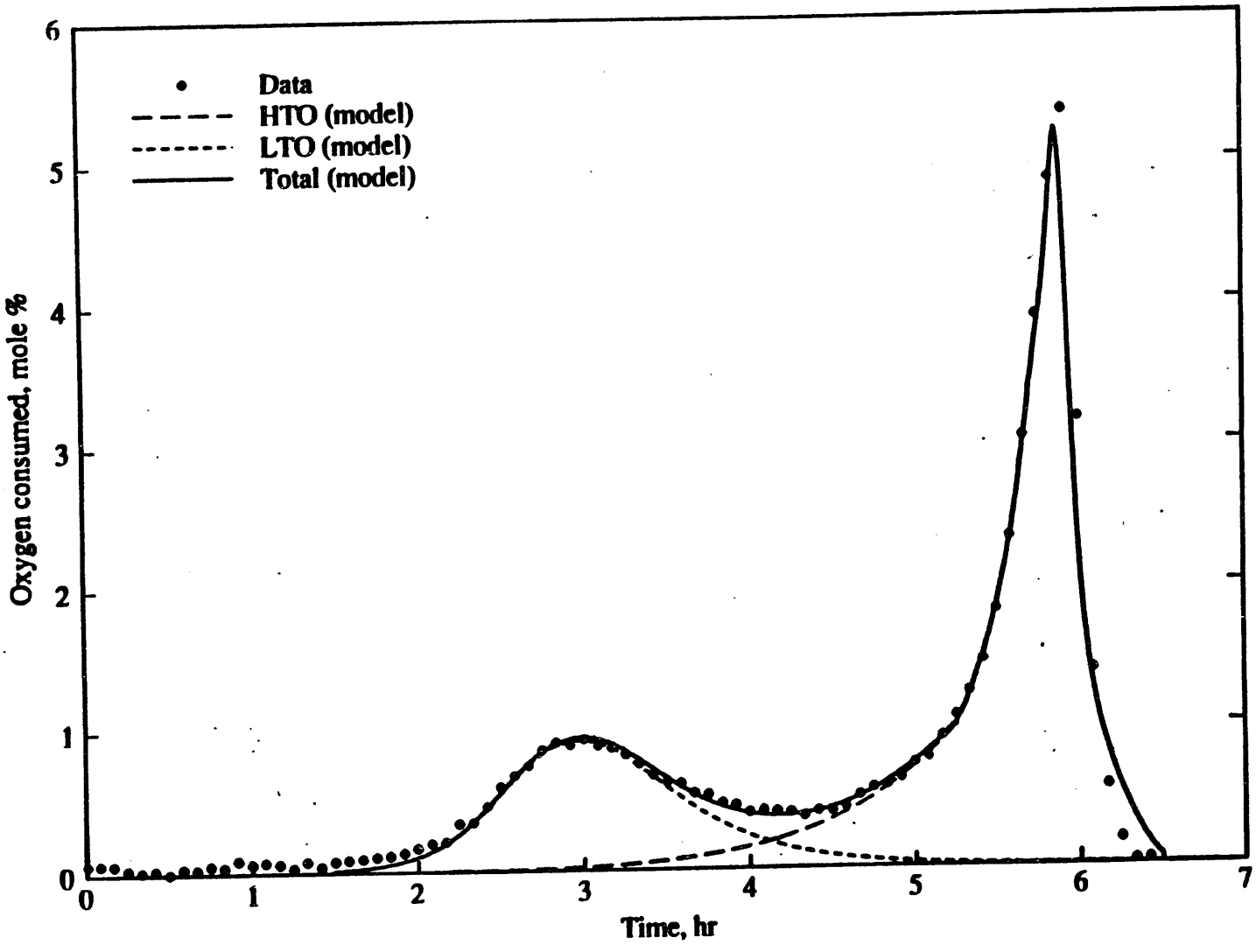

2.1.6 Oxygen consumption: model results and data (run no. CL5)

2.2. FORUM ON IN-SITU COMBUSTION

(L.M. Castanier)

This is a summary of notes received from participants in the AOSTRA/SUPRI In-Situ Combustion Forum held at Tulsa, OK, April 20-21, 1992. Fifty-two experts on the topic representing major oil companies, independents, research organizations and government reviewed the state of the art of the in-situ combustion technology both in terms of field results and laboratory research. A list of the participants is attached as an appendix as well as the technical program. The purpose of this summary is not to comment on the technical program but to present ideas on the past and the future for in-situ combustion and how, in the opinion of the forum participants, future work on this topic should be conducted.

These were some of the concerns of the forum:

1. Status of field projects, worldwide
2. Status of combustion research in industry and academia
3. Future research needs

2.2.1 STATUS OF FIELD PROJECTS

Currently, there are at least 10 projects in the U.S. producing at least 6,000 BOPD, down from 21 projects and 10,000 BOPD in 1986. From the Oil and Gas Journal, one can find the information listed in Table 2.2.1.

In summary, one must conclude that, currently, the oil industry has a minimum interest in fireflooding. Current world-wide production from fireflooding is probably less than 10,000 BOPD. By comparison, steam produces over a million barrels of oil per day. Except for the 1991 Santa Fe Energy pilot fireflood in the Tulare formation in the Midway-Sunset Field and the recent firefloods by Koch Exploration in the Red River reservoirs in North and South Dakota, all of the U.S. and Canadian firefloods are at least 10 years old. No new firefloods are presently being planned in the U.S. or Canada. No doubt there are firefloods being planned in other parts of the world, such as Indonesia. Activity in Russia and China are unknown but are felt to be small.

2.2.2 STATUS OF COMBUSTION RESEARCH IN NORTH AMERICA

Both industry and academia have limited combustion research activities, as outlined below.

2.2.2.1 Industry

The only known fireflood research that is being carried out by industry is being done by Amoco Production Research in Tulsa, Oklahoma through their Air Injection Consortium. Amoco is interested in conducting research for deep (to 10,000 feet), high pressure (up to 6,000 psi) reservoirs with the purpose of repressuring these reservoirs when they reach the mature stage. Currently, Koch Exploration is conducting fireflood field projects in deep reservoirs in North and South Dakota, without laboratory research. Interestingly, Koch is giving Amoco access to their data.

Table 2.2.1: Status of Field Projects

Company	Field	Reservoir	BOPD
USA: Current			
Bayou State	Main Consolidated	Nacatoc	420
Chevron*	W. Heidleberg	Cotton Valley	400
Greenwich	Forrest Hill	Harris	400
Mobil	Midway-Sunset	Moco	900
Mobil	West Newport	Miocene	980
Santa Fe	Midway-Sunset	Potter	700
Santa Fe	Midway-Sunset	Tulare	700
Texaco	Bellevue	Nacatoch	200
Koch Expl.*	Buffalo, SD	Red River	500+
Koch Expl.*	Medicine Pole, ND	Red River	500+
**using the repressuring of the reservoir as the main mechanism*			
USA: Shut-in			
Bayou State	Caddo Pine Island	Nacatoch	100
Cities Service	Bellevue	Nacatoch	600
Marathon	Main Consolidated	Robinson	80
Mobil	San Ardo	Aurignac	360
Mobil	South Belridge	Tulare	400
Mobil	Lost Hills	Tulare	520
Unocal	Brea-Olinda	Miocene	300
Canada: Current			
Amoco	Lindbergh	Cummings	-
Amoco	Morgan	Lloydminster	940
BP/PetroCanada	Wolf Lake	Clearwater	-
Mobil Oil	Battrum	Battrum/Roseway	3800
Mobil Oil	Battrum	Battrum/Roseway	1600
PanCanadian	Countless	Upper Mannville	-
PanCanadian	Countless	Upper Mannville	-
Canada: Shut-in			
Husky	Tangleflags	GP	550
Mobil Oil	Kitscoty	Sparky	600
Mobil Oil	Fosterson, NW	Roseway	50
Murphy	Evehill	Cummings Waseca	350
Hungary: Shut-in			
MKFV	Demjen East	Oligocene	60
Romania: Current			
PETROM	Balaria	-	100
PETROM	Videle, East	-	100
PETROM	Videle, West	-	100

Others:
Firefloods in other countries are not known but China and the CIS may have some field projects.

2.2.2.2 Academia

The University of Calgary (UC) conducts extensive (several million dollars per year) in-situ combustion research, including kinetics and tube test runs at pressures up to 3,000 psi. UC designs projects for independents. Stanford University conducts research in combustion tubes and also in kinetics cells, which has funding of about $100,000 per year. Stanford tube runs are currently limited to 500 psi.

No other university or research organization in North America conducts research on in-situ combustion, to our knowledge. One of the objectives of the forum was to suggest means to improve research and field applications of this process.

2.2.3 MAIN PRIORITIES FOR FUTURE RESEARCH

This section deals with possible directions for research by academia, government support and industry contribution, as suggested by the participants in the meeting.

2.2.3.1 How Can Universities Contribute to In-situ Research?

Identify major chemical reactions taking place during combustion. Prioritize and rank the importance of each. Assess effects of minerals and matrix on the combustion process and low temperature oxidation) L.T.O.

A "state-of-the-art" manual or analysis and review paper should be written by an unbiased researcher to establish what is known (and what is still not understood) about the kinetics and mechanisms of the combustion process for oil recovery. This should emphasize the mechanisms and kinetics rather than the engineering design and/or operation of the process.

Assess kinetics of combustion for crudes of various API gravities. Determine what is the chemical composition of the fuel and the kinetics of the reactions involved for the components identified as major contributors to the process. What is the energy delivered in each case?

Determine combustion ignition and process efficiency for crudes of a variety of API gravities to establish low and high limits, and changes in the process due to different mechanisms occurring as a function of crude oil composition and characteristics.

Incorporate basic research results into numerical simulation in order to better understand and/or evaluate the sensitivity of the controlling mechanisms.

Develop numerical models that can follow fronts, either with fine moving grid blocks or by other appropriate numerical means.

Determine the advantages/disadvantages of enriched oxygen over air in a variety of conditions.

Conduct basic research to improve formation evaluation methods to better understand reservoir heterogeneities, with the ultimate goal to improve conformance. A long term goal is to determine how to maintain a uniform supply of oxygen to a front for combustion in heterogeneous reservoirs.

2.2.3.2 What Incentives Should Governments Offer?

Equal match programs are good incentives. They should be limited, however, for the tax payer should not be responsible for making oil recovery economic. A secure energy source should have a valid price, however, and the government needs to develop a consistent policy to decide what range this should be. The important operating word is "consistency".

Encourage DOE to support (matching funds) field tests for application to specific types of reservoirs, or specific situations (tertiary after waterflood, etc.). These projects should be ranked on technical merit and difficulty only. Industry and universities should help with the rankings.

Develop a "state-of-the-art" manual-type document for distribution by DOE, slanted primarily at independents operating in the U.S.A. This manual would emphasize practical engineering design and operating techniques.

Encourage DOE to develop a "Consulting Bureau" or "Advisory Engineering Group," or some such technical group to advise or do the engineering and laboratory work necessary, for independent operators who wish to use, or consider using, in-situ combustion as an EOR tool.

Encourage DOE to promote workshops (annually? every two years?) that would be slanted more at independents than majors, but to which majors will be cheerfully invited.

Involve the Interstate Oil Compact Commission in the process of preserving the technology because of their interest in maintaining resources.

Promote, or arrange, field trips to currently operating in-situ combustion projects, perhaps in conjunction with CIM, SPE, AOSTRA, or UNITAR sponsored technical conferences.

Encourage the Canadian government to continue price support, royalty relief, etc. of field tests of such projects. Consider a similar scheme for the U.S.

2.2.3.3 What Should be Done by Industry to Further In-Situ Combustion Field Projects?

Test new ideas for better control of the "burn front", and have dedicated personnel conduct these tests for better chance of success.

Optimize contact area and minimize by-passing, override, fingering, etc. This is only possible if design and operations of field projects are based on good reservoir knowledge.

Establish means to mitigate the corrosion and erosion that are two of the main operating hurdles in in-situ combustion. Solve the severe emulsion problems associated with in-situ combustion production.

Establish acceptable monitoring and field procedures for compliance with EPA requirements; for example, the clean-up the produced gases.

Investigate methods of completing wells or improving wells so they can withstand high temperatures associated with this process.

Engineering to reduce capital/operating costs.

Develop generic process optimization scenarios or programs.

Develop process control schemes. Define specific needs and solutions.

2.2.3.4 Specific Research Topics Related to Combustion

This section deals with ideas on specific types of unusual reservoirs or improved oil recovery methods that could be investigated by researchers also working on combustion.

1. **Light Oils**

   This topic was identified as a priority by many participants, as indicated by the following suggestions.

   - Continue research investigating fuel laydown, or coking, by catalytic or other means using additives.
   - Determine the rate of frontal advance and the rate of oil bank movement for light oil cases to determine if the oil is chased ahead of the front before fuel laydown is possible. Determine if there is a correlation with API gravity, and a gravity beyond which the process is no longer possible.

- At higher injection pressures the in-situ combustion process has the reported ability to recover 25-35 °API oils. Research this range of applicability and verify the assumption. Extend research range to include lighter crude oils, to API gravity over 40°. Determine what are the specific limitations to the use of in-situ combustion for the recovery of light crude oils as a function of their composition.

2. Tar Sands

- Can a burn front be propagated in a direction normal to a fracture face? Perhaps the air would propagate through the fracture in a forward combustion mode and the matrix contribution to the recovery would be in a reverse combustion mode.
- Would the fracture have to be "propped" in Conoco's FAST steam process? More basically, can a burn front be propagated toward the fuel source by an oxygen supply flowing normal to the "burn" front?

3. Horizontal Wells

- The combustion process in thick reservoirs depends heavily on gravity drainage. Horizontal wells strategically located in the lower portion of a stratum could prove very beneficial. Research that idea in the laboratory and with proper numerical simulation techniques.
- Establish how horizontal wells should be used for the application of in-situ combustion as one of the primary EOR recovery processes in difficult oil fields as a means to assist the process of heating and mobilizing the oil (e.g., very heavy crude oils or tars).

4. Tertiary or Quarternary Applications

This work will depend on the amount of oil remaining in the reservoir at the start of combustion. Like any thermal recovery method, combustion is only possible when the ϕS_o of the reservoir considered is over a certain minimum.

- What is the limiting oil saturation and porosity that would prevent in-situ combustion from being used as a tertiary process?
- Can in-situ combustion be used to follow waterflooding? Are there any limiting water saturations above which the process would always be quenched?
- Can the "sweep" of an in-situ combustion process be controlled (or diverted by foam, etc.) to recover oil from the unswept regions of a successful waterflood? Extending this idea, can a control procedure be used to recover the residual oil saturation left in the zones swept by a waterflood?
- Can in-situ combustion be used following steamflooding to recover oil from a zone that had override?

2.2.3.5 Other Priorities

The personnel who have had experience in fireflooding, both laboratory research and field tests, are now "senior citizens." Within the next few years, many of these experts will be no longer be with us. It appears that some method should be found to record their experiences and transfer existing technology to younger generations.

One such method would be to hold are In-situ Combustion Forum every few years and publish the Proceedings. Another, would be for DOE to fund a project to pick the brains of these "old experts" and summarize this knowledge as a DOE publication.

2.2.3.6 Stanford View on Priorities

The above paragraphs were a summary of suggestions made by the participants in the forum. Although most of the suggestions seemed well worth pursuing; some, in the view of the Stanford participants, are inappropriate, or require some modification.

1. The suggestion was made that a monograph or an analysis and review paper be written on combustion by a university team. Although this work is worth doing, it seems more appropriate that it be done by a knowledgeable professional outside the university environment.

2. Field experience of successful fire floods show that they all had gravity override. The secret to their success was to recognize this fact and allow the reservoir to control the process. Thus suggestions to reduce override are not appropriate. Also, under this operating scenario, emulsion problems are not severe, nor are high temperature producing wells. Further, since the reservoir dictates the flow behavior, it is not appropriate to try to control sweep efficiency.

3. A number of suggestions related to combustion after other processes: tertiary after waterflood, combustion of light oils after other processes have been used, looking at applicable limiting water saturations, and combustion following steam flooding. All of these can be grouped into a single question – what is the present ϕS_o product in the reservoir? This is the primary term defining whether combustion is an appropriate recovery process to consider, virtually independently of other variables.

4. Numérical simulation is a very important problem that needs to be addressed, and it is quite difficult because of the very large grid block dimensions needed for numerical simulation, and the very small dimensions of the burn front when the heat is generated.

5. Combustion in tar sands is a completely different problem than in light of heavy oils. The tremendous difference in the mobility of the tars forces entirely different thinking on how to operate these systems.

2.2.4 CONCLUSIONS

The main conclusions reached were:

1. In-situ combustion is a viable EOR process for both heavy and light oil reservoirs with the number of new projects tied directly to the price of oil.

2. New projects will most probably use repressuring of the reservoir plus gravity drainage for recovery rather than pattern flooding.

3. The current research now being conducted at Stanford University on the kinetics of in-situ combustion and tube runs should be continued as well as the research performed at the University of Calgary. There will only be a few new field projects as long as the price of oil remains low.

4. At any rate, for heavy oil reservoirs where steam flooding is economically marginal today, fireflooding is the only available alternative.

5. Fireflooding, using oxygen as the fuel, has considerable potential for deeper reservoirs. The technology has been designed to supply oxygen safely and routinely.

6. Combustion producing wells should be pumped off in order to take advantage of gravity drainage.

2.2.5 APPENDIX

Why is Combustion Less Popular Than Steam?

The literature, which was quite prolific over the last forty years, indicates a sharply increased interest in in-situ combustion until the seventies followed by an equally sharp decline, in favor of steam injection. So, we witness combustion competing against steam. This competition should become more open with each method having a chance to be chosen, provided both methods are well understood. The final decision should be based on economic criteria. In this discussion, we will try to look at the assets and weaknesses of each method.

2.2.5.1 General Comparison "Steam vs. Combustion"

Combustion and steam injection have different strengths and weaknesses from an operating point of view. The strengths of each are summarized here.

1. The assets of continuous steam injection (steam drive) over in-situ combustion:

   - Simpler on the whole regarding: feasibility studies, preliminary preparations, experiments, and control methods.
   - Applicable to thicker formations.
   - Low corrosion effects.
   - Quicker response time, hence a more rapid payout.
   - Flexibility in shutting-in and reopening wells, in accordance with the operator's schedule.
   - Easier to operate on a routine basis

2. The assets of in-situ combustion over steam flood:

   - More efficient overall drive mechanism.
   - Less sensitive to permeability variations and water saturation values.
   - Wider applicability range as regards thickness and specific gravity.
   - No heat loss in wellbores and transportation lines, and lower reservoir heat losses, thus it is applicable to deeper reservoirs.
   - Less energy consumption.
   - Less total pollution.
   - No danger of mineralogical incompatibility with the rock.
   - A significant number of naturally flowing wells.
   - Better efficiency in reservoirs with low natural energy, and gravity drainage.

2.2.5.2 Discouraging Factors for Combustion Compared to Steam

From the above, the score seems to be in favor of combustion. And yet, in real life it is the other way around. Why? Here are the discouraging factors in order of their significance.

1. More engineering effort is required for in-situ combustion than for steam.

   More difficult technical, operating and control problems including coke deposition near wellbore and corrosion; more complex monitoring is required, with more people, also more equipment, hence more money; but these could be compensated for by a higher recovery.

2. Combustion leads to a moderate or even low rate of return.

   This problem is mostly caused by the fact that combustion tests have been run on poorer quality reservoirs than steam projects. Economics studies done on reservoirs such as Belridge where both steam and combustion were tried in about the same conditions show very similar rates of return for both methods. (See Williams and Ramey, 1981, and Ramey et al., 1986, for example.)

3. Failures arise in reservoirs with unfavorable characteristics

   Too high oil viscosities, or permeabilities below the minimum admissible value. In August 1991, at "The Fifth UNITAR Conference on Heavy Crude and Tar Sands," in Caracas a U.S. representative pointed out that, "most of the projects that have failed in the US. were attempts at 10,000 to 50,000 cp.; the fluid was basically immobile, and combustion has a very difficult time there. So, it's the application of the process in the right reservoirs, if you're to be successful." One additional point to make here is that low initial oil saturations before the start of the combustion often caused failures in the early tests.

   It is likely that many of these failures have not been reported, but they have discouraged the operators. We think one of the important issues in the future should be a more detailed definition of the criteria for the selection of reservoirs lending themselves to in-situ combustion.

4. Computer simulation is difficult.

   For conventional methods (such as waterflood), computer simulation enjoys a long, well established tradition, with satisfactory matchings of field data. On the contrary, in-situ combustion is considerably more complex and much less applied. Although correlations exist to predict in-situ combustion recoveries, no computer model has shown reliable predictive capability for this process. Significant differences exist between the laboratory results or the computer simulation on the one hand, and the real data obtained from the field, on the other hand. This is a deterrent for the managers of oil companies, for economic decisions must take into account uncertain predictions of oil recovery.

NOTE: See Appendix A for Agenda and List of Attendees

3.1. STUDY OF STEAM INJECTION IN FRACTURED SYSTEMS

(M. Deniz Sumnu-Dindoruk)

3.1.1 INTRODUCTION AND LITERATURE REVIEW

This report summarizes the progress in the research project "Study of Matrix-Fracture Transfer in Steam Injection". The first part of the report consists of a brief literature review. The second part is a summary of numerical studies, experimental design and accomplishments. Finally, the report concludes with the planned future work.

Several fracture flow models have been developed in the literature for modeling flow in fractured media for isothermal processes. The models used in thermal simulators are usually the extensions of those models to thermal processes.

Generally, the models can be classified into two groups, dual porosity and dual permeability models. These models will be discussed in the following sections.

3.1.1.1 Dual Porosity Models

All of the dual porosity models assume that fractures constitute the main path for fluid flow, and matrix blocks act as sources or sinks to the fracture network.

Basic double porosity model

In this model, matrix and fracture communicate through a single exchange term in the flow equations. Neighboring blocks are connected through fracture flow only. Fluid or heat inside the matrix can be transfered only to the fracture, and fracture and matrix within a grid block are at the same depth neglecting gravitational effects.

Kazemi et al. (1976) developed a 3-dimensional, 2-phase model to simulate flow in a fractured system. In their model, oil from matrix blocks flows into fracture space, and is carried to the wellbore by the fractures. Water may imbibe into the matrix blocks to displace oil. The simulator equations are two-phase extensions of the single-phase flow equations derived by Warren and Root (1963).

Thomas et al. (1983) developed a model for 3-phase flow in fractured systems. Their matrix-fracture transfer function is also based on an extension of the equation developed by Warren and Root (1963), and assumes one dimensional horizontal flow between block centers of the matrix and the fracture.

Multiple interacting continua model

In this model, the matrix is divided into nested volume elements which communicate with each other. The model was first used in geothermal reservoir simulation by Pruess and Narasimhan (1985). This model assumes transient flow of fluid and heat between matrix and fracture. The flow domain is partitioned into computational volume elements such that all interfaces between volume elements in the matrix are parallel to the nearest fracture face. Heat is transfered from the matrix to the fracture by means of fluid convection and heat conduction.

Gilman (1986) applied this model to the simulation of hydrocarbon reservoirs. In his model, the matrix blocks are represented by several subdomains in a given grid block. The model is used to show gravity segregation effects in the matrix. The representation of matrix blocks by several

subdomains enabled him to simulate the transient flow in individual matrix blocks. These domains can be connected to one another and/or to the fracture. A gravity term is added to the matrix-fracture transfer function.

Pruess and Wu (1989) developed a semianalytical model to simulate matrix-fracture transient flow. In their dual porosity approach, the flow in the system is considered to occur only through the network of interconnected fractures and rock matrix, and fractures may exchange fluid and heat locally (interporosity flow). A new approach was developed to deal with transient interporosity flow. The idea is to describe fluid and heat exchange between matrix blocks and fractures by semianalytical means using simple trial functions for temperature and pressure distributions in the matrix blocks.

3.1.1.2 Dual Permeability Models

The other major model for fractured systems is the dual permeability model, which also takes into account flow in matrix, incorporating matrix-matrix transfer into the material and heat balances (Hill and Thomas, 1985, Lee and Tan, 1987, Gilman and Kazemi, 1987 and Chen et al., 1987).

Material and heat balance equations used in fractured reservoir simulators can be written as follows (Chen et al., 1987).

Mass balance for matrix:

$$\nabla \bullet \left[k \sum_{l=1}^{n_p} \frac{k_{rl}\rho_l}{\mu_l} x_{il} \nabla \Phi_l \right]_m - \sum_{l=1}^{n_p} x_{il}\rho_l q_{m,f,l} = \frac{\partial}{\partial t} \left[\phi \sum_{l=1}^{n_p} x_{il}\rho_l S_l \right]_m \quad i = 1, \cdots, n_c + 1 \tag{3.1.1}$$

Energy balance for matrix:

$$\begin{aligned} \nabla \bullet \left[k \sum_{l=1}^{n_p} \frac{k_{rl}\rho_l}{\mu_l} h_l \nabla \Phi_l \right]_m + \nabla \bullet (K_T \nabla T)_m - \sum_{l=1}^{n_p} h_l \rho_l q_{m,f,l} - (\theta_{hl})_m \\ = \frac{\partial}{\partial t} \left[\phi \sum_{l=1}^{n_p} \rho_l S_l U_l + (1-\phi)\rho_r U_r \right]_m \quad i = 1, \cdots, n_c + 1 \end{aligned} \tag{3.1.2}$$

Mass balance for fracture

$$\nabla \bullet \left[k \sum_{l=1}^{n_p} \frac{k_{rl}\rho_l}{\mu_l} x_{il} \nabla \Phi_l \right]_f - \sum_{l=1}^{n_p} x_{il}\rho_l q_{m,f,l} + \sum_{l=1}^{n_p} x_{il}\rho_l q_l = \frac{\partial}{\partial t} \left[\phi \sum_{l=1}^{n_p} x_{il}\rho_l S_l \right]_f \quad i = 1, \cdots, n_c + 1 \tag{3.1.3}$$

Energy balance for fracture

$$\nabla \bullet \left[k \sum_{l=1}^{n_p} \frac{k_{rl}\rho_l}{\mu_l} h_l \nabla \Phi_l \right]_f + \nabla \bullet (K_T \nabla T)_f - \sum_{l=1}^{n_p} h_l \rho_l q_{m,f,l} + \sum_{l=1}^{n_p} h_l \rho_l q_l - (\theta_{hl})_f$$
$$= \frac{\partial}{\partial t} \left[\phi \sum_{l=1}^{n_p} \rho_l S_l U_l + (1-\phi)\rho_r U_r \right]_f \quad i = 1, \cdots, n_c + 1 \tag{3.1.4}$$

where,

h_l	enthalpy of phase l
k	absolute permeability
k_{rl}	relative permeability of phase l
K_T	thermal conductivity
n_c	number of hydrocarbon components
n_p	number of phases
q_l	injection or production rate of phase l
$q_{m,f,l}$	volumetric flow rate of phase l between matrix and fracture
S_l	saturation of phase l
U	internal energy
x_{il}	mole fraction of i^{th} component in phase l
θ_{hl}	heat loss to the strata
μ_l	viscosity of phase l
ρ_l	density of phase l
Φ_l	potential of phase l

The important term in these equations for this study is the matrix-fracture flow term ($q_{m,f,l}$) which is not fully understood for nonisothermal processes .

3.1.2 OBJECTIVE

Steps to be followed in this research are:

- Fine grid simulations will be performed with a commercial thermal simulator to understand the flow behavior and to help design the experiment.
- A fractured model experiment will be constructed and steam injection experiments will be performed.
- A matrix-fracture transfer function will be developed based on the experimental runs. This will be achieved by matching the experiments with a double porosity simulator using the developed functions.

3.1.3 SIMULATION RUNS

Simulation runs for the experiment were done by using Computer Modelling Group's STARS thermal simulator. The grid system used in the simulations is given in Fig. 3.1.1 and the simulator parameters are shown in Table 3.1.1.

One of the most important parameters in the experimental design is the steam injection rate. To understand the effect of injection rate, four rates were used in the numerical experiments. Figure 3.1.2 shows the oil produced as a function of steam injected at different flow rates. Higher oil recovery is observed with lower steam rate, and a steam zone was observed even at the lowest rate. All of the rates are within our pump limitations.

Pressure distribution in the system during a run is shown in Fig. 3.1.3. The spatial variations in pressure are quite small, indicating the range of pressure transducers that should be used in experiments. More accurate pressure transducers are required to detect these small changes. Knowledge of the expected pressure variations is also crucial in the choice of core holder material.

Another set of simulation runs were made to understand the effects of capillary pressure in fracture and matrix. Fig. 3.1.4a shows that matrix gas-oil capillary pressure has no effect on the oil recovery. On the other hand, water-oil capillary pressure affects the oil recovery dramatically. (Fig. 3.1.4b) Due to water imbibition and displacement of oil by water, oil recovery is increased. The oil and water saturation maps given in Figs. 3.1.5b and 3.1.6b also show movement of the water inside the matrix and displacement of oil by water due to capillary forces, compared to virtually no movement when capillary pressure is zero, Figs. 3.1.5a and 3.1.6a.

Figures 3.1.7a and 3.1.7b show the effects of fracture water-oil and gas-oil capillary pressure. Fracture water-oil capillary pressure decreases water imbibition, and, therefore, oil recovery. Fracture gas-oil capillary pressure increases the oil recovery significantly due to the flow of the gas into matrix, decreasing oil viscosity. The increase of gas saturation in the matrix can be seen in Fig. 3.1.8b compared to Fig. 3.1.8a. More runs will be performed to look at different rates and sensitivities of different capillary pressure combinations at different rates.

Another important design parameter, that can be determined from simulation runs, is the injection/production scheme for cleaning the model. Cleaning the model is essential after each experiment to obtain the same initial saturations. To determine the locations of the cleaning wells, a set of runs were made with the black oil simulator, ECLIPSE. Mineral spirits are injected into the system to displace oil. The pseudo-miscible option of ECLIPSE is used for the cleaning problem. Several injection/production schemes were tested. Figure 3.1.9 shows the cumulative oil removed due to solvent injected for two different injection/production schemes. These schemes are shown schematically in Fig. 3.1.10. Figure 3.1.11 shows the effect of completion locations. These figures show that the best injection/production combination is to use four injectors and one producer, with production from the middle layer, keeping the injector completions fixed. Two of them are completed at the top and two at the bottom of the model. More runs will be performed to look at different combinations of completion locations.

3.1.4 EXPERIMENT DESIGN

The core holder design was worked out so that heat losses and fluid control could be integrated and incorporated into the experimental system, as discussed in some detail in the next section.

3.1.4.1 Heat Transfer Calculations

Both steady state and transient heat flow calculations were made to help in designing the experimental system.

Steady State Heat Transfer

In any steam injection run, maximum heat loss should be calculated to determine the minimum insulation thickness needed to assure that the steam zone will develop at the minimum planned steam injection rate. The assumptions used in the steady state heat loss calculations are,

- Both the rock and fracture are at steam temperature. ($140°C$)
- The ambient temperature is $20°C$.
- There is conductive heat transfer between the layers of insulation and convective heat transfer between insulator and air .
- Steady state heat transfer is assumed. The heat loss calculated will be the maximum steady state limit during a steam injection run.

The model consists of 2 different layers. The first layer is a polysulfone coreholder which has a fixed thickness of 1.5 cm. The second layer is the Fiberfrax insulation, the thickness of which should be determined based on the heat loss calculations. A polycarbonate layer behind the polysulfone was not considered in these calculations, to produce the maximum heat loss possible.

Since the model is not one dimensional, the shape factor should be incorporated in the heat loss formula. The heat loss formula is given by,

$$q = K\Delta T \tag{3.1.5}$$

where,

q	heat loss per unit area
K	thermal conductance of the system
ΔT	overall temperature difference

The shape factor for a parallelepiped shell is used in the calculations as given by Rohsenow and Hartrett, 1973.

$$K = k\left[\frac{S_1}{\delta} + 2.16(a+b+c) + 1.20\delta\right] \tag{3.1.6}$$

where,

k	thermal conductivity
S_1	total inner surface area of the shell
δ	thickness of the shell

and a,b and c dimensions are shown in Fig. 3.1.12.

Figure 3.1.13 shows the heat losses calculated at different injection rates for different insulation thicknesses. Since low rates will be used in the experiment, a Fiberfrax thickness of at least 1.5 cm is needed to overcome the heat loss at the lowest rate of 1 cc/min.

Transient 1-Dimensional Heat Transfer

To determine the time at which steady state is reached, the one-dimensional transient heat conduction equation is solved for a three layer composite insulation system. The schematic drawing of the problem is given in Fig. 3.1.14. In this system, the first layer is polysulfone with a thickness

of 1.5 cm, the second layer is polycarbonate of the same thickness and the third layer is Fiberfrax with a thickness of 2 cm.

The equation describing the conductive transfer of heat in this system is given by,

$$\frac{\partial^2 T}{\partial x^2} = \frac{1}{\alpha}\frac{\partial T}{\partial t} \tag{3.1.7}$$

The equation and the boundary conditions can be put into dimensionless form by defining the dimensionless variables as follows. Selecting the first layer as reference layer,

$$\alpha_{Di} = \frac{\alpha_i}{\alpha_1} \tag{3.1.8}$$

$$k_{Di} = \frac{k_i}{k_1} \tag{3.1.9}$$

$$x_D = \frac{x}{c'} \tag{3.1.10}$$

$$a = \frac{a'}{c'},\ b = \frac{b'}{c'},\ c = \frac{c'}{c'} = 1 \tag{3.1.11}$$

$$t_D = \frac{t\alpha_1}{c'^2} \tag{3.1.12}$$

$$T_D = \frac{T - T_A}{T_S - T_A} \tag{3.1.13}$$

where,

k_i	thermal conductivity of each layer (i=1,2 or 3)
α_i	thermal diffusivity of each layer (i=1,2 or 3)
T_S	steam temperature
T_A	ambient temperature
a', b', c'	distances shown in Fig. 3.1.14
t	time
T	temperature
x	distance

Then the dimensionless forms of Eq. 3.1.7 for each layer, initial conditions and boundary conditions become,

$$\frac{\partial^2 T_{Di}}{\partial x_D^2} = \frac{1}{\alpha_{Di}}\frac{\partial T_{Di}}{\partial t_D} \tag{3.1.14}$$

$$T_{Di}(0, x_D) = 0 \tag{3.1.15}$$

$$T_{D1}(t_D, 0) = 1 \tag{3.1.16}$$

$$T_{D3}(t_D, 1) = 0 \tag{3.1.17}$$

$$T_{D1}|_{x_D=a} = T_{D2}|_{x_D=a} \tag{3.1.18}$$

$$k_{D1}\frac{\partial T_{D1}}{\partial x_D}\bigg|_{x_D=a} = k_{D2}\frac{\partial T_{D2}}{\partial x_D}\bigg|_{x_D=a} \tag{3.1.19}$$

$$T_{D2}|_{x_D=b} = T_{D3}|_{x_D=b} \tag{3.1.20}$$

$$k_{D2}\frac{\partial T_{D2}}{\partial x_D}\bigg|_{x_D=b} = k_{D3}\frac{\partial T_{D3}}{\partial x_D}\bigg|_{x_D=b} \tag{3.1.21}$$

The dimensionless form of the transient heat conduction equation was solved by Laplace transformation and inversion by the Stehfest Algorithm (Stehfest, 1970).

Figure 3.1.15 shows the calculated dimensionless heat flux and cumulative heat flux as a function of time and Fig. 3.1.16 shows the temperature history at different locations. Steady state is characterized by a plateau in the temperature and heat flux plots, and a straight line portion in the cumulative heat flux plot. It takes nearly three hours to reach steady state for all locations of interest. Since the time to reach steady state is relatively large compared to the estimated duration of the experiments, the early time behavior cannot be neglected and transient heat transfer models should be used in calculating the heat loss from the system for the experimental design. Heat loss calculations to determine the minimum insulation thickness will be repeated using transient heat transfer models.

3.1.4.2 Core Holder Design

Due to material restrictions in the Cat scanner, different high temperature plastics are considered. Polysulfone which is a high strength transparent thermoplastic, having an operating temperature range between $-150°F$ and $300°F$, was chosen for the core holder. It is also a good insulator and has a low coefficient of thermal expansion. It is resistant to steam and compatible with the solvents, alcohols and oils that will be used in the experiment.

The core will initially be placed inside the polysulfone core holder using 0.07 cm polysulphone spacers to simulate the fracture aperture. The spacing between the polysulfone box and the core will form the fracture.

The front and back plates of the coreholder will be removable and O-rings will be used on these plates to seal the model. For extra strength and support, polycarbonate plates of 0.5 in. thickness will be used behind the polysulfone back and front plates. Finally the whole rectangular box will be cast with Fiberfrax insulation in a circular shape. Firebricks cut in a circular shape will be placed on top of the model before it is cast with Fiberfrax. These bricks will help avoid the scanning artifacts as will be discussed in Section 3.1.5.

This coreholder design will be the same for both the 2-D and the 3-D model. The 2-D model of core dimensions $20 \times 4 \times 10$ will be constructed first. Front, top and side views of the 2-D model are given in Figs. 3.1.17- 3.1.19.

A total of 24 thermocouples will be used. Nine of them will measure the temperature inside the rock, and 15 will measure the temperature inside the fracture. The temperatures will be measured as close to the matrix-fracture interface as possible.

Heat flux sensors will be placed on the polysulfone core holder to measure the heat losses from the system during the experiments.

The injection/production wells will be located diagonally in the fracture at the corners of the model. The injection corner of the model will be slightly different than the production corner. To make sure that steam of 100% quality at $120°C$ is injected to the fracture, a 1/8 in. firerod heater will be placed in a groove in the plastic at the injection corner. The injection tube will

be attached to the heater. A thermocouple will be placed at the same location to monitor the temperature at the injection well (Fig. 3.1.20).

The 2-D core will be scanned at two different planes. Fig. 3.1.21 shows the front scan view. For the 3D model of $20 \times 8 \times 10$ cm dimensions, scanning will be done in two different orientations, front scan and side scan. A side scan view of the model is given in Fig. 3.1.22.

3.1.5 EXPERIMENTAL ACCOMPLISHMENTS

Dimensions were determined for the rectangular Boise sandstone cores to be used in the experiments. Two different cores will be used. The one with $20 \times 4 \times 10$ cm dimensions will simulate a 2-dimensional model, and the one with $20 \times 8 \times 10$ cm dimensions will simulate a 3-dimensional model.

First the surfaces of the cores were ground to make them smooth. Then some basic properties of the cores were measured.

3.1.5.1 Porosity and Permeability Measurements

The porosity was determined by the saturation method. The porosity was found to be 0.30 which agreed with the porosity values for Boise sandstone reported in the literature (Sanyal, 1971).

The permeability of the sandstone was determined using two different methods. The first was the Ruska liquid permeameter. The measurements were made on 1 in. round core plugs cut from a larger block. The results ranged from 900-1700 md depending on the cut directions.

The second method was the measurement of point permeabilities by a minipermeameter. For this purpose, a minipermeameter was built, and the method of Goggin et al. (1988) was used to calculate permeability. The permeability measurements were made directly on the Boise blocks which will be used in the experiments. The measurements are in reasonable agreement with the standard permeability measurements. The x, y and z-direction permeability maps for the 2D block are given in Figs. 3.1.23-3.1.25.

3.1.5.2 Cat Scan Trial Runs

Before building the model, a number of trial scans were made on mockups to determine the ideal core holder design and the scanner settings for the best scan results.

Since the model is rectangular, artifacts from corners should be reduced to obtain CT numbers which will yield correct saturations . For this purpose, a mock model was made using the actual rock to be used and the plastic to be used for the core holder. First, two firebricks were used; one at the top and one at the bottom of the model. The artifacts were reduced significantly (Fig. 3.1.26).

To eliminate the artifacts as completely as possible, it was decided to make the rectangular system appear to be circular to the scanner. To do this, Fiberfrax insulation was cast around the core holder combined with firebricks in a circular shape. Figure 3.1.27 shows the scan picture for this configuration. The result is quite satisfactory. The circular shape helped eliminate artifacts. Figures 3.1.28 and 3.1.26 compare two different scans with and without Fiberfrax.

3.1.6 PLANNED FUTURE WORK

The construction of the experimental setup has been started. After the equipment has been built and tested, the steam injection experiments will begin. Saturations will be measured by the CT-scanner. After the completion of the experiments a new calculation method will be developed for matrix-fracture transfer of both fluids and heat.

Table 3.1.1: Fine Grid Simulation Parameters

Matrix porosity, %	30
Matrix x-dir. permeability, md	900
Matrix y-dir. permeability, md	1400
Matrix z-dir. permeability, md	1400
Fracture permeability, md	84400000
Initial reservoir pressure, psia	25
Initial reservoir temperature, K	297
Initial oil saturation (matrix)	0.8
Initial oil saturation (fracture)	1.0
Steam injection rate (Water eq.), cm^3/min	1.0
Production pressure, psia	20

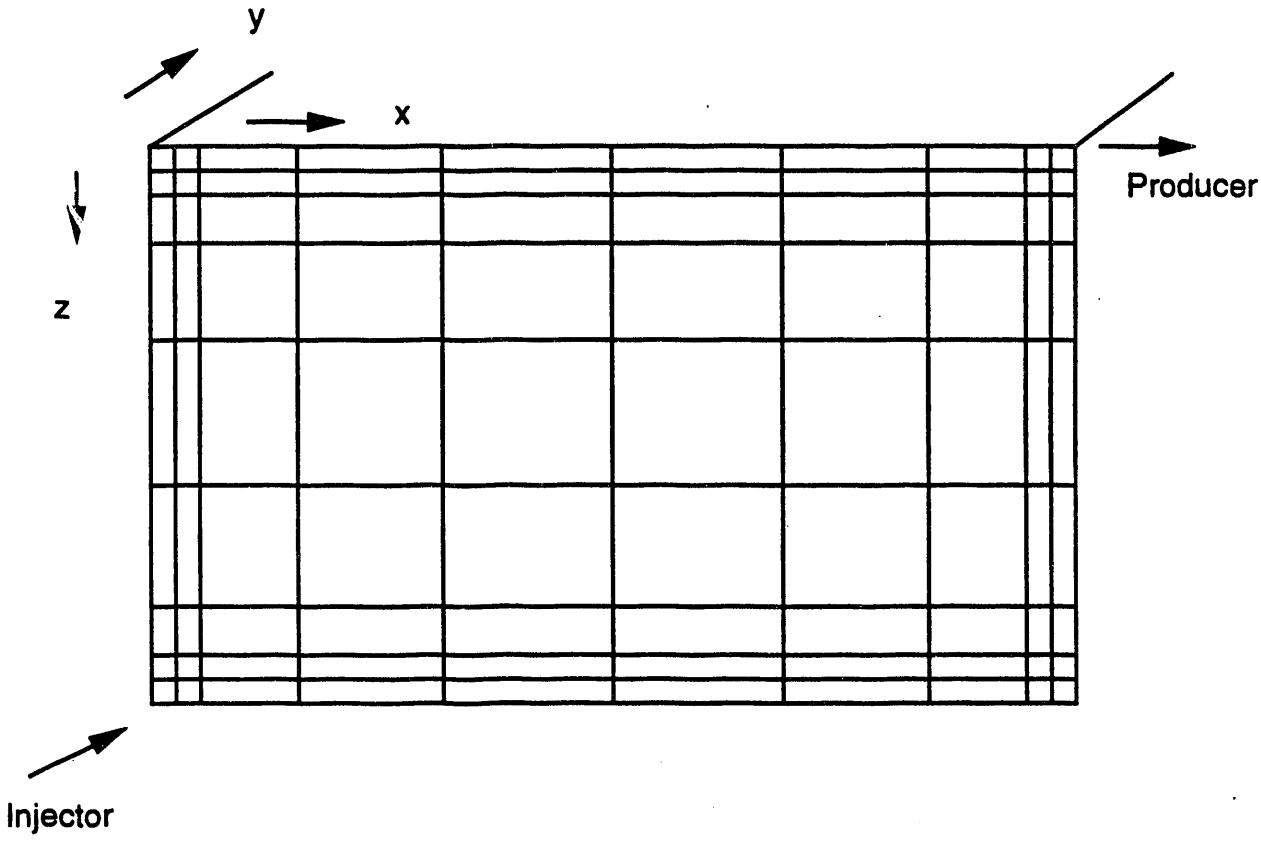

Figure 3.1.1: Grid system used in the simulations.

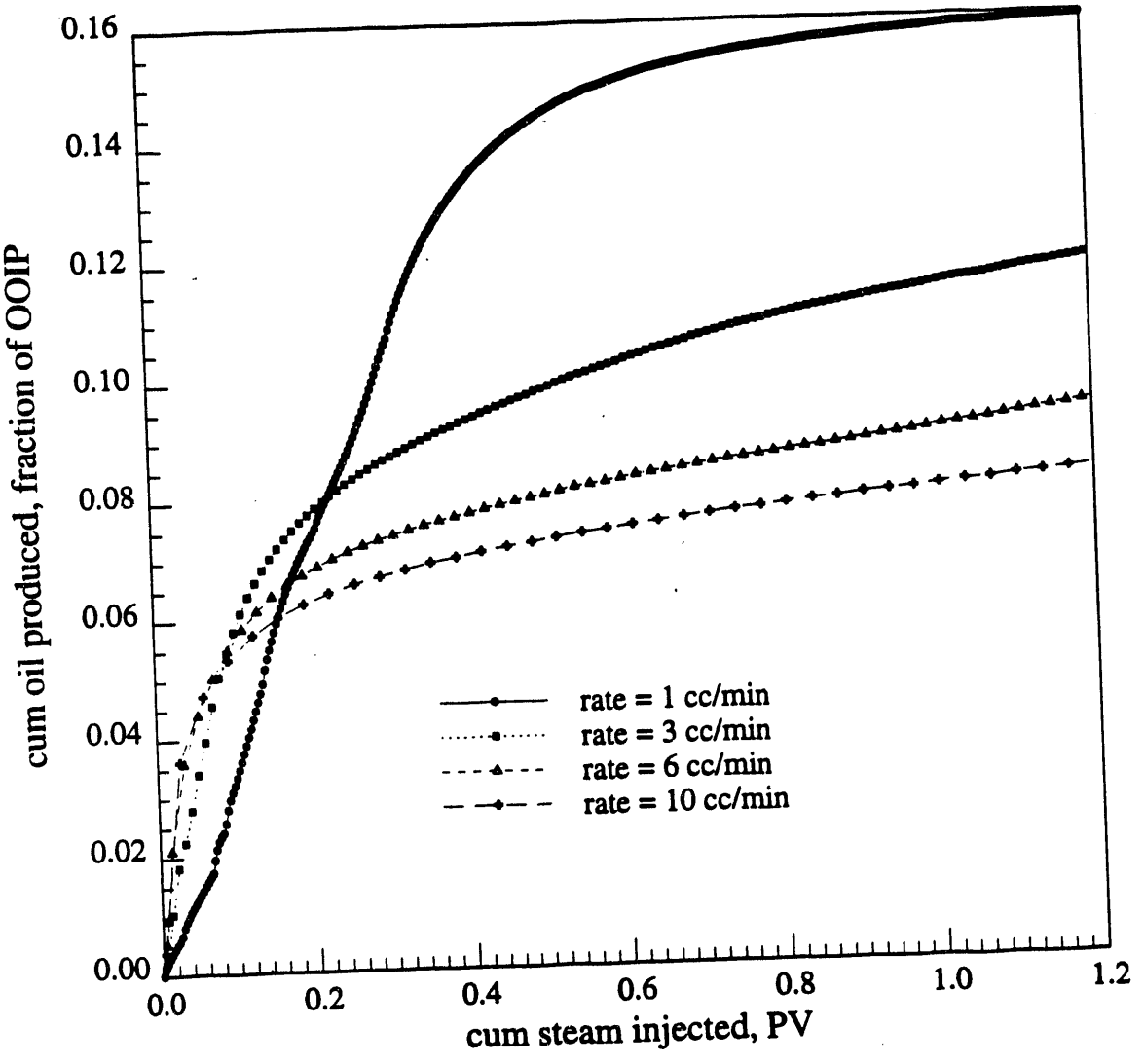

Figure 3.1.2: Cumulative oil produced versus cumulative steam injected at different injection rates.

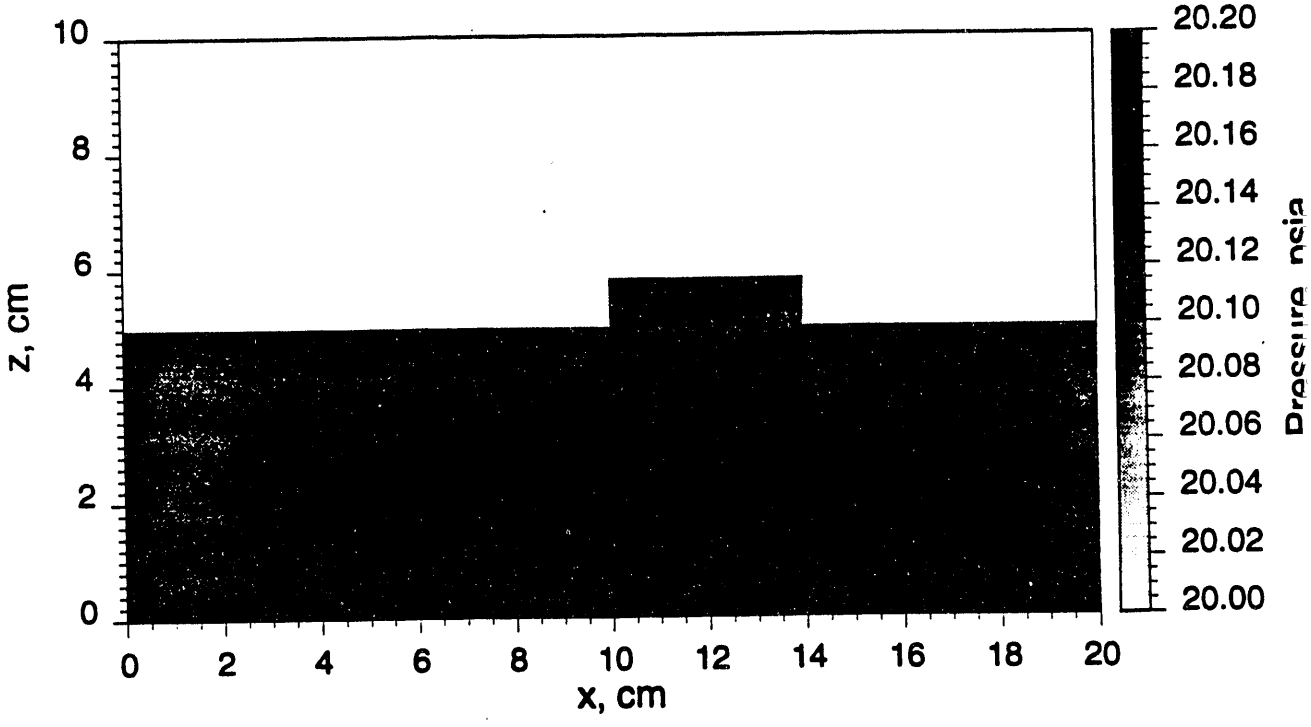

Figure 3.1.3: Pressure distribution throughout the system.

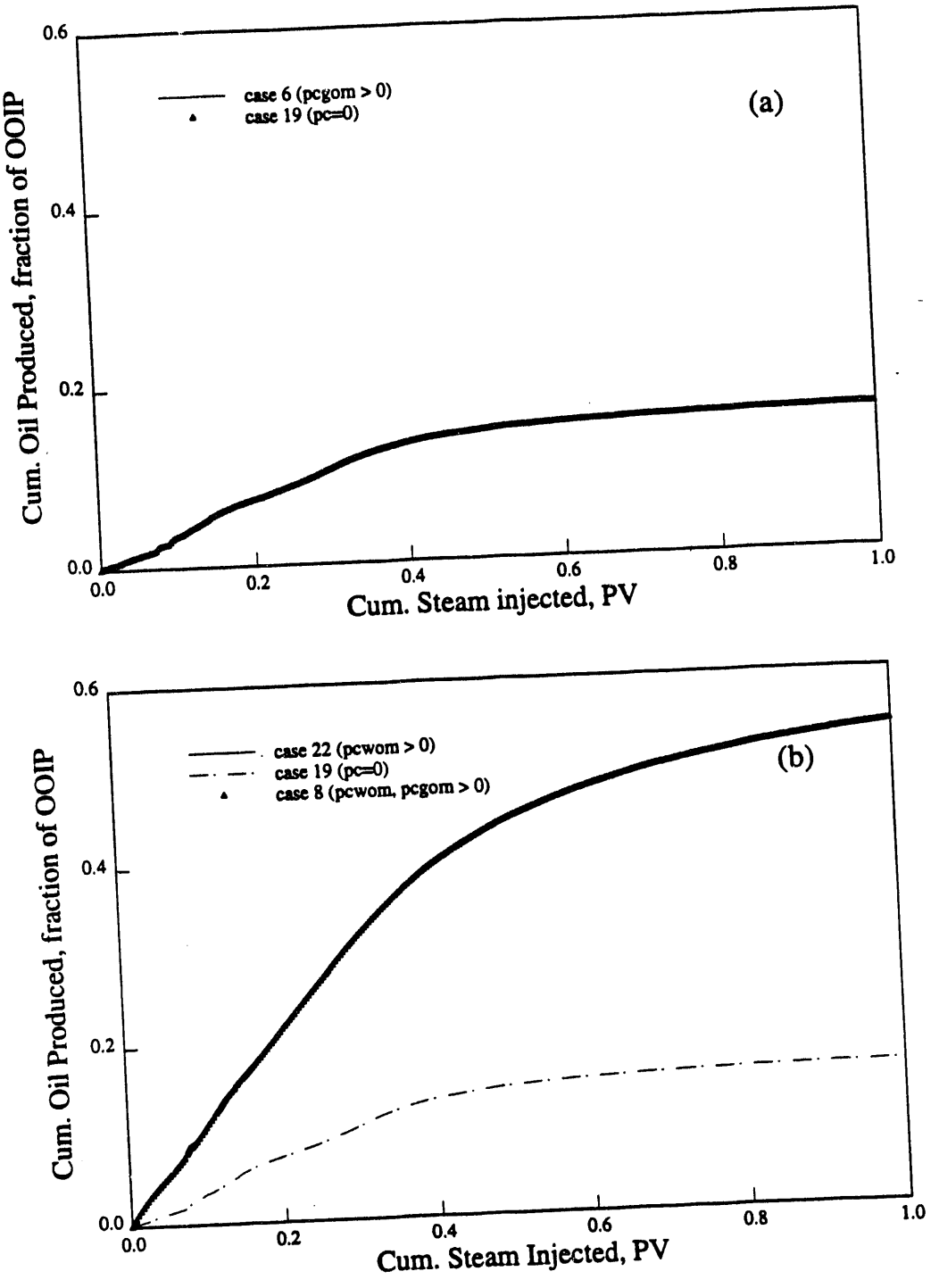

Figure 3.1.4: Effect of gas-oil, (a), and water-oil, (b), capillary pressures of matrix on cumulative oil recovery.

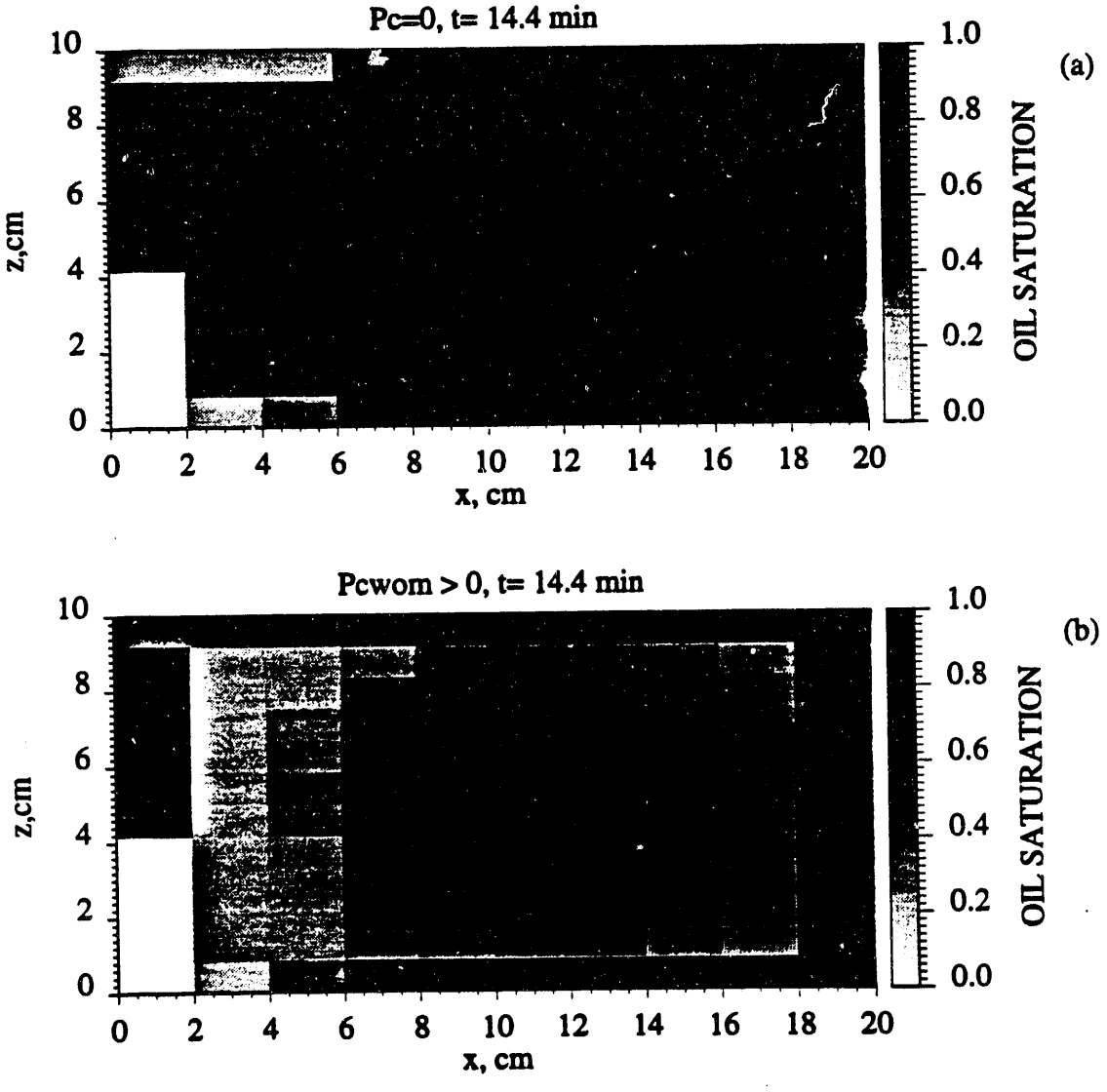

Figure 3.1.5: Oil saturation maps: zero capillary pressure, (**a**), and nonzero water-oil capillary pressure, (**b**).

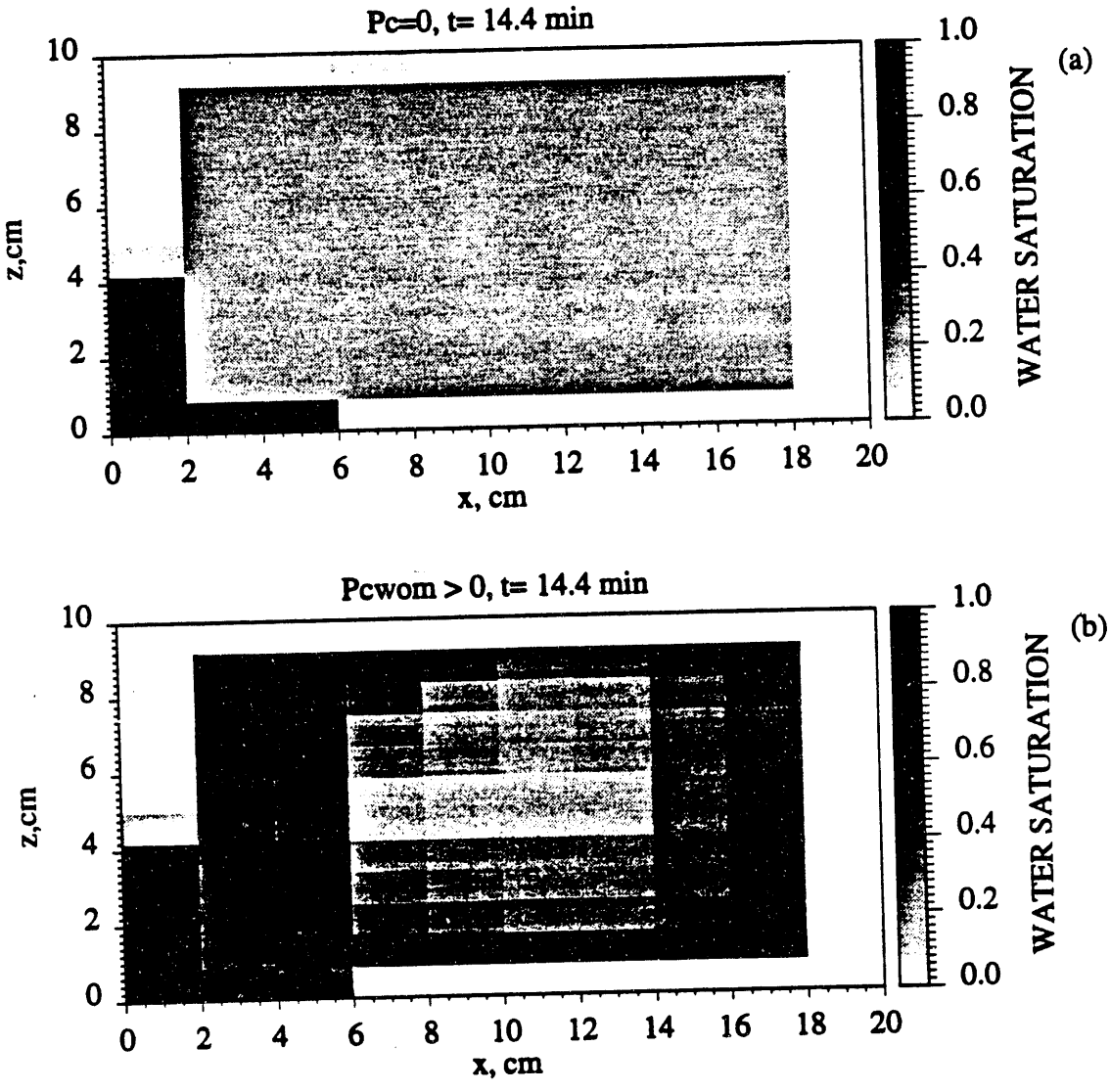

Figure 3.1.6: Water saturation maps: zero capillary pressure, (**a**), and nonzero water-oil capillary pressure, (**b**).

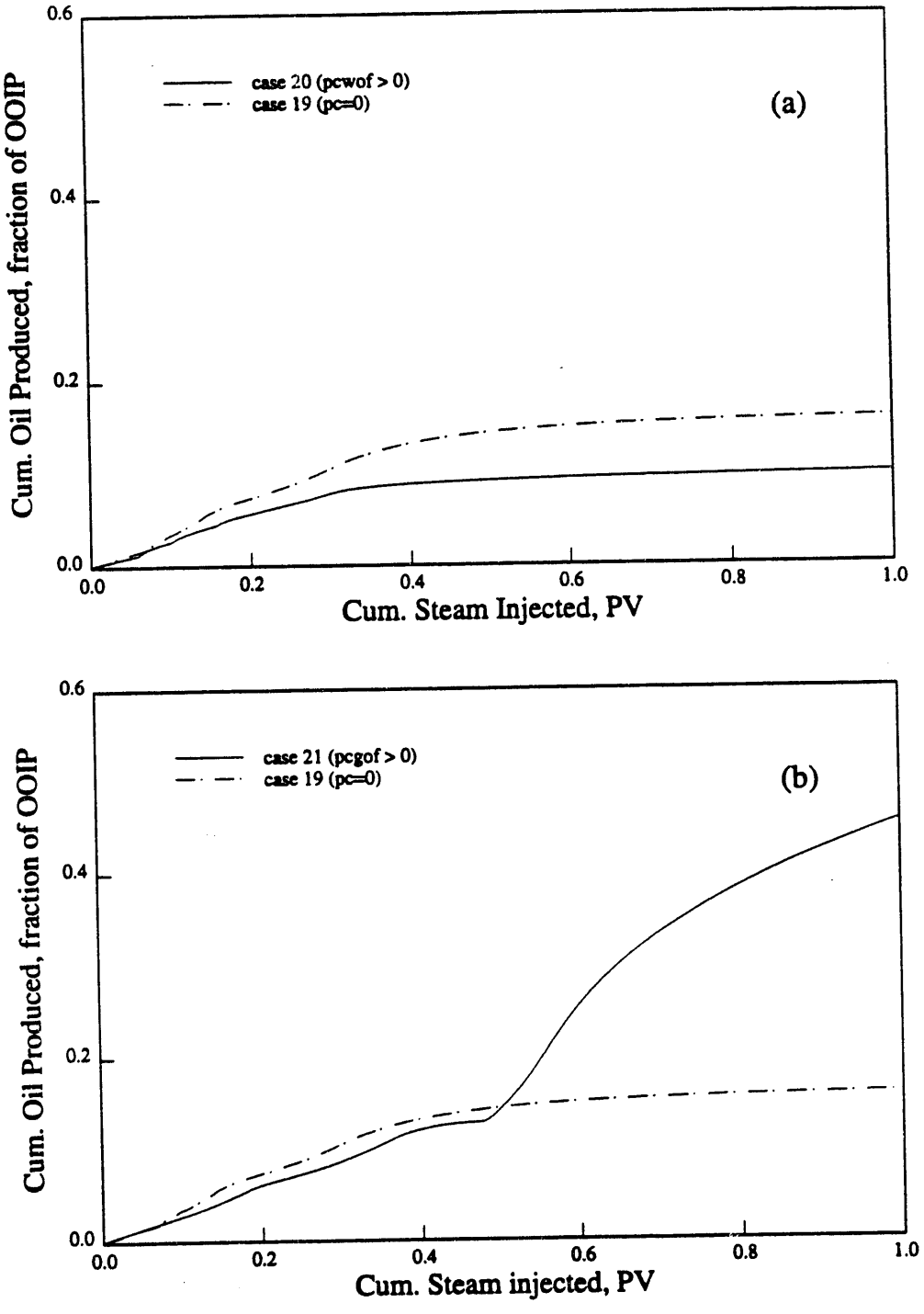

Figure 3.1.7: Effect of water-oil, (**a**), and gas-oil, (**b**), capillary pressures of fracture on cumulative oil recovery.

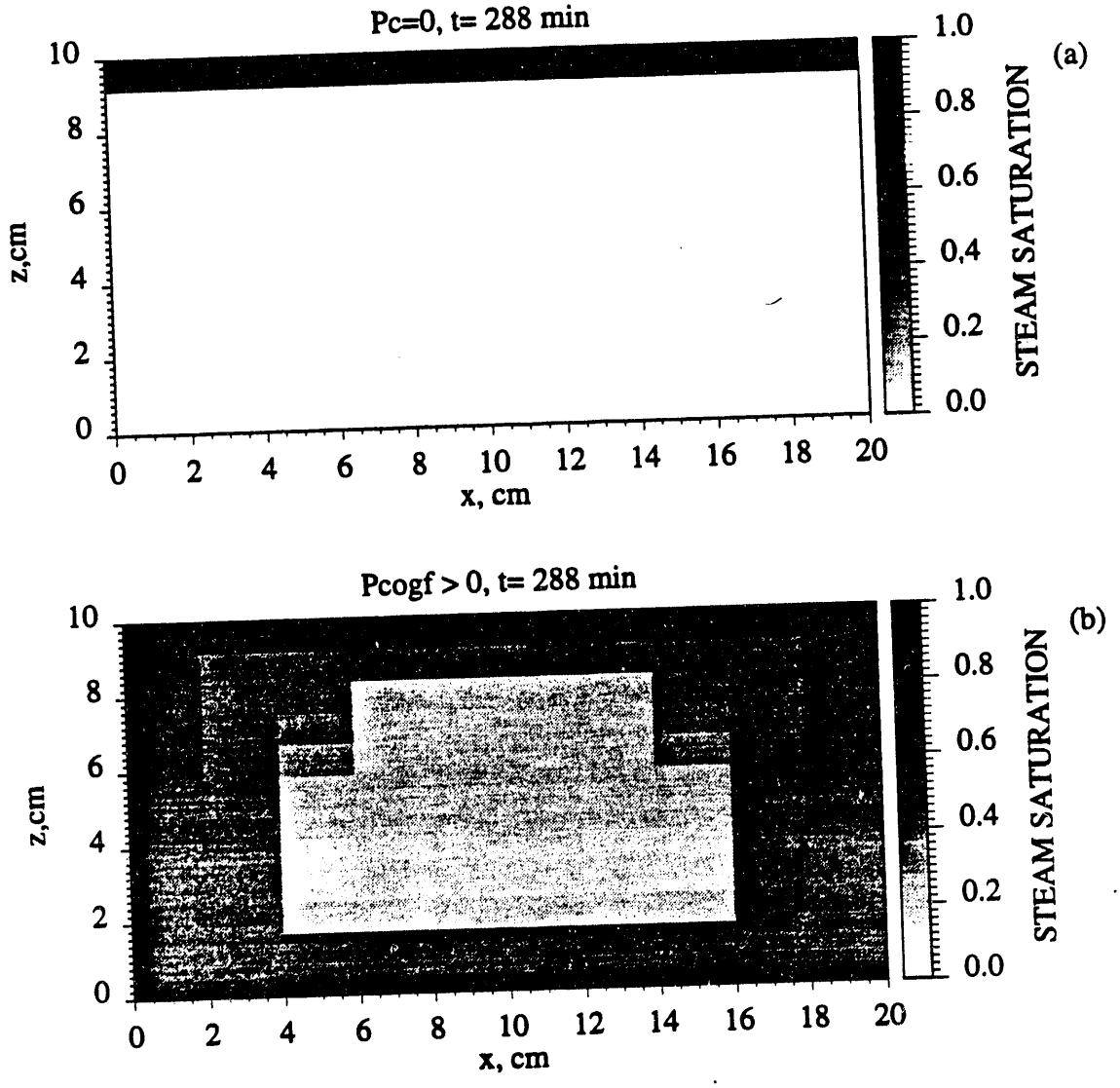

Figure 3.1.8: Gas saturation maps: zero capillary pressure, **(a)**, and nonzero gas-oil fracture capillary pressure, **(b)**.

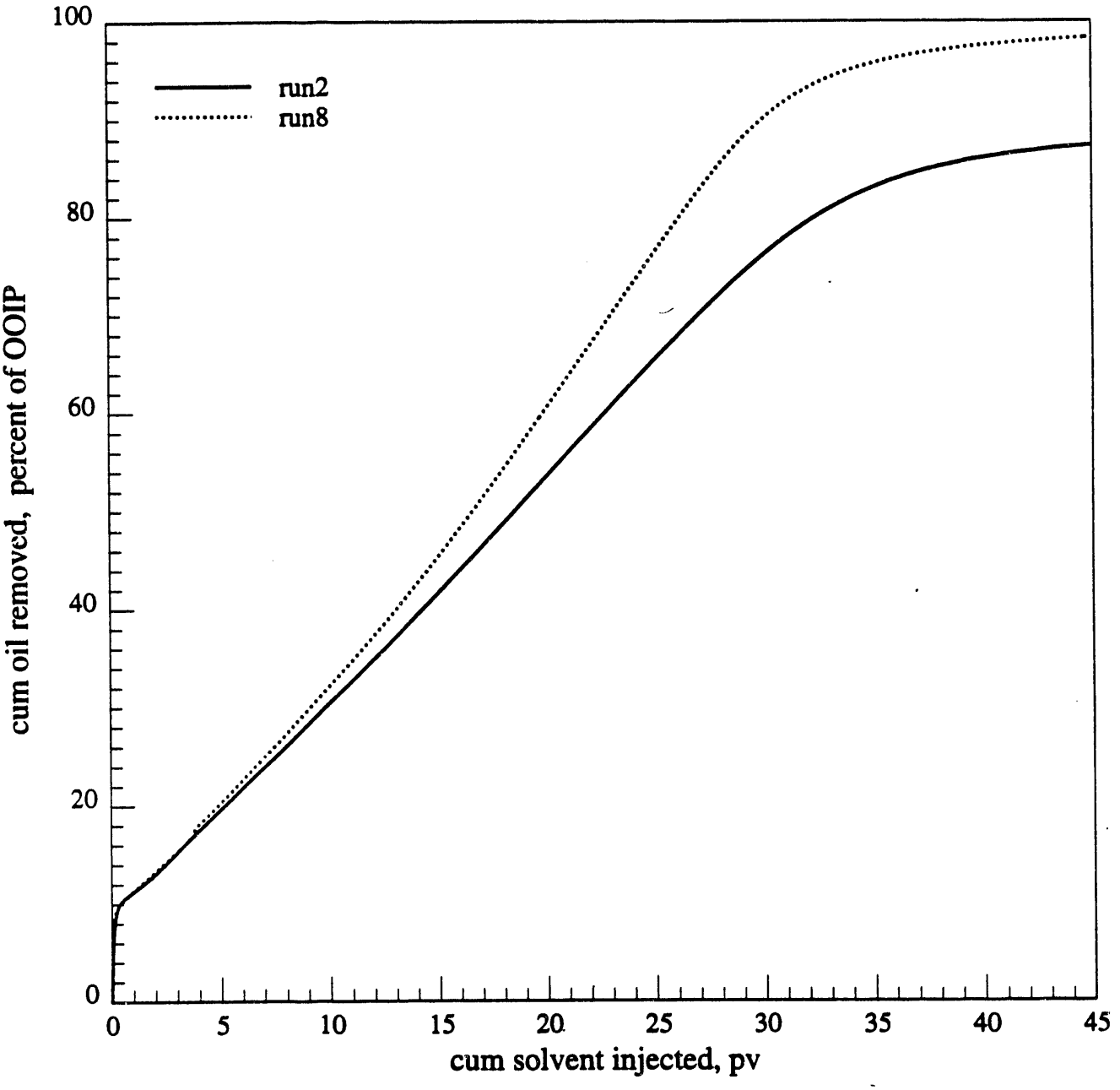

Figure 3.1.9: Oil recovery comparison for two different injection-production schemes

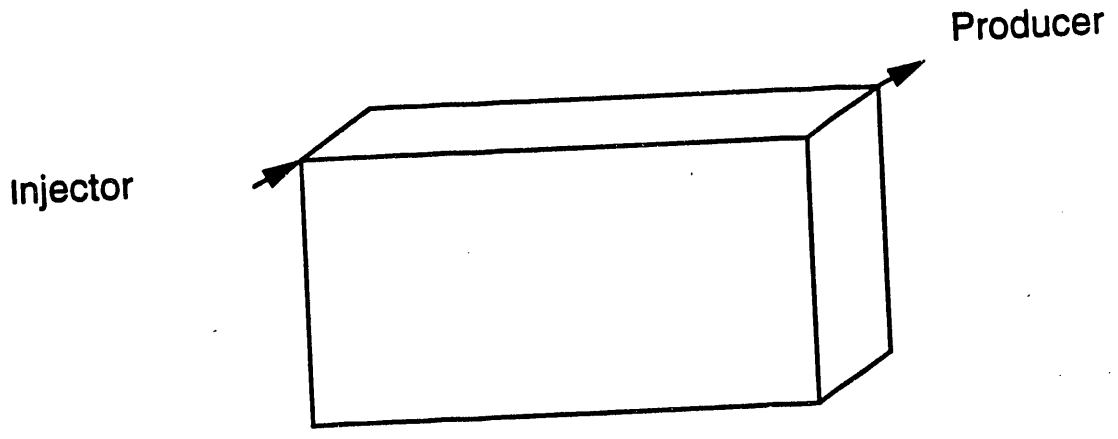

Injection-production
scheme Run 2

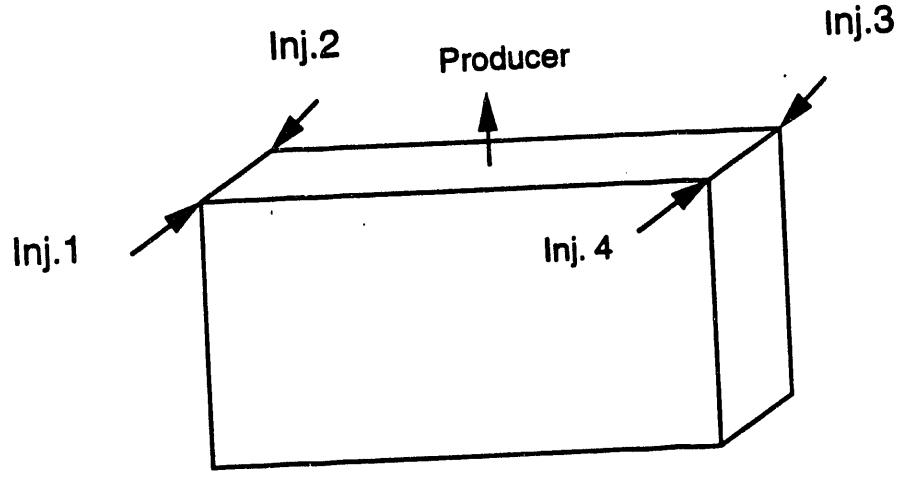

Injection-production
scheme Run 8

Figure 3.1.10: Two different injection-production schemes used in the pseudo-miscible simulations

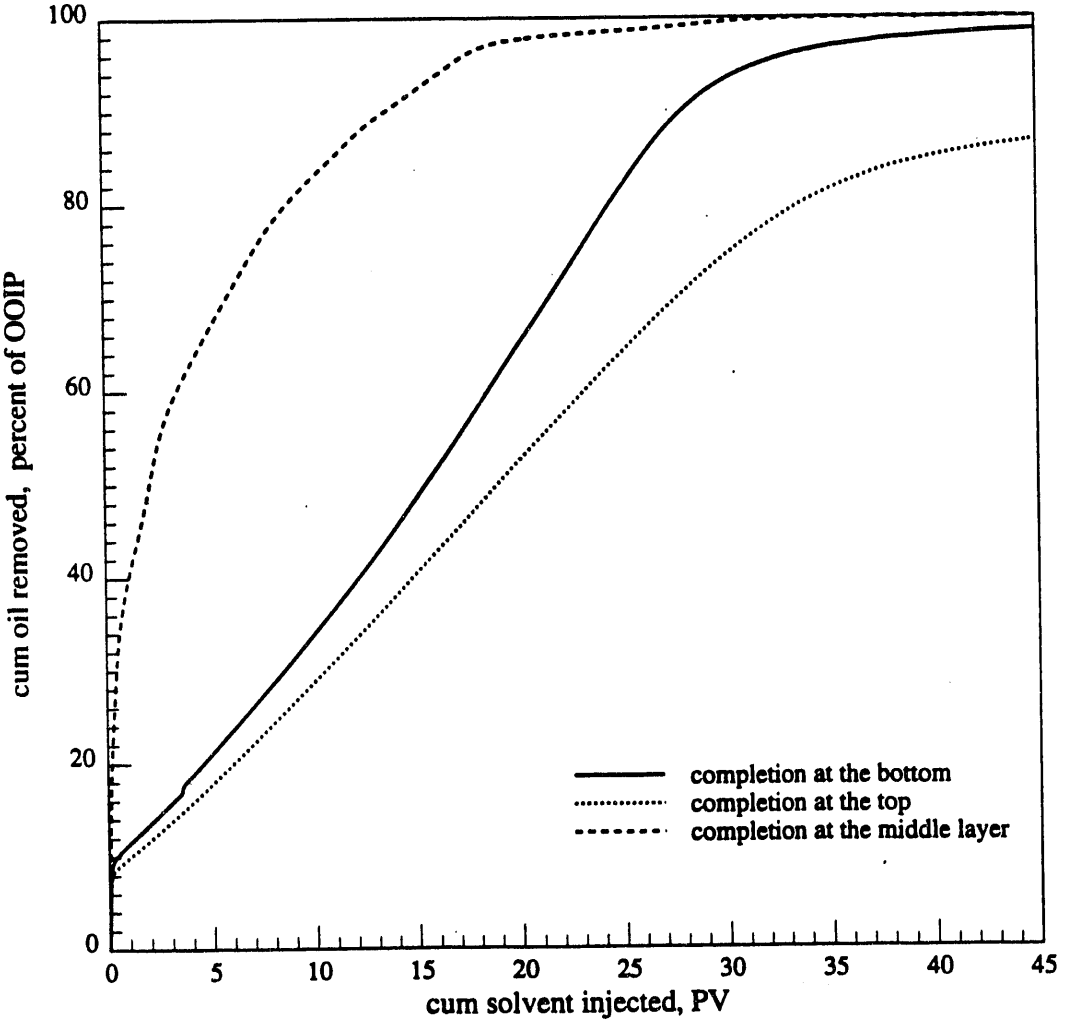

Figure 3.1.11: Oil recovery comparison for different completion locations

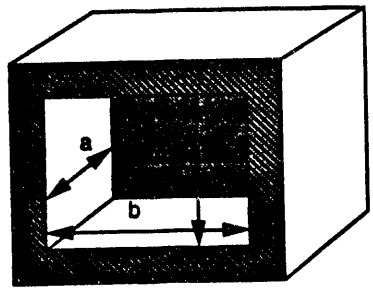

Figure 3.1.12: Parallelepiped shell

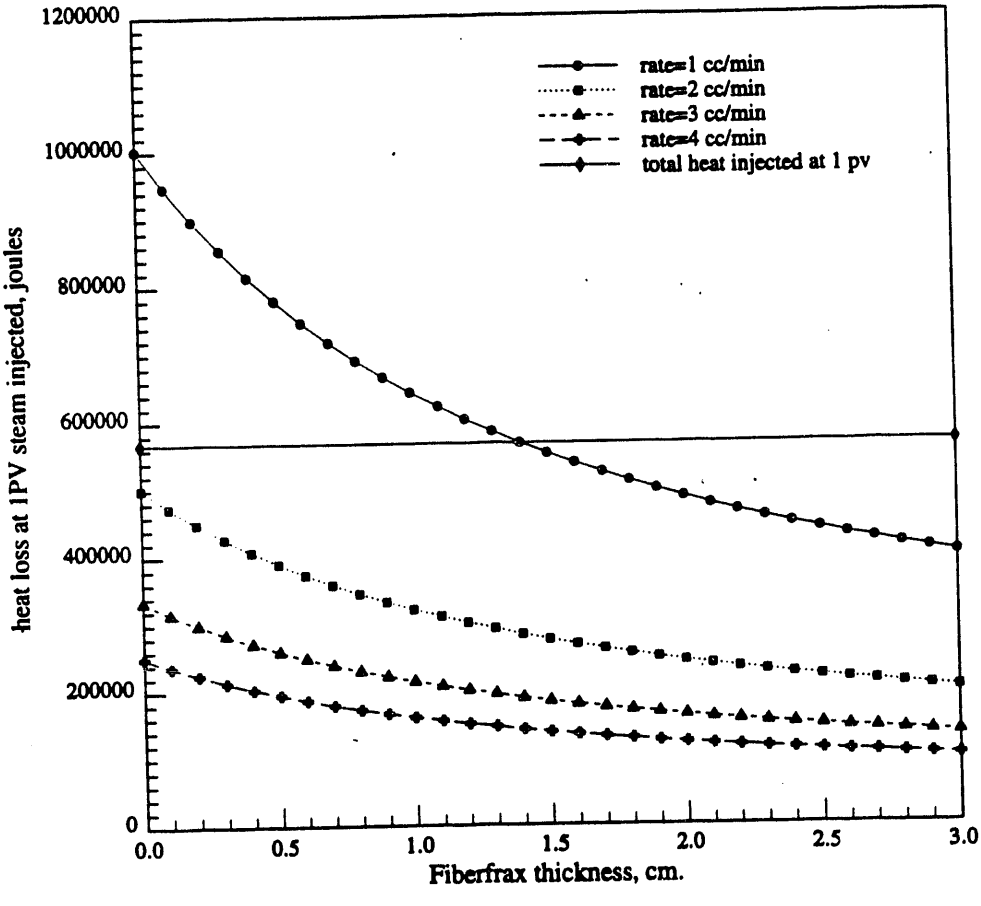

Figure 3.1.13: Steady state heat losses at different rates vs. insulation thickness

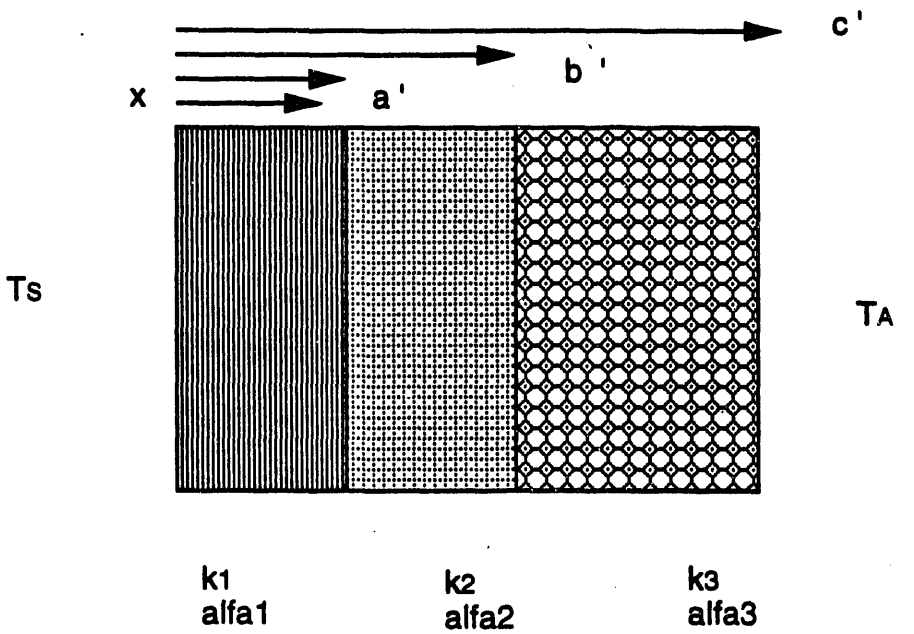

Region 1 = polysulphone
Region 2 = polycarbonate
Region 3 = fiberfrax

Figure 3.1.14: Sketch showing the system solved

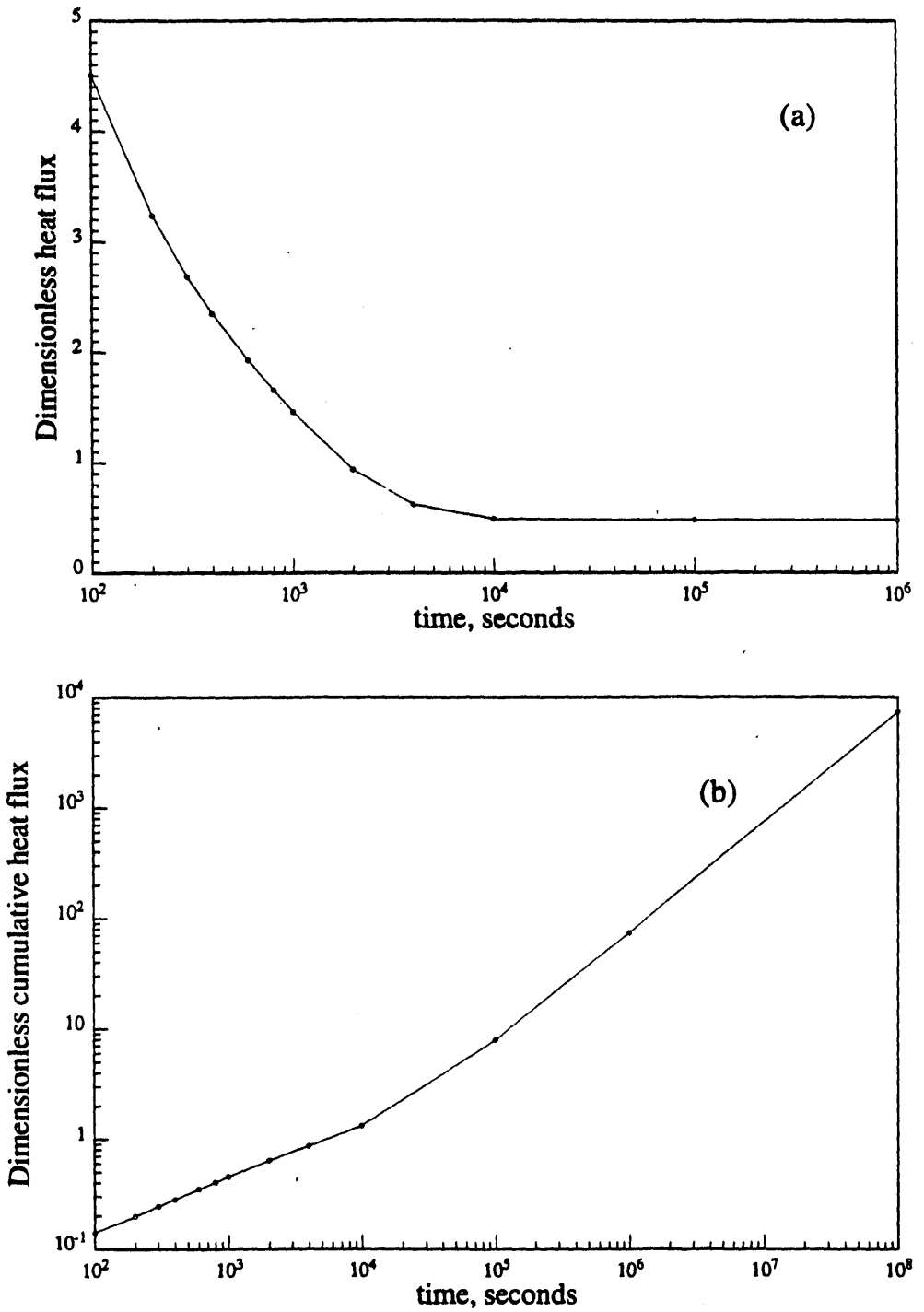

Figure 3.1.15: Heat flux vs. time, (**a**), and Cumulative heat flux vs. time (**b**)

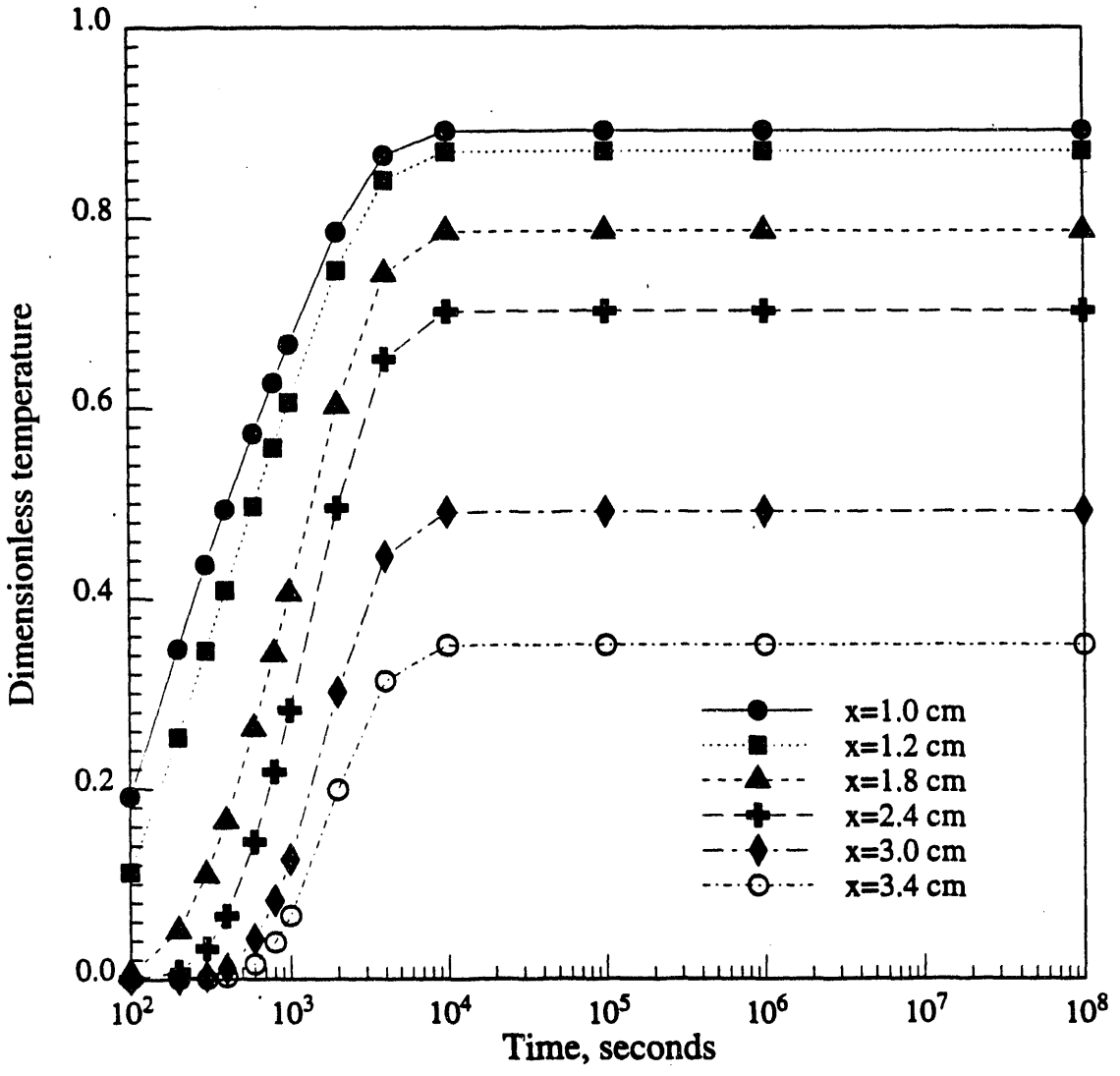

Figure 3.1.16: Temperature history at the three layer system at different locations

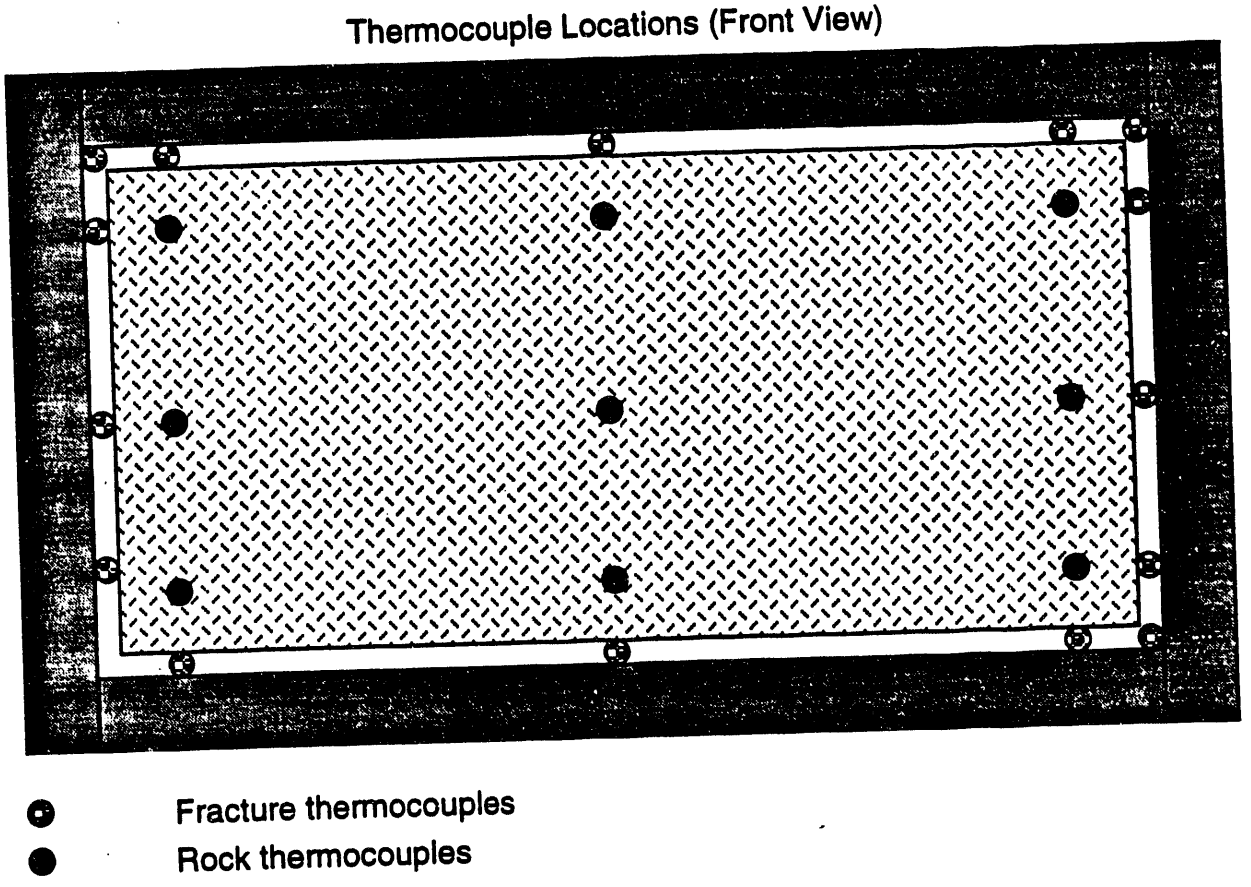

Figure 3.1.17: Front view of the system

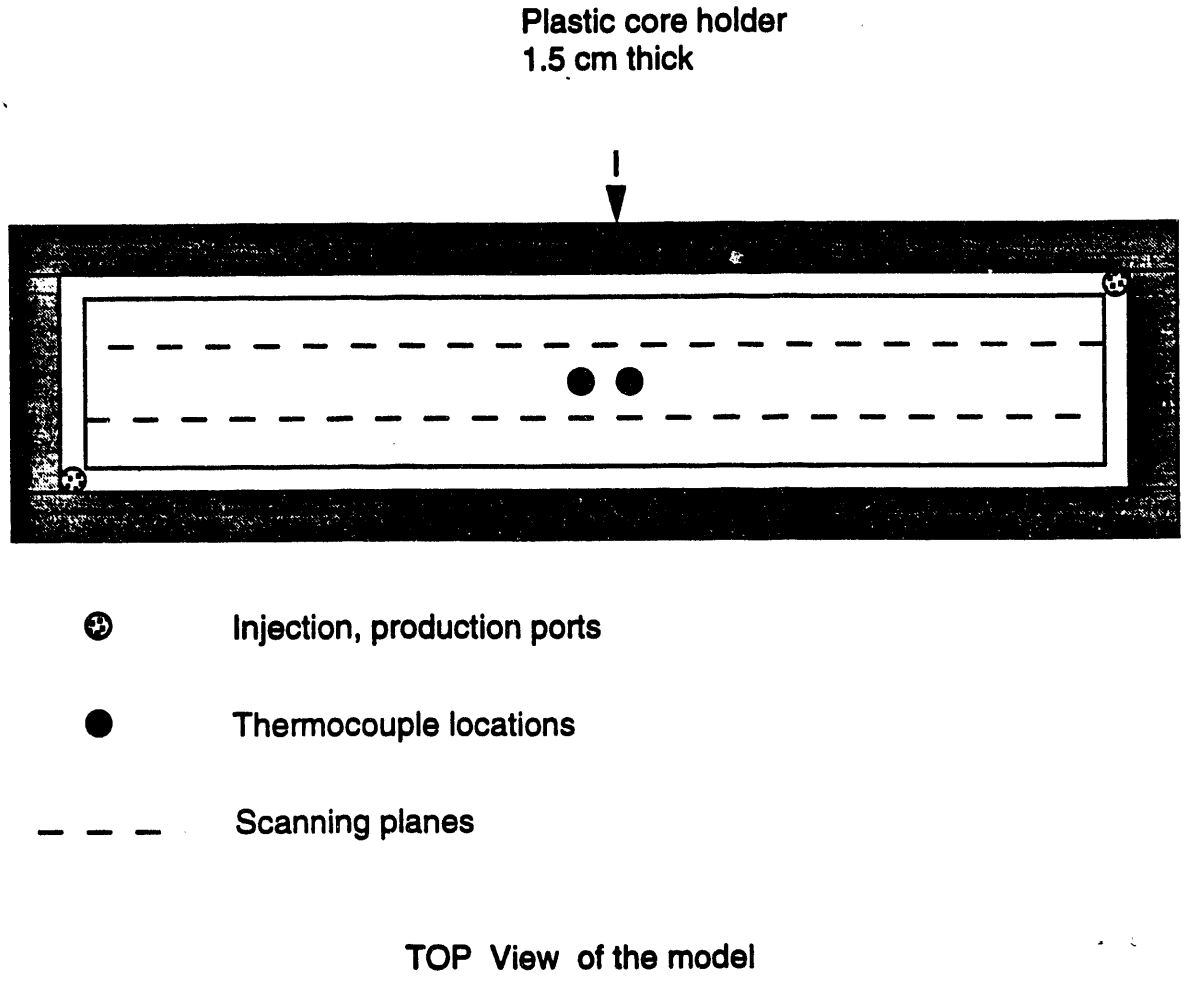

Figure 3.1.18: Top view of the system showing the scanning planes

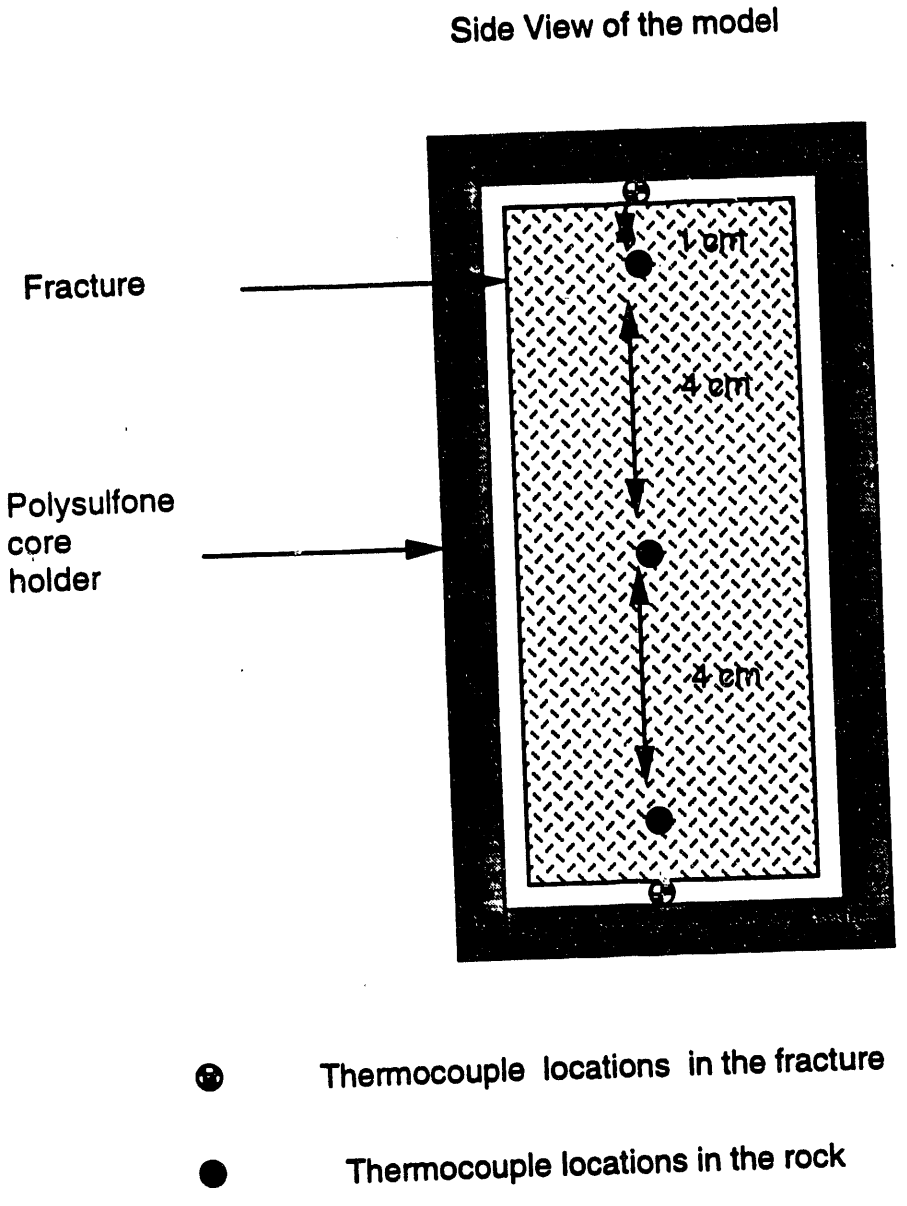

Figure 3.1.19: Side view of the system

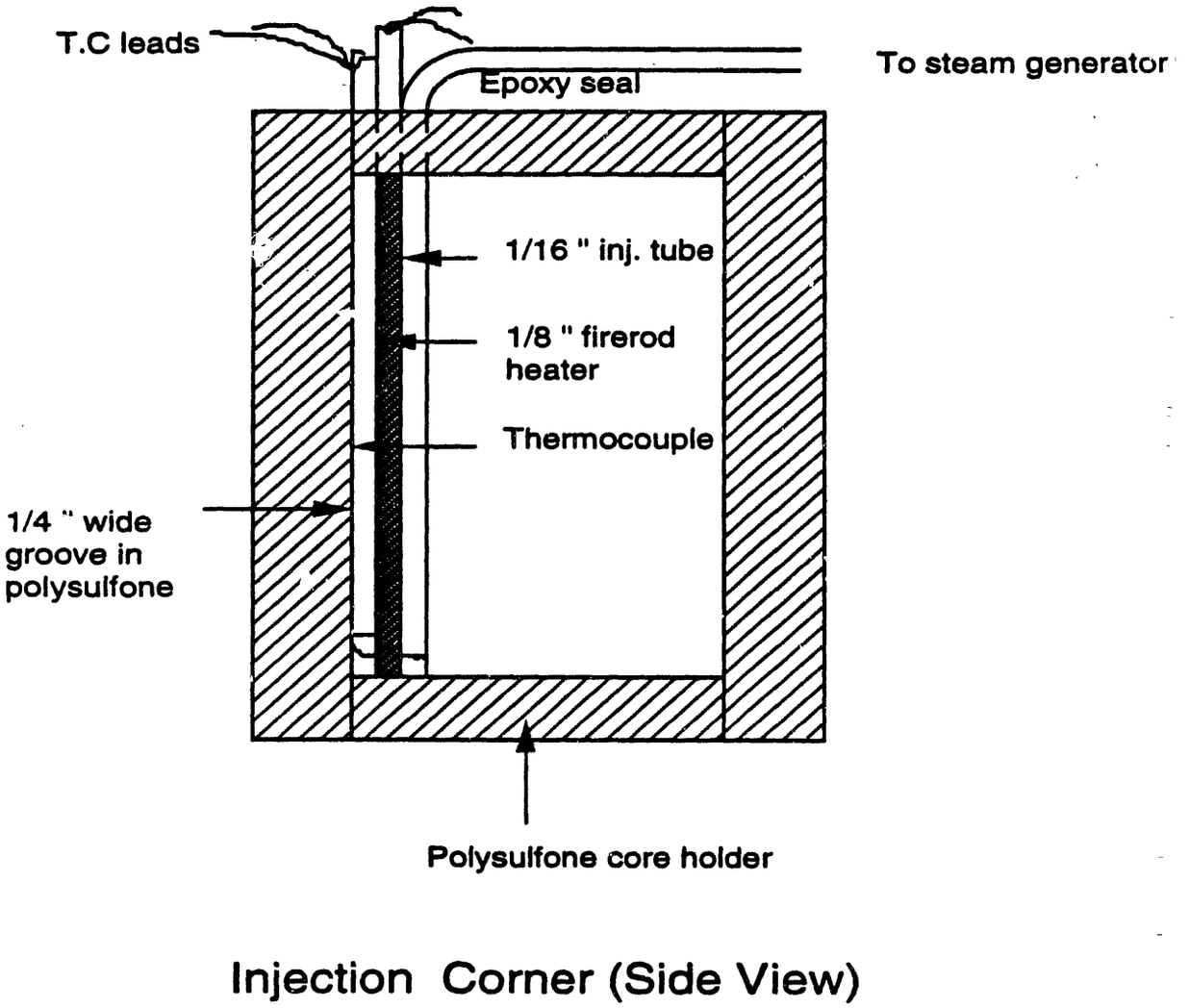

Figure 3.1.20: Sketch showing the injection corner

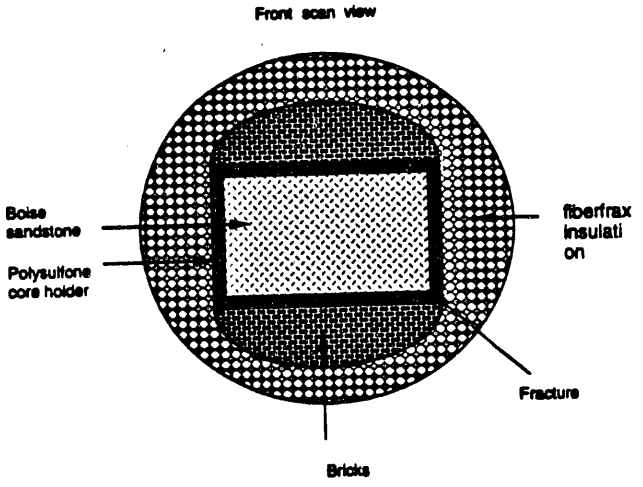

Figure 3.1.21: View of the model from the front scanning plane

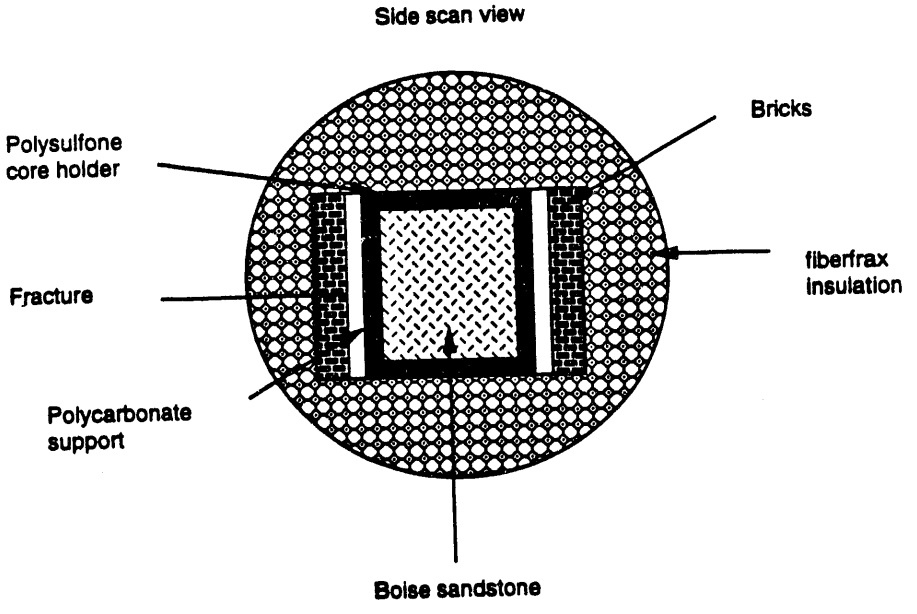

Figure 3.1.22: View of the model from the side scanning plane

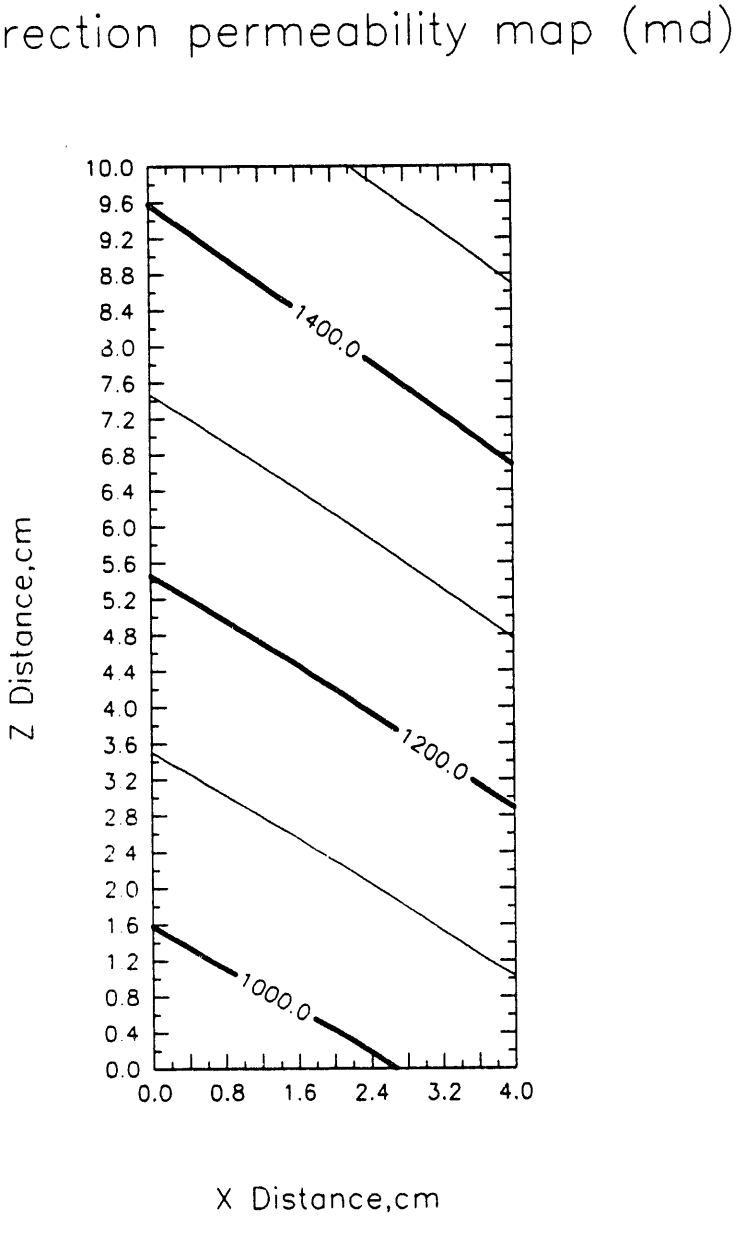

Figure 3.1.23: Permeability map of Boise 2D block (x-direction)

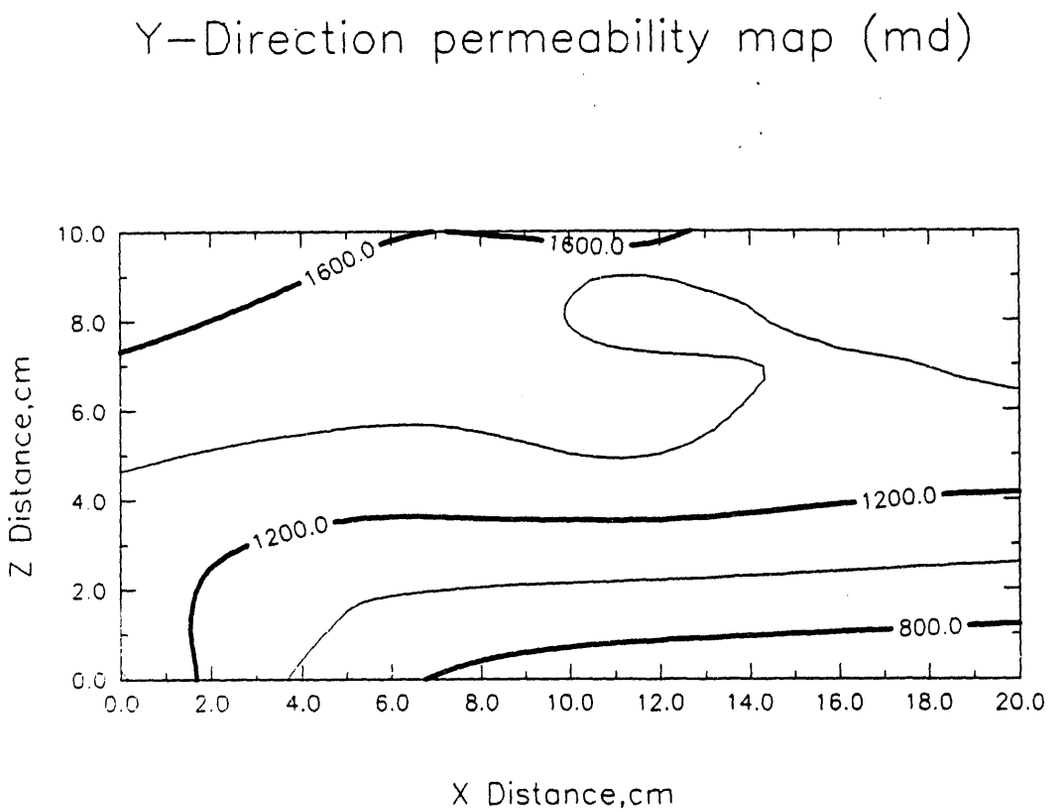

Figure 3.1.24: Permeability map of Boise 2D block (y-direction)

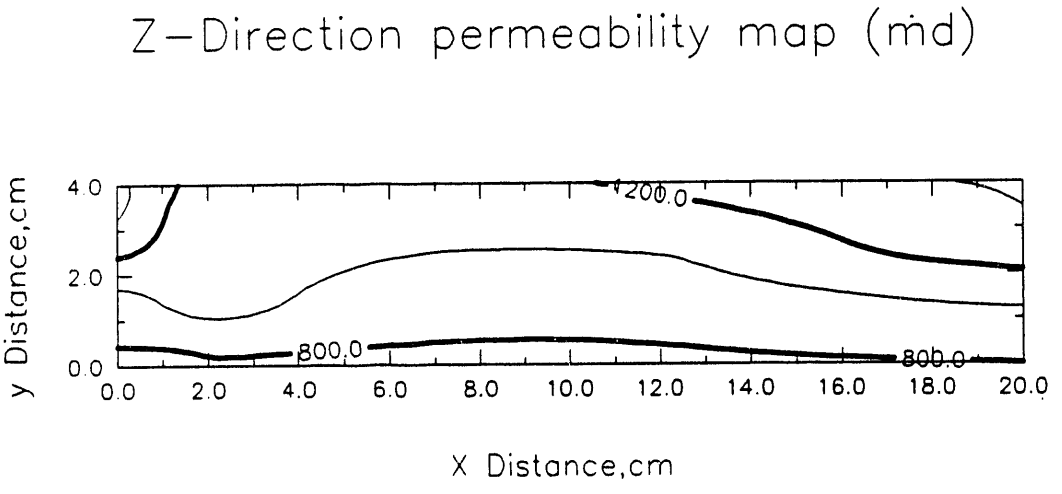

Figure 3.1.25: Permeability map of Boise 2D block (z-direction)

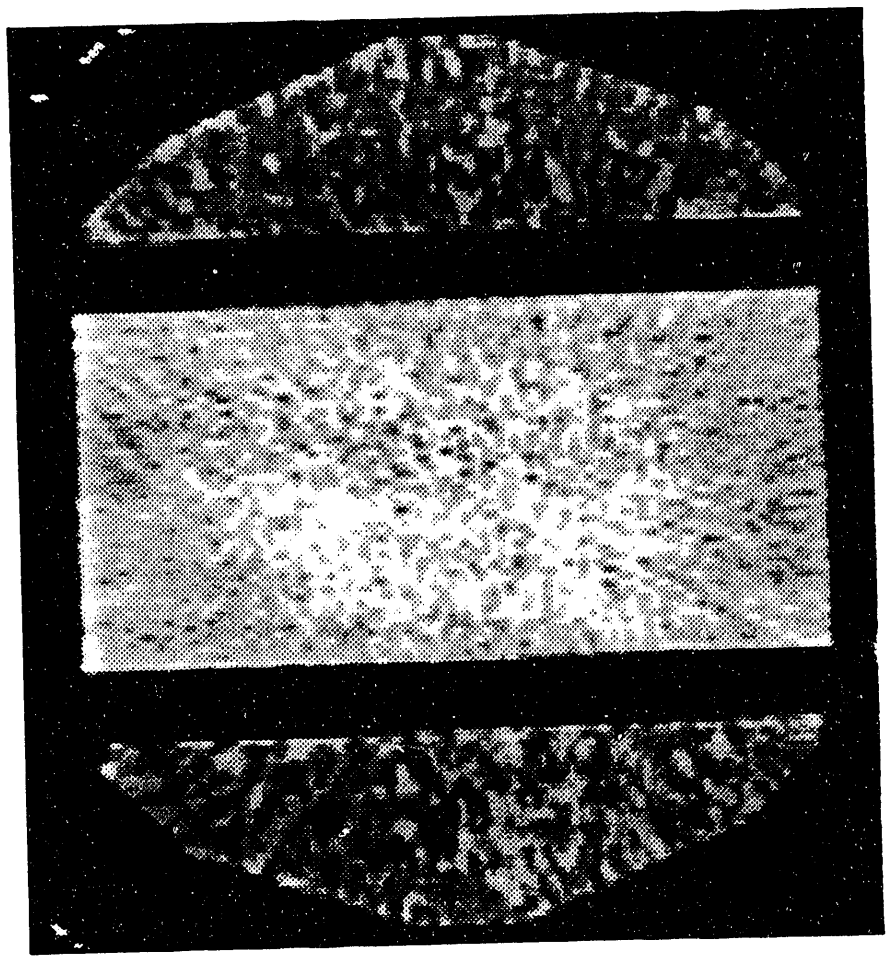

Figure 3.1.26: Scan picture with bricks

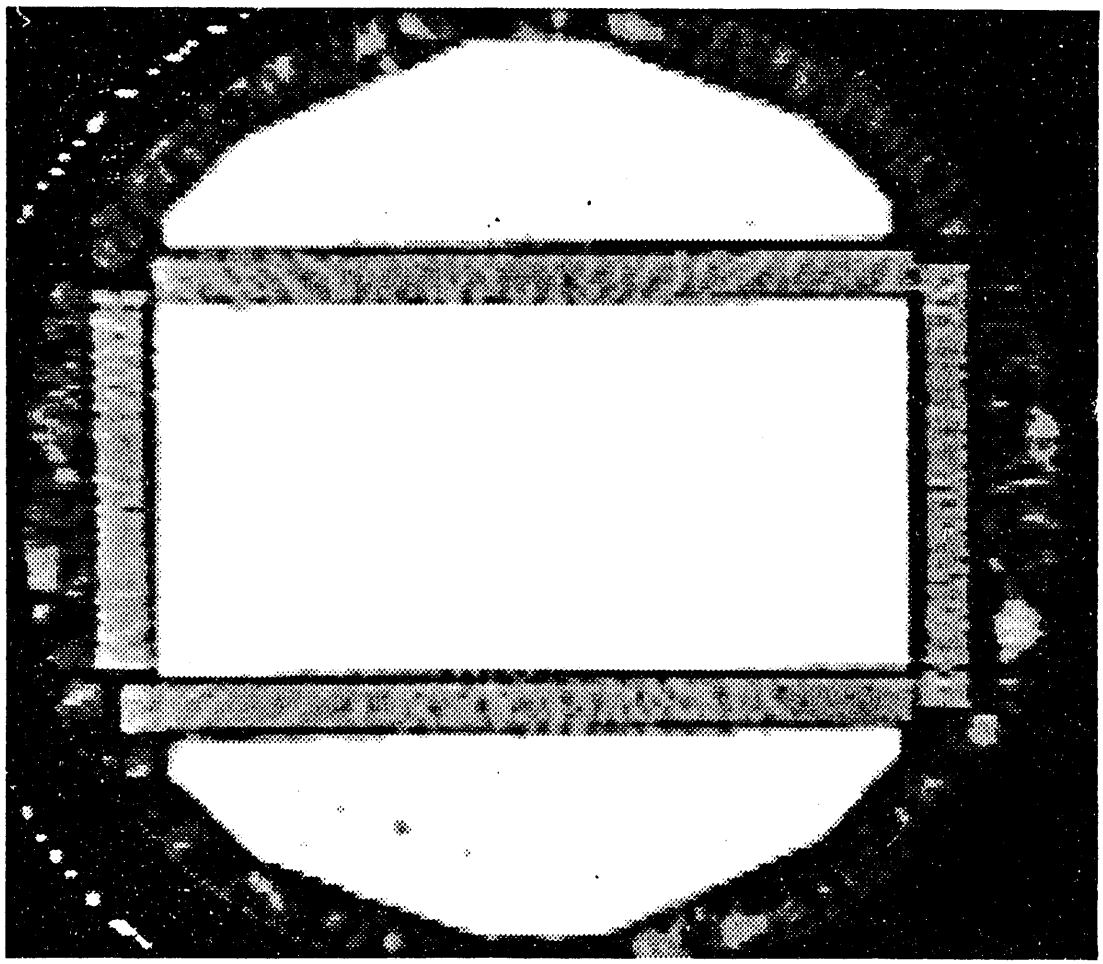

Figure 3.1.27: Scan picture with fiberfrax

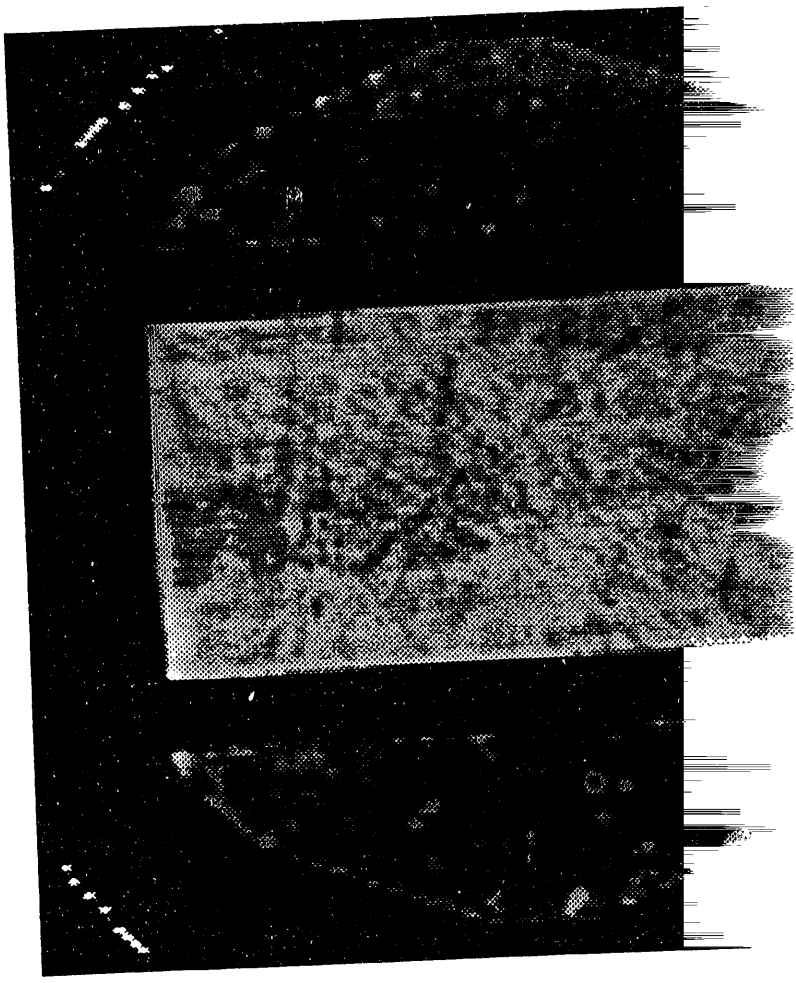

Figure 3.1.28: Scan picture without fiberfra

3.2. COMPUTER MODELING OF THE SUPRI-A 3-D STEAM INJECTION MODEL

(Sameer Joshi)

3.2.1 AIM

This research project has the aim of computer modelling the experimental results obtained with the SUPRI three-dimensional steam injection model (Demiral et al. 1991, 1992) , using the STARS (Steam and Additives Reservoir Simulator) compositional reservoir simulator. This would be useful in predicting the results of further experimental runs with the apparatus. The results could also be applied to field studies using appropriate scaling parameters.

3.2.2 EXPERIMENTAL BACKGROUND

Demiral et al. had idealized and constructed their experimental steam injection model based upon one quadrant of a theoretical 5-spot pattern. The model was designed and constructed in such a way that it could be used to measure temperature , pressure and heat-flux data in addition to being capable of easy scanning in the SUPRI-A C.T. scanner. The experiments were carried out on steam-flooding and steam-flooding with additives and nitrogen of the water saturated model. The primary aim was to utilize the C.T. scanner to visualize the saturation distributions and displacement fronts during the course of the experiment. A large amount of data has been collected regarding the saturation, temperature and pressure distributions within the model as well as heat flux rates during the course of the experiment.

3.2.3 COMPUTER MODELLING

Computer modelling of the experiments has been carried out using the STARS compositional simulator. This is a three-phase multi-component thermal and steam additive simulator. Some of its features are:

- Modelling using dispersed components including foam.
- Four different models for simulating fractured reservoirs.
- Adaptive implicit formulation including fully implicit wells.
- Flexible grid system with local grid refinement.

Proper modeling of the experimental results requires calculation of the physical parameters of the apparatus.These include reservoir description parameters like porosity, permeability, transmissivities and compressibility as well as rock thermal properties. Other important parameters are component properties and rock-fluid interaction parameters like IFT's and relative permeability tables. The proper heat loss model also must be specified.

The primary heat loss model used in STARS is a semi-analytical infinite-overburden method. It uses a semi-analytical procedure to solve the one-dimensional linear heat conduction equation, with the following assumptions:

- Conduction within the cap rock wipes out any sharp temperature differences. Thus, the temperature in the cap rock varies smoothly.
- Longitudinal heat conduction in the cap rock can be neglected.
- The most important features of the heat loss process are good descriptions of the boundary conditions at the interface and conservation of cap rock energy.

These points suggest that the temperature profile into the cap or base rock can be adequately approximated by a fitting function with a few parameters. The function chosen is:

$$T(t,z) = (\phi + pz + qz^2)e^{-z/d}$$

where p and q are the fitting parameters, ϕ is the temperature at the interface between the reservoir and the cap or base rock and d is the diffusion length, where d is chosen as

$$d = \sqrt{kt}/2$$

Utilizing a finite difference scheme into the equation of heat flow along with the appropriate boundary conditions gives the parameters p and q. The heat loss rate can also be calculated. In addition there is a facility for applying a constant or convective heat loss rate to selected grid blocks. This is done by specifying a convective heat transfer coefficient for the selected block. Since the laboratory model has a large component of convective heat loss, this is an important part of the modelling.

3.2.4 RESULTS OBTAINED

There is a fairly good match between the experimentally obtained saturation and temperature distributions and those calculated from the simulator.

As far as heat losses are concerned it was found that it is not possible to match the heat losses using solely the semi-analytical model. However with the addition of the convective heat loss model there is a closer agreement. This is as expected since the original design calculations for the model were made with the assumption that the heat transfer mechanism between the outer insulator surface and air is natural convection only.

One problem faced in modelling the experimentally observed heat losses is that theoretically the rates of heat loss from the symmetric sides of the 5-spot should be similar if the steam front is propagating symmetrically. A typical areal temperature distribution during the experiment shows that the isotherms are almost symmetrical. However the measured rates of heat losses from the symmetric sides of the 5-spot are always unmatched. The hypothesis put forward to explain this phenomenon is that there are local temperature differences around the lab model, which cause the differences in heat loss rates.

The simulator results on the other hand show an almost perfectly matching rate of heat loss from the symmetric sides of the 5-spot, as expected. There is no facility in the simulator to model an asymmetrical local temperature distribution around the model.

3.2.5 FURTHER WORK

Additional work is continuing to model further experimental runs and make a final selection of appropriate input parameters for the simulator.

A program has been written to extract data from the simulator and process it by a gridding and graphics program. This work is necessary as there is no graphics module available in the department for this simulator, and manual processing of the data is quite tedious. Some further improvements are being made to this program.

3.3. CHARACTERIZATION OF SURFACTANTS IN THE PRESENCE OF OIL FOR STEAM FOAM APPLICATIONS

(Abdul-Razzaq)

The steam foam process has been applied in oil fields since the late 1970ś. The mechanism of the process, however, is not known fully; particularly the detrimental effects of oil on foam, while known, are still unexplained. This hinders field application as the behavior of surfactants cannot be predicted under field conditions. The understanding of the mechanisms of foam generation and stability, and the mobility of foam to improve the development of field level projects have been the focus of the attention of many workers in the oil industry. Extensive laboratory studies have been carried out, mostly without oil, but some with oil. This study falls in the later category.

A one dimensional sandpack (6 ft by 2.15 in diameter) model was used to investigate the behavior with steam of four anionic sulfonate surfactants of varying chemical structure. The study was performed with an crude oil at residual oil saturation of about 12 percent of the pore volume. The observed pressure drops across the various sections of the pack were used to study the behavior of the surfactant.

The tested surfactants vary in chain length, aromatic structure and number of ionic charges. A linear toluene sulfonate produced the highest strength foam in the presence of the oil at residual saturations, as compared to the alpha olefin sulfonates. This is in contrast to the behavior of the surfactants in the absence of oil, where the alpha olefin sulfonates perform better. The reason for this change in behavior is the relative propagation rate of the foams produced by the surfactants. This conclusion is based on the observation that increase in propagation rate decreases the detrimental effect of oil; while the propagation rate is of little significance without oil.

The disulfonate performed better in the presence of oil. The improvement in the performance is embedded in the propagation rate of these surfactants as the rate of propagation in this case is also high. But the true mechanism of improvement in the strength of the foam, instead of deterioration, needs further study.

The detailed report has been published as DOE TR-88.

4.1. DRAWDOWN BEHAVIOR OF GRAVITY DRAINAGE WELLS

(J. Aasen)

A study was undertaken to develop an analytical solution to the transient free-surface gravity drainage flow problem. The behavior of wells producing under the action of gravity is a classic problem in the groundwater literature, and pressure transient testing of such systems appears to be an important problem for many heavy oil reservoirs considered targets for enhanced oil recovery.

The Green's function was derived in Laplace domain as the linearized solution to the highly nonlinear flow problem. This analytical solution was obtained by specifying uniform flux at the wellbore, and the inner boundary condition was later modified to that of uniform potential.

The model was compared with a finite difference simulator, and there is reasonable agreement between the calculated values of wellbore pressure drop, seepage face, and wellbore flux. The analytical model coincides with the radial flow equation for confined reservoirs after reaching the pseudosteady state flow regime.

4.2. A FINITE DIFFERENCE MODEL FOR FREE SURFACE GRAVITY DRAINAGE

(F.R. Couri)

The unconfined gravity flow of liquid with a free surface into a well is a classical well test problem which has not been well understood by either hydrologists or petroleum engineers. Paradigms have led many authors to treat an incompressible flow as compressible flow to justify the delayed yield behavior of a time-drawdown test.

A finite-difference model has been developed to simulate the free surface gravity flow of an unconfined single phase, infinitely large reservoir into a well. The model was verified with experimental results in sandbox models in the literature and with classical methods applied to observation wells in the Groundwater literature. The simulator response was also compared with analytical *Theis* (1935) and *Ramey et al.* (1989) approaches for wellbore pressure at late producing times.

The seepage face in the sandface and the delayed yield behavior were reproduced by the model considering a small liquid compressibility and incompressible porous medium.

The potential buildup (recovery) simulated by the model evidenced a different phenomenon from the drawdown, contrary to statements found in the Groundwater literature. Graphs of buildup potential vs. time, buildup seepage face length vs. time, and free surface head and sand bottom head radial profiles evidenced that the liquid refills the desaturating cone as a flat moving surface. The late time pseudo radial behavior was only approached after exaggerated long times.

This study has been completed and the results will be published as a separate DOE report.

5.1. CRITIQUE OF A STEAM FOAM FIELD PILOT

(L.M. Castanier and W.E. Brigham)

5.1.1 ABSTRACT

From 1981 to 1983, the Stanford University Petroleum Research Institute (SUPRI) performed a field test of steam with foaming additives in the McManus lease of the Kern River field. The test was operated by CORCO on a Petrolewis lease. The goal of this communication is to review the monitoring techniques and injection procedures used during this test in light of the advances in technology that have been made in the past ten years. We hope to draw on a successful but imperfect experiment to provide information that can be used by field operators who wish to run similar pilots.

The discussion will start with the choice of a surfactant as foaming agent for a specific field and will point to the importance of laboratory screening. Injection mode (continuous or multiple slugs) and the effect of noncondensable gases will be evaluated. Evaluation of production results and problems experienced during this evaluation will be described in detail. A new method to accurately measure oil production was developed during the project and we will comment on its applicability.

We will show how the logging program that was implemented during the SUPRI test could be improved by better temperature and neutron logging. Tracer tests, pressure transient tests and injection profile determination methods all showed some limitations during the pilot. We shall discuss the gap between the information available in theory from those methods and what was really achieved in the field. We shall also make suggestions for improvement in designing and interpreting such formation evaluation methods.

The goal of a pilot is to provide information on the application of a process to a reservoir. The best monitoring methods should be used to ensure that this objective is met. Examination of past results can be an excellent way to improve current and future projects.

5.1.2 INTRODUCTION

Steam/foam has been used as a way to improve the efficiency of steam injection for over 15 years. In a typical steam/foam project, aqueous solutions of surfactants are injected, often with a small amount of noncondensable gas, to generate a foam when mixed with the steam. The foam in turn increases local pressure gradients, improving the sweep efficiency of the steam.

A Department of Energy contract for a field pilot was initiated in October, 1980. The field work lasted from 1981 to 1983. The test was preceded by extensive laboratory studies performed at Stanford University. The goals were to obtain field scale data unobtainable in the laboratory and to test the effectiveness of the steam/foam process. This project was concluded at the end of 1983. The results were presented by Brigham. (Brigham, 1989; Brigham, 1984) The purpose of this communication is to review the results of this test, to constructively criticize the methods and operational procedures used in view of recent progress of technology, and to provide recommendations for the design and operation of future tests of the steam/foam process.

5.1.3 LABORATORY STUDIES AND FOAMER SELECTION

The SUPRI pilot was initiated after a comprehensive laboratory evaluation of various surfactants. (Owete, 1980; Al-Khafaji, 1982) Selection of a proper product involves screening for thermal stability, adsorption, and partitioning into the oil phase. Cost of the surfactants should also be considered. The number of suitable thermally stable surfactants has greatly increased in the last ten years, thus allowing more flexibility in the search for the optimum product.

We feel that the laboratory screening program implemented prior to the test was adequate. The adsorption measurements were only performed at static conditions while dynamic adsorption data would be more realistic. However, collection of dynamic adsorption data is costly and usually such data can be inferred from static adsorption measurements. These experiments should be performed with cores, brines and crudes from the pilot area at steam injection temperatures and pressures. Core selection for the laboratory studies are now easier than at the time of the pilot through proper use of CT scanners and better description of mineralogy.

An interesting technique to select the best surfactant for a given reservoir was suggested by Mohammaddi and McCollum, (Mohammaddi, 1986) to supplement laboratory studies. In the field, a small slug of foamer was injected with the steam and the pressure increase in the well treated was monitored with time. This procedure was repeated in different injection wells for three of the foamers preselected from laboratory studies. The criteria for the choice of the best product were pressure response and speed of pressure buildup. This approach is probably more suitable to full scale field applications than for pilot studies, but it allows at least partial confirmation of the validity of the laboratory work at low cost to the operator. It also allows a small scale rehearsal of the injection procedure that could warn of future operational problems during the main injection period.

5.1.4 SITE SELECTION

The MacManus lease, operated at the time by Petrolewis was chosen as the test site. The choice was based on the need for a mature steam drive project where there would be adequate production and injection facilities. Chemical Oil Recovery Corporation (CORCO) was selected as the field manager because of their experience in steam/foam operations.

The oil in the lease is heavy (12! API) and the water slightly brackish. This last point is important because the chosen foamer would have been adversely affected if any divalent ions had been present in the MacManus water. The reservoir is shallow (180 to 500 ft) and parts of it had been under steam drive for several years prior to the project. The reservoir pressure was low (50 psig in the test pattern) ensuring moderate steam injection temperatures and pressures.

A geological model of the field site was developed and two confined inverted 5 Spot patterns (2.25 acres) were chosen, one for a test pattern where steam/foam would be used, and the other a control pattern where steam only would be used (Fig. 5.1.1).

One of the problems experienced was the differing stages of exploitation of those two patterns. While the test pattern (centered on Well 208) had been under steam drive for several years, the control pattern (centered on Well 214) was not even drilled. Because of changes of operators on the lease prior to the start of the pilot, it was not possible to obtain details of the production data for all wells before 1980. This made direct comparisons between the two patterns impossible.

Another problem was the lack of time between site selection and the start of the project. A baseline production curve for the test pattern could not be generated from existing data on the pattern itself. It had to be inferred from only three months of good data prior to the test and from lease-wide decline curves obtained from the California Department of Oil and Gas database. Ideally a pilot test site should be well monitored by the pilot operator for several months before the start of a project. It is difficult to distinguish between the production increase due to the EOR process being tested and the increase caused by better monitoring and more efficient operational practices during the project. These two factors need to be decoupled to evaluate the effectiveness of the process. The best way to obtain that evaluation is to have the same personnel operate the pilot site for some time before the test.

5.1.5 DRILLING AND OBSERVATION WELLS

The two observation wells were drilled in August, 1981 in the 208 and 214 patterns. As direct comparison of the test pattern and control pattern was impossible, it would have been better in retrospect to drill two observation wells in the test pattern at various distances from the injector to better follow foam propagation in the reservoir.

Core recovery was poor because of the presence of large boulders and the unconsolidated nature of the formation. Advances have been made in coring techniques in the intervening ten years. Of particular importance is the preservation of cores for use in the laboratory screening process. Changes in core wettability can greatly affect the results of laboratory tests and can give erroneous information about steam/foam feasibility. We were lucky that our pilot test results confirmed the laboratory data, for the core material we received in the laboratory had been damaged by exposure to air and desaturation.

The observation wells were cased to total depth after an extensive suite of open hole logs had been run by several companies. Observation wells were not perforated during the project thus loosing sampling opportunities for surfactant and or tracers. A possible further improvement would have been nonmetallic casing in these wells. This would have allowed modern monitoring methods such as electromagnetic or acoustic logging and tomography to locate the steam invaded region and its changes with the use of steam foam. It also would have allowed the use of some open hole logs that are not normally of use through metallic casing.

5.1.6 INJECTION PROGRAM

The SUPRI pilot project was a demonstration project designed to show the feasibility of the steam foam process. As a result, only a very crude attempt was made to optimize the surfactant injection process.

5.1.6.1 Preliminary Injectivity Tests

Two preliminary injection tests gave useful information. The first test was the injection of 2,300 gallons of 15% active surfactant without nitrogen. It was a failure because of a faulty batch of surfactant. This showed the need for better coordination with the supplier and on site quality control. No further problems with surfactant quality were experienced during the project. The second preliminary test consisted of injection of 1,400 gallons of 15%

active surfactant with no nitrogen, followed by another 1,100 gallons with nitrogen. The resulting pressure data showed the importance of adding a noncondensable gas to improve the foam stability. It was decided to inject nitrogen at about 5% of the mole fraction of the steam. During these tests, the injection equipment performed as planned.

5.1.6.2 Main Injection Program

Three main slugs of surfactant were coinjected with steam and nitrogen. The same amount of surfactant (about 22,000 gallons of 15% active solution) was injected in each slug but the concentration was halved for the second slug and halved again for the third. As a result the second slug injection lasted twice as long as the first while the third lasted four times as long. The laboratory data showed the need for a concentration of 0.25% or above for optimum results, this number being the critical micelle concentration of the Suntech IV surfactant. The design concentrations for each slug were 4%, 2% and 1%, respectively. This was a deliberate overkill to take into account possible surfactant losses due to adsorption or phase partitioning.

No effect of the decreases in surfactant concentration were seen in the pressure responses at the injector, showing that indeed the surfactant concentration had been higher than needed. The longer duration of the second and third slugs caused injectivity profile effects for a longer time and greater response at the producers.

Since the SUPRI pilot, many attempts have been made to optimize surfactant use in a steam foam project.(Eson, 1989; Castanier, 1989) It appears that injection of small slugs of surfactant for a short time can be effective. Continuous injection to generate a large foam bank is probably not economical.(Patzek, 1989) Preflush of the near wellbore region by alkali or by a liquid slug of surfactant could improve the economics of the process.(Lau, 1989) As no predictive model yet exists for steam foam applications, the best optimization method to date is to monitor injection pressure and injectivity profiles. Experience gained from small pilot tests can help in planning injection programs for fieldwide operations. Economic optimization should be the ultimate objective of the engineer.

5.1.7 LOGGING PROGRAM

The logging program was comprehensive. Table 5.1.1 lists the logs run in the observation wells. Qualitative analysis of the logs allowed geological description of the layers present in the test and control patterns. Figure 5.1.2 shows a cross-section between the test injector (Well 208) and the updip producer (Well 114). Four major slices can be identified. Steam channeling was detected using one or more of the following: (1) gamma ray spikes, (2) high electrical conductivity in shales, (3) high core porosity indicating possible high permeability streaks, and (4)

high temperature. Porosity and saturations were estimated from logs and cores and appeared to give reasonable values.

It was hoped that C/O logs could be used to follow oil saturation changes in the observation wells. These logs were run every three months but the accuracy was not sufficient to distinguish saturation changes. Temperature and neutron logs have been shown by others (Hirasaki, 1984; Mohammadi, 1987) to be a good combination to follow the growth of the steam invaded zone at observation wells.

Production logging, particularly periodic temperature surveys should also prove useful as a tool to follow the effect of steam/foam on sweep efficiency near the producers. In the

SUPRI project, marked decreases were observed in the producers' temperatures in the test pattern, especially at the updip producer (Well 114), while no similar decrease was seen in the control pattern. Although the data were scattered and difficult to analyze, this temperature decrease was interpreted as further evidence of steam diversion.

New tools, now under development by the service companies, allow flow measurements at any given interval of a producer. Such data would be valuable , for rate and temperature data from each of the producing layers could provide evidence of steam diversion.

5.1.8 PRESSURE TRANSIENT TESTING

Pressure fall-off surveys were performed on Wells 208 and 214. The testing equipment consisted of a capillary tube filled with helium, a helium purge system, a downhole pressure chamber, a recorder, and a quartz-crystal pressure gauge. All components performed well during three surveys made at four month intervals: October '81, February '82 and May '82. The setup provides pressure change readings accurate to 0.01 psi under ideal conditions.

The goal of such tests is to provide an estimate of the volume of the steam zone. (Walsh, 1981). Analysis of the data obtained in Well 214 which had been under steam injection only since October 1981, gave reasonable estimates for the steam zone volume. The data from Well 208, however, could not be analyzed. (Messner, 1982) This well had been under steam injection for over three years prior to the first survey. Breakthrough of steam at the producers was probably the cause of the problem. Fall-off pressure transient data are difficult to analyze. (Messner, 1982) New developments in the analysis of such tests were published by Ambastha and Ramey, (Ambastha, 1987) and computer aided well test analysis can also allow better test interpretation. (Horne, 1990) It is certain that the results of these tests are more reliable for wells that have received steam for a short period of time than they are for mature injectors. In summary, the data obtained during the pilot were of good quality but interpretation techniques needed improvement.

5.1.9 INJECTION PRESSURE DATA

Monitoring of the injection pressure was continuous. The reservoir pressure was about 50 psig. Injection pressure increased to 80 psig under 500 bbl/day CWE steam injection at about 80% quality. Addition of surfactant and nitrogen increased the injection pressure to 150 psig. This level was maintained during the injection of surfactant, then reverted slowly to 80 psig in about thirty days after completion of each surfactant slug. This increase in injection pressure is far too large to be explained by the additional fluids injected. Most of the increase can be attributed to foam generation blocking the steam. In shallow reservoirs, care must be taken not to exceed fracturing pressure. An optimum pressure increase should exist for each pattern and could be approached by changing the concentration or rate of foamer injected, depending on the pressure response at the injector.

5.1.10 TRACER TESTING

Tracer testing can be a useful technique to define reservoir heterogeneity (well-to-well) or to study flow behavior near a given injector (injectivity profiles). This section deals with SUPRI experience with tracers during the pilot test.

5.1.10.1 Well-to-Well Radioactive Tracers

A radioactive tracer survey was conducted in November, 1981. The objective of this survey was to define the reservoir. A technique for the analysis of tracer breakthrough curves has been developed by Abbaszadeh and Brigham. (Abbaszadeh, 1984) Although this method is only valid for a mobility ratio equal to one, it was hoped that the data from the survey would be amenable to a similar analysis.

Tritium, krypton 85, sulfur hexafluoride and Freon 14 were injected into Well 208 and tritium and krypton 85 were injected into Well 214. As an experiment, gamma ray logging of the observation wells was attempted to try to detect the radioactive tracers–to no avail. No tracer response was seen. Nor were Tritium or Freon 14 detected in any of the producers. Krypton 85 and sulfur hexafluoride were observed in Well 120 (see Fig. 5.1.1) and a smaller amount was seen in Well 119. The data from these wells could not be analyzed using the technique of Ref. 16.

No samples were taken from Well 114, the most updip producer in the test pattern. This was unfortunate. The results of the inorganic tracer tests (discussed later) and the temperature surveys showed that most of the steam injected into Well 208 moved towards Well 114. The oversight in not sampling this well probably cost access to valuable data.

Timing was faulty on the sampling program. As shown by the inorganic tracer results, described in the next section, steam traveled from Well 208 to Well 114 in less than half an hour, much faster than expected. As a result we may have missed most of the tracer responses by sampling too late. One other reason for the failure of the radioactive tracer program lays in the small amounts of tracers that can be injected under California law. Present restrictions are even more stringent, thus it is difficult to design a good radioactive well-to-well tracer testing program in California.

Nitrogen was injected as a noncondensable gas to improve the efficiency of the steam/foam test. It would have been useful to use nitrogen as a tracer and obtain information in that manner. No sampling facilities for nitrogen were available at the time.

5.1.10.2 Inorganic Well-to-Well Tracers

Due to the poor results of the radioactive tracer survey, an attempt was made to use sodium bromide and sodium nitrate as tracers. These salts are water soluble, are supposed to be nonvolatile and their transport properties in steam/water systems are not understood. Even though the inorganic tracers are nonvolatile, a strong tracer response was observed in the most updip wells in less than half an hour. This can only be explained by some transport of the tracers by the steam. Since no theory exists for this behavior, quantitative analysis of the breakthrough curves is impossible. It was possible, however, to qualitatively compare surveys performed before the steam/foam test (Fig. 5.1.3a) and during injection of foam (Fig. 5.1.3b). Evidence of steam diversion from Well 120 to Wells 113b and 119 can be inferred from the changes in relative amounts of tracers recovered at the producers.

Inorganic tracer surveys are inexpensive. They can provide useful qualitative data; but, as no interpretation method exists to extract quantitative reservoir information from such tests, they should be used only as a supplement to other monitoring methods.

5.1.10.3 Injectivity Profiles

Injectivity profiles are used in wells where spinner surveys are not accurate enough to provide information on the amount of fluids entering a given interval of the formation.

That happens when rates of injection are too low or when two phase flow effects perturb the measurements. Spinner surveys have been successfully used (Keijzer, 1986; D'Orazio, 1987) in Venezuela and should be preferred when possible. The SUPRI test was in a lease operated at conditions where the spinner surveys are not reliable. We decided to use injectivity profiling instead.

Injectivity profiles are obtained by injecting a water soluble radioactive tracer with the steam and making repeated passes over the perforated interval with a detector. The procedure is repeated for the gas phase, this time using a gas soluble tracer. The amount of fluid entering a given interval of the formation is calculated from the intensity and the rate of decay of the radioactivity detected. Interpretation procedures of these tests vary for different service companies, and no sound theory seems to be available to analyze them. We feel, consequently, that quantitative analysis of these tests should be used with caution.

Profiles were taken in Well 208 before, during and after every surfactant slug injection. They provided useful qualitative information. The same profile patterns with time were obtained for each of the three main slugs. Before the slug, injectivity profiles in our test pattern were atypical; for instead of normal steam override most of the fluids went into the bottom of the well in the fourth layer. We found later that there had been additional unreported perforations in that interval. During the treatment, injectivity into this zone was reduced and Slices 1 to 3, previously poorly swept, were contacted by the steam (Fig. 5.1.4). The profiles reverted to the original values a few days after completion of each surfactant slug injection.

In the SUPRI test, we planned a deliberate overkill in the amount of surfactant injected. As a result, the steam diversion was not perfect during injection of the first slug. The profiles showed improvement at the beginning with steam being diverted from Slice 4 to Slices 1 to 3; then they reverted to the original profiles as surfactant injection continued. We feel that the excess foam reduced the injectivity of Slices 1 to 3 after a few days and that the steam then swept back into the higher permeability desaturated layer, Slice 4. When the surfactant concentration was reduced during injection of the two later slugs, this problem disappeared and better vertical sweep was achieved throughout the injection sequence.

In theory, one would like to compare spinner surveys and injectivity profiles from radioactive tracers. Both techniques are useful in detecting injectivity changes near the wellbore caused by the additives, and in qualitatively monitoring the near wellbore vertical sweep efficiency.

5.1.11 SAMPLING AND PRODUCED FLUIDS ANALYSIS

Sampling could have been attempted in the observation well located in the test pattern. Designing a sampling program should be done carefully for it can complicate later logging operations. However, it is worth the effort , for knowledge of surfactant transport through the reservoir can lead to better modeling of foam propagation for a given site and offer some predictive tools for management decisions. A good example of such an approach was presented by Patzek and Myhill.(Patzek, 1989)(Patzek, 1989) Detection of surfactant, and/or degradation by-products, could have provided insight on the validity of the laboratory studies. Surfactant transport is an important problem, as noted by Lau and Borchardt (Lau, 1989), and Liu et al. (Liu, 1992), for transport properties can directly affect the economics of the steam foam process.

Produced fluids were sampled during the SUPRI pilot. The water samples did not show either surfactant or products resulting from possible surfactant degradation. Other projects (Eson, 1989; Castanier, 1989; Patzek, 1989) have found surfactant transported to the producers.

The fact that surfactant can be transported to the producers has led to fear of emulsion problems. The surfactants used in steam/foam projects are not designed to reduce oil/water interfacial tension. In the laboratory, the lowest IFT measured by SUPRI in oil/foamer systems was several dynes/cm. This is probably the reason why no emulsion problems have been attributed to the surfactants in published steam/foam projects.

5.1.12 PRODUCTION RESULTS

Two sets of production data were obtained during the field experiment. One set was provided by the lease operator and proved to be radically different from the second set collected by CORCO, the operator of the pilot test. A testing procedure was designed to evaluate the production data.

Both sets of data were obtained by testmeters where total production of oil and water was measured using turbine flowmeters and the water cut was determined by sampling. Such meters require careful handling and calibration. To check the accuracy of the production measurements, 500 bbl tanks were installed on site and the production from individual wells was tested periodically in these tanks. To obtain the exact cut of oil in the tanks a new sampling device was constructed, (Brigham, 1989; Brigham, 1984) Fig. 5.1.5. This device was needed because of the problem of separating oil and water in the tanks. The CORCO set of data was found to be the more reliable by comparison with the tank measurements.

Unfortunately these test measurements were not available during the entire pilot test, so there is some doubt about the accuracy of the production data. We recommend the use of tanks for individual wells whenever possible.

Oil production estimates from the test pattern are shown in Fig. 5.1.6. A pronounced upward trend was observed within days of the start of each of the slugs. These increases are remarkable in light of the general decline of about 16% per year observed on the lease as a whole as can be seen from one of the dashed lines in Fig. 5.1.6. The baseline production trend is not accurately known, but an increase in rate is clear. The increase can be attributed to the steam foam treatments because no significant operational changes were made in the test pattern during the life of the project. Economic projections performed on a leasewide basis (Strom, 1984) show the process to be economic. This conclusion was later confirmed by others. (Eson, 1989)

Measuring produced fluids in heavy oil reservoirs is not simple. Even if a correct baseline or decline curve for the test area has been established, care has to be taken to assess individual wells' oil and water rates. Use of individual tanks with proper determination of the oil cut is one of the best methods. Overall lease data should be viewed with caution because of normal variations between individual wells and sometimes insufficient operating personnel or equipment. As oil production is the main indicator of economic success of a process, every effort should be made to obtain accurate data.

5.1.13 CONCLUSIONS

Even in a carefully designed research pilot, we have seen that significant improvements could have been made in the design and operation of the SUPRI project. The goal of a pilot test is to obtain information. This information is valuable for it allows understanding of a process behavior in a given reservoir. In the search for accurate field data, redundant monitoring methods can and should be used to forstall unexpected problems or equipment failures. The reservoir is not often going to behave as expected. It is important to understand the reservoir physics prior to the application of any enhanced oil recovery process. Time and money spent on reservoir characterization and proper monitoring methods are a wise investment.

Table 5.1.1: Logging Program in the Observation Wells

TABLE 1
LOGGING PROGRAM IN THE OBSERVATION WELLS

OPEN-HOLE LOGS	COMPANY
FDC-CNL Gamma Ray	Schlumberger
Nuclear Magnetic Log	Schlumberger
Electromagnetic Propagation Tool	Schlumberger
Dual Induction-SFL	Schlumberger
Cyberlook	Schlumberger
Spectralog	Dresser-Atlas
Dielectric Constant	Gearhart Industries
CASED-HOLE LOGS	**COMPANY**
Dual Spacing Thermal Neutron Decay Time	Schlumberger
Cement Bond	Schlumberger
Gamma Ray Spectroscopy (in Well 214M only)	Schlumberger
Carbon/Oxygen	Dresser-Atlas
Temperature	USGS
COMPUTER-PROCESSED LOGS	**COMPANY**
VOLAN	Schlumberger
Production Management	Schlumberger

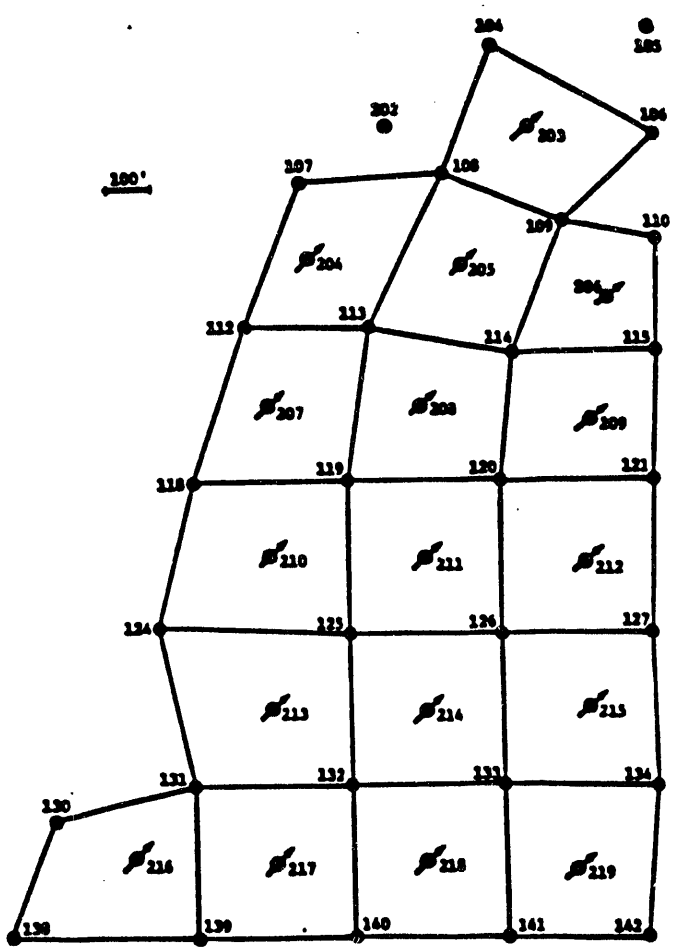

Figure 5.1.1: MacManus lease test and control pattern location.

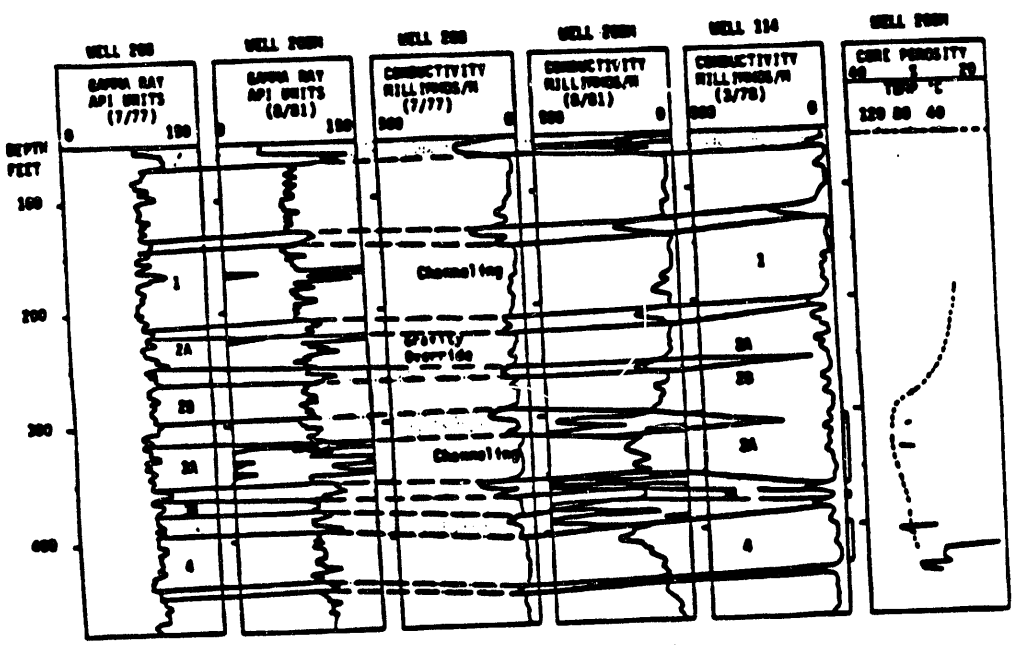

Figure 5.1.2: Cross section test pattern.

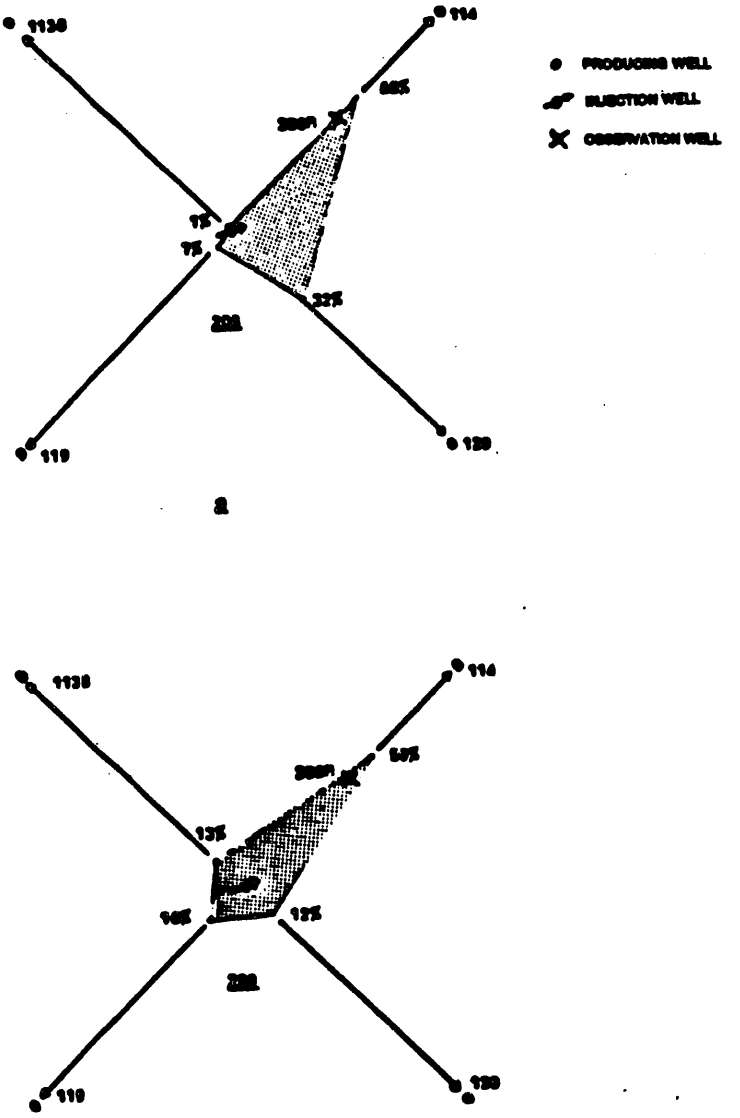

Figure 5.1.3: Tracer response: (a) before and after second slug injection; (b) during second slug injection.

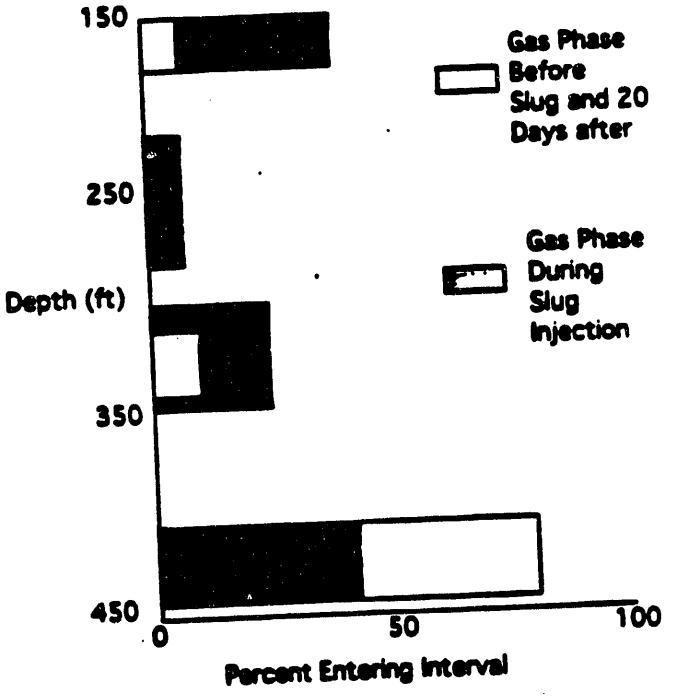

Figure 5.1.4: Injection profiles during first slug injection.

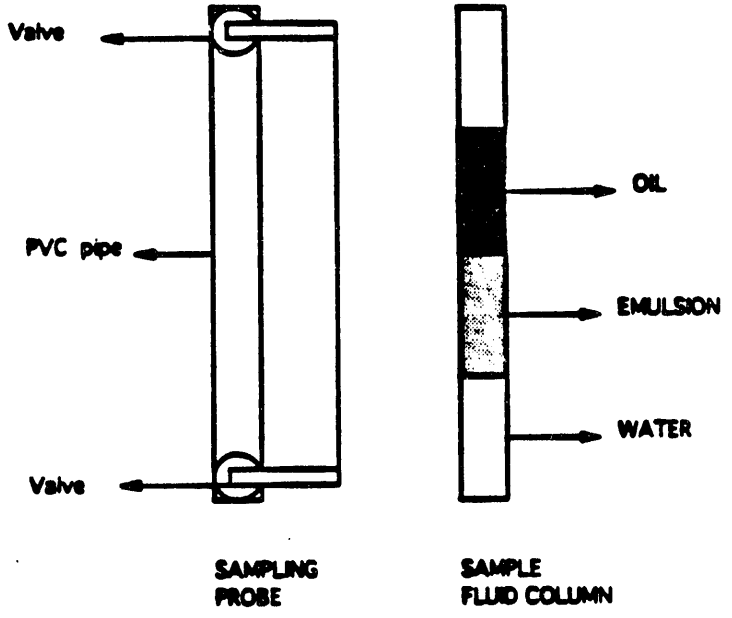

Figure 5.1.5: Sampling probe assembly.

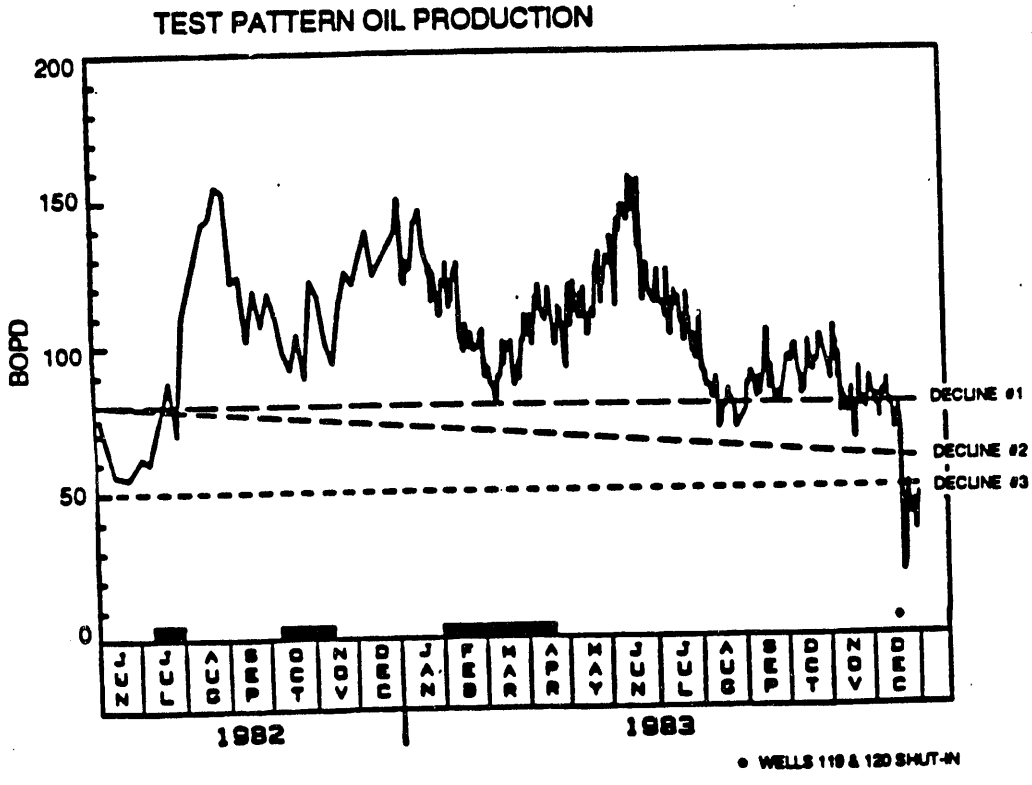

Figure 5.1.6: Test pattern oil production.

5.2. INJECTIVITY CALCULATIONS FOR VARIOUS FLOODING PATTERNS

(W.E. Brigham)

Whenever an enhanced recovery process is used, there are two factors that affect the economics of the process. One is the recovery as a function of the volume injected; the other is the rate of injection and production as a function of time (or volumed injected). There is considerable literature which addresses recovery predictions for various enhanced recovery techniques, but there is surprisingly little on the rate functions.

It is surprising that this situation exists; for whenever an engineer makes an economic evaluation he finds that the rate is the most important single variable effecting the economics of a project. Particularly important are the rates to be expected during the earlier years of any project. This is because the cash flow stream normally is discounted in value at later times. The purpose of these notes is to show how rate calculations can be made easily and rapidly using simple analytic approximations.

If a reservoir is nearly depleted, under primary production, early injection rate predictions can be made using simple radial flow formulas and the concept of a succession of steady states. This idea is shown in detail for waterfloods–but the concepts are of general value for any recovery process.

If the reservoir is liquid filled, analytic equations are available to handle various flooding patterns whenever the mobility ratio is unity. The material in these notes shows how to approximate these exact solutions using simple geometric construction concepts. The value of using these approximations is that the engineer can gain considerable insight on the effects of changing the operating variables. As a result, a large number of practical problems can be addressed rapidly and accurately using those ideals. Examples are:

1. Wellbore Radii. If some of the wells are fractured or damaged, the effect on injectivity can be calculated exactly.

2. Non-Unity Mobility Ratio. The analytic solutions can be easily changed to handle the more common cases of non-unity mobility ratio.

3. Permeability Anisotropy. Often reservoirs have permeabilities that differ in the two main directions. These equations can be used to model this situation.

4. Complex Flooding Patterns. Patterns such as the 9-spot have production histories that appear anomalous but which can be predicted by these equations.

5. Non-Pattern Flooding. The ideas in the work can be used to handle the behavior of any balanced flooding arrangement. And it can be done using simple equations.

IN-SITU COMBUSTION FORUM

DOUBLETREE DOWNTOWN HOTEL

PROGRAM
(April 20-21, 1992)

Monday, April 20

FIELD I

9:00 - 9:30	In-Situ Combustion Performances in Romania (V. Machedon)
9:30 - 10:00	Case History of South Belridge (H.J. Ramey, Jr., V.W. Stamp, F.M. Pebdani and J.E. Mallinson)
10:00 - 10:15	**Break**
10:15 - 10:40	Experience in Hungary (M. Toth)
10:40 - 11:00	An Overview of Some Texaco In-situ Combustion Research and Field Projects (M. Fontaine and J. Prieditis)

FIELD RESULTS II

11:00 - 11:30	Forrest Hills Pilot with Oxygen (L. Hvizdos)
11:30 - 12:00	Application of In-Situ Combustion (D.W. Bennion)
12:00 - 1:30	**Lunch**

LIGHT-OIL APPLICATIONS

1:30 - 2:30	Air Injection into Deep Light Oil Reservoirs and the Resulting High Pressure Oxidation Kinetics (D. Yanimaras)
2:30 - 3:00	Combustion Experience in Light Oil Systems (A. Barnes)
3:00 - 3:15	**Break**

FUEL LAYDOWN

3:15 - 3:45	Are Gasification Reactions Important? (J. Donnelly)
3:45 - 4:15	Effect of Oil Type and Other Operating Parameters on Fuel Laydown (M.R. Fassihi)
4:15 - 4:45	Numerical Simulation Study of Cyclical Processes of In-Situ Combustion and Steam Injection (P. Colonomos)
4:45 - 5:05	A New Model for In-Situ Combustion Kinetics (D. Mamora)

April 16, 1992

Tuesday, April 21

LABORATORY STUDIES

8:30 - 9:00	Esso Canada Three-Dimensional Model (R. Leaute)
9:00 - 9:30	Combustion Experiments and Kinetics Data (E. Okandan)
9:30 - 10:00	Amoco's High Pressure Combustion Tube Studies (D. Tiffin)
10:00 - 10:15	**Break**
10:15 - 10:50	Texaco's Laboratory Results (S. Boussaid)
10:50 - 11:30	Why are Combustion Kinetics Important? (G. Moore)

DISCUSSION

11:30 - 12:30	Panel discussion on future of combustion
12:30 - 2:00	**Lunch**
2:00	Departure to Amoco's Research Center
4:00	Return to Doubletree Hotel, Adjourn

IN-SITU COMBUSTION FORUM, TULSA, APRIL 20-21, 1992

Name	Address
John Alexander	Conoco, Inc. P.O. Box 1267, Ponca City, OK 74603 (405) 767-3294, Fax (405) 767-6569
Ralph Avellanet	DOE FE-33, Washington, D.C. 20545 (301) 903-2737, Fax (310) 903-2713
A.L. Barnes	ARCO 2300 W. Plano Parkway, Plano TX (214) 754-6079
Douglas W. Bennion	Hycal Energy Research Laboratories, Ltd. 1338A-36 Ave. NE, Calgary, Alberta, T2E 6T6 (403) 250-5800, Fax (403) 291-0481
Sam Bousaid	Texaco, Inc. - EPTD P.O. Box 770070, Houston, TX 77215 (713) 954-6011, Fax (713) 954-6911
William E. Brigham	Stanford University 350 Mitchell Bldg. Petroleum Research Institute, Stanford, CA 94305 (415) 723-0611, Fax (415) 725-2099
Louis M. Castanier	Stanford University 350 Mitchell Bldg. Petroleum Research Institute, Stanford, CA 94305 (415) 723-2223, Fax (415) 725-2099
Peter Colonomos	Intevep P.O. Box 76343, Caracas, Venezuela (582) 908-6442, Fax (582) 908-7633
Ted Cyr	AOSTRA 10010-106 St., Edmonton, Canada, T55 3L8 (403) 427-7623, Fax (403) 422-9112
John K. Donnelly	Independent consultant Box 13, Sitel RRZ, Calgary, Alberta, T2P 265, Canada. (403) 932-4162, Fax (403) 932-4068

Grant Duncan	Petro-Canada P.O. Box 2844, Calgary, Canada T2P 3E3 (403) 296-4606, Fax (403) 296-3030
M. Reza Fassihi	Amoco Production P.O. Box 3385, Tulsa, OK 74105 (918) 660-3963, Fax. (918) 660-4163
Marc F. Fontaine	Texaco, Inc. - EPTD P.O. Box 770070, Houston, TX 77215 (713) 954-6064, Fax (713) 954-6911
Norman Freitag	Saskatchewan Res. Council 515 Henderson Drive, Regins, Sask. (306) 787-9349, Fax (306) 787-8811
Claude Gadelle	Institut Francais du Petrole 1 et 4 Av. du Bois Preau 92500 Ryeil-Malmasson, France 33-1-47526297, Fax 33-1-47490411
Fevzi Gürnrah	Middle East Technical University Petroleum Engineering Dept, 06531 Ankara, Turkey Fax (904) 286-8630
W. Carey Hardy	Sun E&P (ret) 1708 Wessex Circle, Richardson, TX 75082 (214) 235-5886, Fax (214) 644-7364
John V. Howard	Greenwich Oil Corp. Suite 200, 6750 Hillcrest Plaza Dallas, TX, 75230 (214) 934-9125, Fax (214) 490-0856
Leonard J. Hvizdos	Air Products Allentown 10, PA (215) 481-7910
John Kirkpatrick	Amoco consultant RT. 3, Box 1310, Afton, OK (918) 257-5881
M. Kumar	Chevron Oil Field Research Co. La Habra, CA 92670 (310) 694-7354

Vinodh Kumar	Kock Exploration P.O. Box 2256, Wichita, Kansas (316) 832-5368
Roland P. Leaute	Exxon Res. & Dev. Labs. P.O. Box 2226, Baton Rouge, LA 70821-2226 (504) 359-1502, Fax (504) 359-8037
Daulat D. Mamora	Stanford University Petroleum Engineering Dept., Stanford, CA 94305 (415) 723-3094, Fax (415) 725-2099
Doug Marjerrison	AMOCO Canada P.O. Box 200, Calgary, Alta, T2M OA5 (405) 234-4014
W.L. (Bill) Martin, Sr.	Conoco, Inc. (ret.) 124 Elmwood Ave., Ponca City, OK 74601 (405) 762-4140
Raj Mehta	University of Calgary Dept. of Chem. & Pet. Engr. 2500 University Drive, N.W. Calgary, Alberta T2N lN4, Canada (403) 220-4804, Fax (403) 284-4852
Gord Moore	University of Calgary Dept. of Chem. & Pet. Engr. 2500 University Drive, N.W. Calgary, Alberta T2N lN4, Canada (403) 220-7217, Fax (403) 284-4852
Scott Northrop	Mobil Research 13777 Midway Road, Dallas, TX 75244 (214) 851-8609
Victor Machedon	PETROM - Romania, Bd-Culturii 29, 2150, Cimpina 973-34831, Fax (73) 35236
J.E. Mallinson	Mobil Oil Box 650232, Dallas, TX 75265 (214) 951-3331, Fax (214) 951-2952

Ender Okandan	Middle East Technical University Petroleum Engineering Dept, 06531 Ankara, Turkey Fax (904) 286-8630
Fred H. Poettmann	Colorado School of Mines Dept. of Petroleum Eng., Golden, CO 80401 (303) 273-3043
John Prieditis	Texaco - EPTD 3901 Briarpark, Houston, TX 77042 (713) 954-6168
H.J. Ramey	Stanford University Petroleum Engineering Department, Stanford, CA 94305 (415) 723-1774
Thomas B. Reid	DOE P.O. Box 1398, Bartlesville, OK 74006 (918) 337-4233, Fax (918) 337-4418
Partha Sarathi	NIPER P.O. Box 2128, Bartlesville, OK (918) 337-4304, Fax (918) 337-4365
W.E. Showalter	400 Ocean Ave., Seal Bc 11, CA (310) 430-4382
Bruce Slevinsky	Petro-Canada P.O. Box 2844, Calgary, Canada T2P 3E3 (403) 296-4606, Fax (403) 296-3030
John Stalder	Conoco Houston, TX (713) 293-1340
V.W. Stamp	Consultant 3640 Ermine Circle, Casper WY 82604 (307) 235-1301
George Stosur	DOE FE-33, GTN, Washington, D.C. (301) 903-2749, Fax (301) 903-2713
Pete Thies	Koch Exploration P.O. Box 2256, Wichita, Kansas (316) 832-5481

David L. Tiffin
Amoco Production Co.
P.O. Box 3385, Tulsa, OK 74102
(918) 660-3728

Maria Toth
Hungarian Hydrocarbon Institute
Budapest III 1311, POB 43
(36) 11800-912, Fax (36) 1180-2145

Larry Treiber
AMOCO Production
P.O. Box 3385, Tulsa, OK 74102
(918) 660-3258

Elena Tzanco
Pan Canadian Petroleum Ltd.
Calgary, AB
(403) 290-2361, Fax (403) 290-2950

Matt Ursenbach
University of Calbary
Dept. of Chemical & Pet. Engr.
2500 University Drive N.W.
Calgary, Alberta T2N 1N4, Canada
(403) 220-4807, Fax (403) 284-4852

Marlene Villalba
Intevep
El Tambor, Los Tegues, Edo Miranda, Venezuela,
(582) 908-6097, Fax (582) 908-7633

Shapour Vossoughi
University of Kansas
4006 Learned, CPE Lawrence, KS
(913) 864-4965, Fax (913) 864-4967

Demetrios Yannimaras
AMOCO Prod. Research
P.O. Box 3385, Tulsa, OK 74102
(918) 660-4148

David R. Zornes
Phillips Petroleum
238 GB-PRC, Bartlesville, OK 74005
(918) 333-6965, Fax (918) 662-2047

END

DATE FILMED

9/30/93